CONTRIBUTION OF COMPLEX FORMATION IN THE *IN VITRO* AND *IN VIVO* ACTION OF *CLOSTRIDIUM PERFRINGENS* ENTEROTOXIN

by

Justin Angelo Caserta

BS Biology, University of Dayton, 2004

Submitted to the Graduate Faculty of

The School of Medicine in partial fulfillment

of the requirements for the degree of

Doctor of Philosophy

University of Pittsburgh

2010

UNIVERSITY OF PITTSBURGH

SCHOOL OF MEDICINE

This dissertation was presented

by

Justin Angelo Caserta

It was defended on

July 9, 2010

and approved by

Billy W. Day, Ph.D., Professor, Pharmaceutical Sciences

Neal A. DeLuca, Ph.D., Professor, Microbiology and Molecular Genetics

Michael A. Parniak, Ph.D., Professor, Microbiology and Molecular Genetics

Russell D. Salter, Ph.D., Professor, Immunology

Dissertation Advisor: Bruce A. McClane, Ph.D., Professor, Microbiology and Molecular Genetics

CONTRIBUTION OF COMPLEX FORMATION IN THE *IN VITRO* AND *IN VIVO* ACTION OF *CLOSTRIDIUM PERFRINGENS* ENTEROTOXIN

Justin Angelo Caserta, PhD

University of Pittsburgh, 2010

Clostridium perfringens enterotoxin (CPE) is a pore-forming toxin that is responsible for causing the symptoms of type A food poisoning, a leading cause of bacterial foodborne illness in the US. CPE-induced pore formation on intestinal epithelial cells results in ion permeability alterations leading to Ca^{2+} influx and activation of cell death pathways. Upon binding to its receptor, certain claudins, the interactions between CPE and the target membrane result in the formation of a series of toxin complexes (CH-1 and CH-2) that represent the formation of the functional CPE pore. Many bacterial toxins, particularly, pore-forming toxins, hijack cholesterol-rich lipid raft domains in the target cell membrane to aid in their virulence. Lipid rafts serve as platforms to cluster receptor proteins to allow for more efficient binding and oligomerization. Due to the pore-forming activity of CPE, we wished to determine if membrane rafts play a role in the mechanism of action of CPE. Interestingly, CPE was found to be a novel pore-forming toxin that does not require raft domains for its action in that CPE complexes do not form within lipid rafts and cholesterol depletion had no effect on CPE-induced cytotoxicity. These findings illustrate the unique interactions between CPE and target cells. Despite recent research findings indicating the presence of claudins in the various CPE complexes, these intricate interactions have not been fully elucidated, and the exact composition of the toxin complexes is unknown. Therefore, the research presented here describes the development of a two-step method of electroelution/immunoprecipitation that allows for the isolation and purification of the CPE

complexes for compositional analysis by mass spectrometry. Finally, a mouse model has been developed and characterized to show that the molecular interactions that occur in cell culture models, such as complex formation and inflammatory cell death, also occur *in vivo*. Furthermore, the mouse model mimics the lethality that is occasionally seen in humans that suffer from type A food poisoning-related deaths.

TABLE OF CONTENTS

LIST OF TABLES

LIST OF FIGURES

PREFACE

Although the goal of earning a PhD in the biomedical field is to train one to become an independent scientist, it is without a doubt more of a team effort. There are many people of whom I could not have accomplished what I have up to this point without their help in one way or another. First, I must acknowledge Dr. Mark Nielsen, my undergraduate research advisor at the University of Dayton, who instilled in me the drive to perform research, and imparted upon me passion for science. Not only his understanding of the research process, but also of life, were true lessons to have learned. Dr. Nielsen once told me that the **people** doing science are more valuable than any reagent that you can buy.

Next, I must recognize my advisor, Dr. Bruce McClane, who has taught me over years what it means to be a scientist. His mentorship was invaluable in my development as an independent scientist. Thank you also to the members of my committee: Dr. Jay Carroll, Dr. Billy Day, Dr. Mike Parniak, Dr. Russ Salter, and Dr. Neal DeLuca. Their guidance and helpful suggestions were instrumental in leading me towards completing my PhD training. I also acknowledge Dr. Joanne Flynn, whose NIH Pre-doctoral training grant partially supported my PhD training.

Many thanks go out to our many collaborators who have helped in one way or another in producing data for this thesis dissertation. Dr. Brad Stiles and Dr. Martha Hale from USAMRIID were instrumental in initiating the lipid raft studies and were kind enough to provide

technical training. Additionally, the assistance provided by Drs. Mani Balasubramani and Manny Schreiber from the University of Pittsburgh Proteomics Core was indispensible in designing and carrying out our proteomics experiments. Lastly, all of our animal experiments were performed by Dr. Francisco Uzal and Juliann Saputo at the CA Animal Health & Food Safety Lab at UC-Davis. The animal data presented here could not have been accomplished without their technical superiority and their assistance is greatly appreciated.

Finally, thank you to my family and friends who have supported me through this challenging process. I appreciate the times that you forced me to not go into the lab and were understanding in the times that you could not convince me to do so. Thank you for not asking too many times, "When will you be finished with grad school?"

Abbreviations used in this Dissertation: AAD: Antibiotic-associated Diarrhea; BBMs: brush border membranes; CDCs: cholesterol-dependent cytolysin; CH-1: CPE Hexamer-1; CH-2: CPE Hexamer-2; cldn: claudin; CPE: *C. perfringens* enterotoxin; DRM: detergent-resistant membrane; EE: electroelution; HUVEC: human umbilical vein endothelial cell; IP: immunoprecipitation; JAM-A: junctional adhesion molecule-A; MβCD: methyl-β-cyclodextrin; mAb: monoclonal antibody; MDCK: Madin-Darby canine kidey; PBMC: Peripheral Blood Mononuclear Cell; PFT: pore-forming toxin; ; rCPE: recombinant CPE (His-tagged); SC: Small Complex; SD: Sporadic Diarrhea; TEER: transepithelial electrical resistance; TJ: tight junction; TX-100: Triton X-100

1.0 INTRODUCTION

1.1 GENERAL BACTERIOLOGY OF *CLOSTRIDIUM PERFRINGENS*

Originally isolated and identified as *Bacillus aerogenes* in 1892 by Welch and Nuttall, and transiently named *Clostridum welchii*, *C. perfringens* is a Gram-positive bacterium of great medical importance as it is a well-recognized cause of both human and veterinary diseases (30). Historically, *C. perfringens* first gained notoriety during World War I when it was discovered that this bacterium was responsible for causing the deaths of many soldiers suffering from gas gangrene wound infections. Known for its wide environmental distribution, *C. perfringens* is a ubiquitous pathogen that can be found in water, soil, and as part of the normal flora of the digestive tract of humans and other mammals; *C. perfringens* is known as the most widely occurring pathogenic bacteria. This ubiquitous nature allows this pathogen ample opportunity to come in contact with humans and other animals in order to cause disease. Additionally, *C. perfringens* has the largest arsenal of toxins within the *Clostridium* genus, with >14 toxins and enzymes, which give this pathogen its exceptional virulence.

As a member of the *Clostridium* genus, *C. perfringens* is part of a diverse group of bacteria that are anaerobic endospore-forming rods of size 0.6-2.4 µm X 1.3-19 µm and form large, regular, round, and slightly opaque and shiny colonies on the surface of agar plates (30). Other distinguishing characteristics include: non-motility, catalase/oxidase negative, optimal

growth at 42°C, lecithinase-positive, double zone of hemolysis on blood agar, and the reduction of sulphite. Additionally, *C. perfringens* alpha toxin works in synergy with Group B Streptococcus toxins, serving as the basis for the Reverse CAMP test (30). In the phylum Firmicutes, *C. perfringes* belongs to the class Clostridia where other medically relevant bacteria such as *C. difficile*, *C. botulinum*, and *C. tetani* are classified.

As a member of the Firmicutes, *C. perfringens* has a low GC content of 24-54%, with the average being 28%. Recently, the genomes of three *C. perfringens* strains were sequenced (140, 174). It was revealed that there is considerable diversity among the strains, with genome sizes ranging from 3 to 4 Mbp. This diversity was explained by the presence of ~300 mobile genetic elements that vary among isolates and encode factors involved in metabolism, capsule synthesis, and toxin production. These mobile elements, thus, convey different virulence advantages between strains which lead to the varying human and veterinary diseases caused by *C. perfringens*.

1.2 TOXINS AND DISEASES ASSOCIATED WITH *C. PERFRINGENS*

1.2.1 Toxinotyping

As mentioned above, *C. perfringens* produces an impressive array of toxins. However, not all these toxins are produced by all strains or at the same time. This allows for a systematic classification of *C. perfringens* isolates based on the expression of four major typing toxins: α, β, ε, and ι. This typing scheme allows for the classification of isolates into five types, A-E, and is illustrated in Table 1.1. Each toxinotype is associated with a particular disease due to the

production of a different set of toxins (Table 1.1). All five types carry the *plc* gene, encoding for α-toxin, on their chromosome, while the other major toxins are located on large virulence plasmids which are variably present in isolates. Plasmid size can vary among isolates within the same type based on the compatibility of different toxin genes with one another (104, 134, 167-168).

The α-toxin is a lethal dermonecrotic toxin with hemolytic, phospholipase C, and sphingomyelinase activities, and has been implicated as the primary cause of myonecrosis (gas gangrene) (9, 197). β-toxin is produced by type B and C strains and is responsible for causing enteric disease in both humans and animals. Specifically, Type B isolates are responsible for causing enterotoxemias in sheep and goats, while type C strains cause can enterotoxemias in both animals and humans. Human necrotic enteritis, also known as Pigbel, is an endemic disease in Papua New Guinea caused by type C isolates and is associated with diets of foods with high amounts of trypsin inhibitor. Recent studies using a type C rabbit ileal loop model with β-toxin knockouts and purified toxin demonstrated that this toxin is responsible for the pathogenic effects of necrotic enteritis (169, 207). Type B and D isolates produce ε-toxin, a potent pore-forming toxin known for its neurotoxicity, allowing it to be classified as a Class B Select Agent by the CDC. Epsilon toxin is the 3rd most potent toxin of the clostridial toxins, behind tetanus and botulinum toxins. Strains producing ε-toxin cause lethal enterotoxemias in lambs and goats, where pathological effects result from the toxin increasing the permeability within the intestine allowing for the toxin to enter the circulation where it can target other organs such as the kidneys, lungs, and brain. The fourth major typing toxin is ι-toxin, produced solely by type E isolates, and is a member of the classical binary toxin family such as *C. botulinum* C2 toxin with

ADP-ribosyltransferase activity. So far, type E isolates have been identified as only associated with veterinary enterotoxemias.

Table 1.1 Toxinotyping classification scheme and associated diseases for *C. perfringens* isolates

Toxinotype	Major Toxins α	β	ε	ι	Genotypes	Diseases
A	+	-	-	-	*plc* *plc, cpe* *plc, cpb2* *plc, cpb2, cpe*	Gas grangrene, diarrhea (dogs, pigs) Food poisoning, antibiotic-associated diarrhea, sporadic diarrhea, necrotic enteritis (fowl)
B	+	+	+	-	*plc, cpb, etx* *plc, cpb, etx, cpb2*	Dysentery (lambs) Enterotoxemia (sheep)
C	+	+	-	-	*plc, cpb* *plc, cpb, cpb2* *plc, cpb, cpe* *plc, cpb,cpb2, cpe*	Enteritis necroticans (pigbel), Necrotic enteritis (piglets, foals) Acute enterotoxemia (adult sheep)
D	+	-	+	-	*plc, etx* *plc, etx, cpb2* *plc, etx, cpb2, cpe* *plc, etx, cpe*	Enterotoxemia (goats, sheep, etc)
E	+	-	-	+	*plc, iap/iab, cpe* *plc, iap/iab, cpe, cpb2*	Enterotoxemia (calves, rabbits)

1.2.2 Non-typing Toxins

In addition to the four major typing toxins, *C. perfringens* produces other biomedically relevant toxins not used in the typing scheme. Theta toxin, also known as perfringolysin O (PFO), is a member of the cholesterol-dependent cytolysin (CDC) family of pore-forming toxins, with structural homology to *Streptococcus pyogenes* streptolysin O, *S. pneumoniae* pneumolysin, and *Listeria monocytogenes* listerolysin O. PFO has been shown to act synergistically with α-toxin in gas gangrene pathogenesis (10), as well as potentiate the lethal effects of ε-toxin in an intravenous mouse model (44). Additionally, PFO has been suggested to be the primary factor in

the killing of macrophages, an aspect which would aid in persistence of the bacterium within muscle tissue during gas gangrene infections (146).

Another example of a non-typing toxin is beta2 toxin, which has been implicated in several animal GI diseases, including equine typhlocolitis, diarrheic disease in piglets and dogs, and bovine enterotoxaemia, as well as some human non-foodborne diseases (47). Other toxins requiring further characterization include lambda protease, collagenase, and the many sialidases that are encoded by *C. perfringens*. Perhaps the most relevant *C. perfringens* toxin, as it relates to human disease, is *C. pefringens* enterotoxin (CPE) which is responsible for mediating the effects of human *C. perfringens* type A food poisoning.

1.3 *CLOSTRIDIUM PERFRINGENS* ENTEROTOXIN

1.3.1 Role in Type A Food Poisoning

1.3.1.1 Clinical and Epidemiological Aspects of Type A Food Poisoning

Clostridium perfringens type A food poisoning ranks among the top 3 causes of bacterial food-borne illness in the US and UK (2, 113) and is a great economic burden (198). This illness was first reported in large-scale outbreaks in England in 1943 and in the US in 1945 (84) and occurs in large institutions such as nursing homes and mental hospitals. A recent outbreak occurred in August 2008 where >100 inmates in a Wisconsin prison became ill due to contaminated food (154). Clinical symptoms of the illness include diarrhea, abdominal pain and cramping, and to a lesser extent, nausea, vomiting, and fever (172). Type A food poisoning is usually mild and

somewhat self-limiting, however, there are deaths commonly associated with this illness, especially within the elderly population. Symptoms usually resolve with 24 hours.

The source of type A food poisoning (Fig. 1.1) is most commonly exposure to high numbers (10^8 organisms) of *cpe*$^+$ vegetative *C. perfringens* present in contaminated meat products, usually beef stews, which have been inadequately cooked or improperly stored. Typically, within 12 hours after ingestion of the high numbers of vegetative cells, exposure to the harsh environment of the gastrointestinal tract will trigger sporulation (through an unknown mechanism, possibly the presence of inorganic phosphate (150)) of these vegetative bacteria. It is during sporulation that CPE production begins, resulting in a buildup of CPE protein within an inclusion body in the sporulating mother cell. At the conclusion of sporulation, the mother cell lyses to release the mature spore, as well as the large amount of CPE, into the intestinal lumen where it can act on target cells of the intestinal epithelium.

1.3.1.2 *In vivo* Effects of Type A Food Poisoning

The *in vivo* effects of CPE-induced type A diarrhea have been elucidated in rabbit animal studies, where it was shown that the rabbit small intestine is the major target of CPE *in vivo*, with the ileum being the most sensitive (123). A recent study additionally showed that CPE binds to human ileal epithelium and induces morphological damage concurrent with reduced transepithelial resistance and net water absorption (45). When tested in rabbit ileal loop models, CPE induces significant damage to the ileum within 15-30 minutes (173). This damage includes villus blunting, epithelial desquamation and some inflammation. Development of this histopathological damage coincides with the arrest of fluid absorption and reverse in fluid transport, suggesting a cause and effect relationship that gives rise to the secretion of fluid into the intestinal lumen which is characteristic of diarrhea. Additionally, doses of CPE within the

range measured in the stool samples of human patients are only able to cause histopathological damage and are capable of eliciting changes in fluid and electrolyte transport.

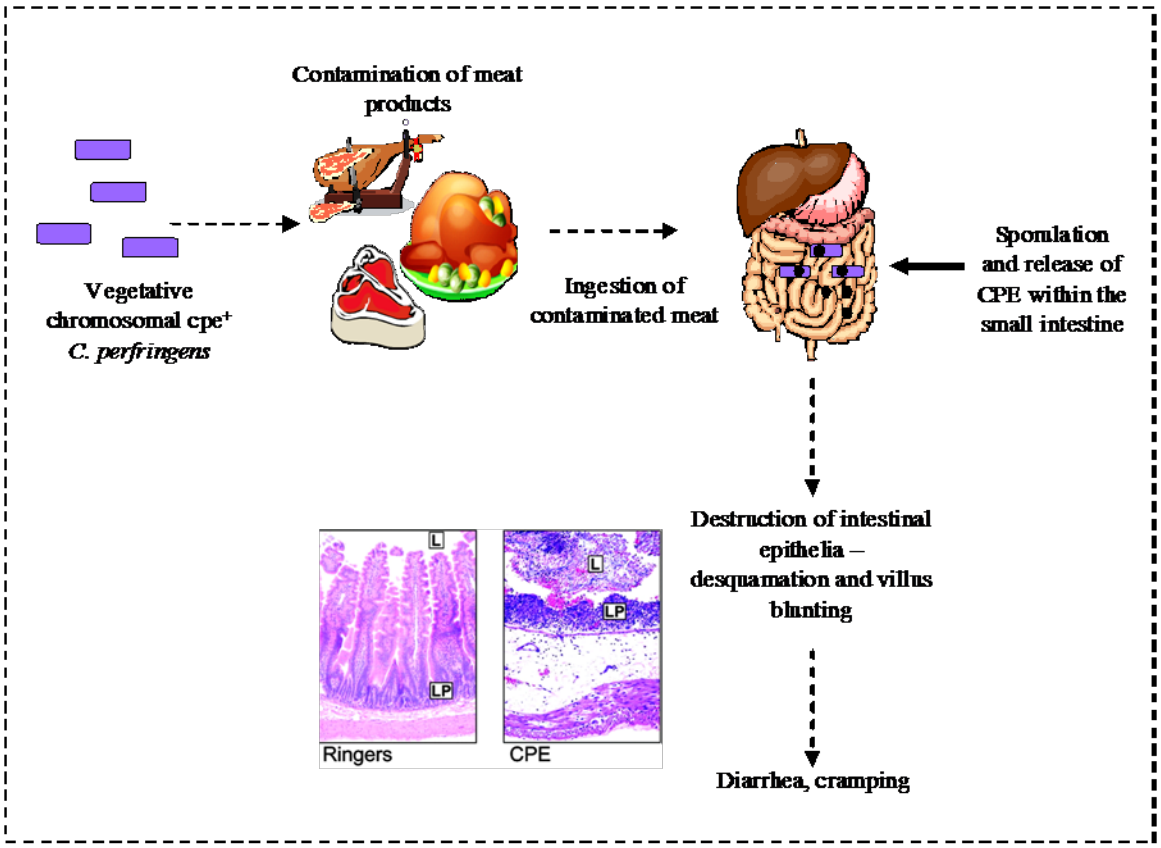

Figure 1.1 ***C. perfringens*** **Type A Food Poisoning.**

After ingestion of improperly stored or cooked food contaminated with vegetative cpe+ C. perfringens, bacteria begin to sporulate and produce CPE. CPE is released at the conclusion of sporulation within the lumen of the small intestine where it causes destruction of the epithelial cells, leading to cramping and diarrhea symptoms. Modified from (183).

A recent study (183) has illuminated the relevance of the CPE cytotoxicity seen *in vitro* (see below) and the entertoxicity seen *in vivo* as described above. This study used two rCPE variants, which are non-cytotoxic to cells *in vitro*, in a rabbit ileal loop model of CPE enterotoxicity *in vivo*. It was revealed that these non-cytotoxic CPE variants did not produce damage of the villus tips such as the necrosis of epithelium and lamina propria, villus blunting

and fusion, and transmural edema and hemorrhage as is seen with wild-type CPE. From this data it was concluded that cytotoxicity is necessary for the enterotoxic effects associated with CPE.

1.3.1.3 Direct Evidence for CPE's Role in Food Poisoning

As illustrated above, there is strong evidence for the role of CPE in the pathological effects of type A food poisoning. Further evidence supporting a role for CPE includes the observation that individuals suffering from food poisoning, but not healthy individuals, have CPE found within their feces (12, 15). Additionally, the levels of CPE found in the feces of patients suffering from food poisoning are similar to those that cause histopathological damage in animals as described above (125). Furthermore, the histopathology and fluid accumulation observed in rabbit ileal loop models can be prevented by neutralizing antibodies against CPE (72). Another piece of evidence comes from a study of human volunteers that were orally administered purified CPE and displayed symptoms consistent with type A food poisoning (181). Lastly, a study in which the *cpe* gene was inactivated in two *C. perfringens* isolates resulted in the complete absence of fluid accumulation and epithelial damage in the rabbit ileal loop model; however, when the wild-type *cpe* gene was complemented back into the isolate, fluid accumulation and blunting and desquamation of the villi returned in the same manner as observed for the parent isolate, thus, satisfying molecular Koch's postulates (165).

1.3.1.4 What is the Reservoir for *cpe*$^+$ Isolates?

Despite being found within retail foods (212), a question that remains regarding the role of *cpe*$^+$ *C. perfringens* in food poisoning is what the reservoir of these isolates is and where it originates within the food supply. Recent efforts have been undertaken to try to answer this important question. A recent study by Li et al. surveyed the presence of chromosomal *cpe*$^+$ type A isolates,

which are responsible for food poisoning (see Section 1.3.3.1), within Pittsburgh-area soil and home kitchens (105). The survey did not find any *C. perfringens* spores or vegetative cells from the 300 samples collected from different kitchen surfaces from 30 homes. Despite being ubiquitous in soil, this study did not find any *C. perfringens* isolates harboring the chromosomal *cpe* gene associated with food poisoning. This is in agreement with a previous US-wide soil survey which found no *C. perfringens* isolates harboring the enterotoxin gene (96).

In addition to environmental reservoirs, the human digestive tract could be a possible reservoir for carrying enterotoxigenic *C. perfringens*, and thus, many studies are now being published examining the presence of these isolates in healthy humans. A 2006 Finnish study examined the distribution of *C. perfringens* fecal carriage in 136 healthy food workers and found 11 (8%) to be cpe^+, however, only one was found to be carrying the enterotoxin gene on the chromosome (74). A Japanese survey of the presence of *C. perfringens* isolates in healthy individuals also found a low frequency of chromosomal cpe^+ isolates, with only two isolates as positive in the sample group (194). Lastly, when fecal samples were examined from 43 North American healthy subjects, no chromosomal-positive isolates were found (28). Taking these studies together, among those surveyed there is only a low incidence of colonization of healthy humans by *C. perfringens* carrying a chromosomal enterotoxin gene. Larger numbers of samples are needed, but one can conclude that healthy humans are most likely not the reservoir for food poisoning isolates. Unfortunately, the question of the reservoir remains unknown. However, additional sites that are likely guesses for the *cpe* reservoir including livestock digestive tracts or slaughter houses and warrant further investigation.

1.3.2 Role of CPE in Non-foodborne Disease

In addition to type A food poisoning, CPE also has a role in non-foodborne related diseases. An example of CPE-related non-foodborne disease is antibiotic-associated diarrhea (AAD). Most commonly implicated by *C. difficile* nosocomal infections, AAD is the result of the disruption of normal flora of the intestine by administration of antibiotics. The gut microflora acts as a barrier against enteropathogens, and as a result, any bacterium that is insensitive or resistant to the prescribed antibiotic can colonize and multiply within the intestine, leading to diarrheal disease. *C. difficile* is the most often documented cause of AAD because of the severe, and often fatal, pseudomembranous colitis that can result, but accounts for only 20-25% of AAD cases. In both North American and Europe, recent attention has been focused on *C. difficile*-related AAD because of the emergence of a hypervirulent, toxin-producing strain that results in not only nosocomal AAD, but also community-acquired infections (160). However, CPE-producing *C. perfringens* has been estimated to cause 5-15% of AAD cases. In 1984, Borriello et al. first described 11 cases of *C. difficile* toxin-negative AAD which harbored enterotoxin-positive *C. perfringens* strains (17). This first study has been extended by many others, confirming a relationship between patients suffering from diarrheal symptoms and receiving antibiotic therapy and CPE-positive *C. perfringens* with varying degrees of incidence (7-8, 16, 18, 80, 162, 203). It must be noted, however, that cases of AAD have been reported where enterotoxin-negative *C. perfringens* have been found within feces of patients (26, 153). In addition to AAD, cpe^{+}-positive *C. perfringens* has been implicated in cases of sporadic diarrhea (SD) in the community, particularly with elderly individuals (20, 139).

Unlike CPE-related food poisoning, symptoms resulting from CPE-positive *C. perfringens* AAD/SD tend to be more protracted and severe with blood and mucous in feces of

patients (138). The symptomatic differences between these CPE-associated diseases were not well understood until recently. In 2005, Fisher et al. performed a survey of the presence of the *cpb2* toxin gene in 61 *cpe*$^{+}$-positive isolates (48 AAD/SD isolates and 13 FP isolates) (47). The *cpb2* gene encodes the beta2 toxin (CPB2) which is mainly associated with animal GI diseases. This PCR study showed that 79% of AAD/SD isolates carried the *cpb2* gene whereas only 2 of the 13 (~15 %) FP isolates had the *cpb2* gene. This relationship of *cpb2* with AAD/SD isolates was later confirmed by Harrison et al. (69). Taken together, these studies indicate CPB2 may serve as an accessory toxin in AAD/SD cases, acting to prolong symptoms not normally seen with CPE alone (i.e. food poisoning).

1.3.3 CPE Genetics

1.3.3.1 The *cpe* Gene and Locus

The *cpe* gene is approximately 1.3 kbp in length and encodes a 319 amino acid CPE protein with a molecular weight of 35,317 Da (36). There exists no significant DNA or amino acid homology with any other known bacterial toxins, except for some limited homology with the non-toxic hemagglutinin from botulinum C1 neurotoxin gene complex (73). The significance of this limited homology is unknown; however, the region of greatest homology lies within the N-terminal cytotoxicity domain of CPE (see below). As described above, CPE can be responsible for both foodborne disease and non-foodborne disease. When the *cpe* gene was sequenced from isolates of each of these types of diseases, no difference in the deduced amino acid sequence was found between the types (33). Yet, *cpe*$^{+}$ isolates are capable of producing quite different disease.

In 1995, Cornillot et al. first demonstrated that the *cpe* gene could be located on either the chromosome or an episomal plasmid (35). Complete sequencing of two types of plasmids

carrying the *cpe* gene revealed that *cpe*-plasmids can vary significantly in their size, encoded open reading frames, and IS elements (134). The chromosomal *cpe* gene can be distinguished from plasmid-encoded *cpe* genes by a PCR assay which amplifies the flanking IS*1470* element of the chromosomal *cpe* gene versus the IS*1151* or IS*1470*-like elements on the *cpe* plasmids (135). The significance of these IS elements is most likely to allow for the mobilization of the *cpe* gene which could allow for horizontal gene transfer.

Collie and McClane demonstrated a strong correlation in which isolates carrying a plasmid-borne *cpe* gene were associated with AAD and SD (non-foodborne disease) while food poisoning isolates typically carry the *cpe* gene on the chromosome (34). Additional observations regarding chromosomal vs. plasmid *cpe* isolates revealed that the vegetative cells and spores of chromosomal *cpe* isolates are much more resistant to heat and chemical treatments than are plasmid isolates (101-102, 166). Insight into the mechanism of this resistance was recently investigated by Li and McClane (103). This study identified a novel member of the DNA binding small acid soluble protein (SASP) family, Ssp4, in which a single amino acid substitution existed in chromosomal *cpe* isolates which conferred greater resistance to temperature and chemical treatments as compared to plasmid *cpe* isolates. A final observation regarding the relationship between FP and chromosomal *cpe* genes comes from a study which described the presence of *cpe*$^{+}$ *C. perfringens* in raw meats in local grocery stores where all samples harbored a chromosomal gene (212).

1.3.3.2 Transcriptional Regulation of CPE

As described previously, CPE expression is tightly controlled and is associated with sporulation of the bacterium. After the development of sporulation media, early investigations demonstrated the sporulation-specific production of CPE that, when purified and administered to, resulted in

diarrhea in human volunteers and fluid accumulation in rabbit ileal loops (39, 71). This transcriptional control is attributed to, at least in part, the presence of three sporulation-specific sigma factor promoters (one SigK and 2 SigE) upstream of the *cpe* gene (225). Sigma factors are transcriptional regulators that direct RNA polymerases to promoter-specific genes that allow for the temporal transcription during sporulation which compartmentalizes the endospore and mother cell. In fact, as CPE is produced, it accumulates in a paracrystalline inclusion body within the mother cell and can account for up to 20% of total protein (36, 109). CPE has additionally been shown to be controlled by the CcpA transcriptional regulator which is a mediator of catabolite repression. CcpA was shown to act as a repressor of CPE expression during vegetative growth but positively regulates CPE synthesis during sporulation conditions (206). Although CPE synthesis is regulated with sporulation in *C. perfringens*, it is not required for expression when transformed and recombinantly-expressed in *E. coli* (36). Furthermore, the mechanisms of sporulation-dependent regulation seem to vary among sporulating Gram-positive bacteria, as evidenced by only moderate CPE expression when transformed into *Bacillus* (130). As mentioned above, CPE is not secreted, but rather, is released in large amounts at the conclusion of sporulation when the mother cell lyses to release the mature endospore.

1.3.4 Mechanism of Action

1.3.4.1 Binding

After release of CPE into the intestinal lumen at the conclusion of sporulation, CPE is able to act on target cells of the intestinal epithelia to induce the pathological effects characteristic of type A food poisoning. Considered a membrane-active toxin, binding of the enterotoxin to target cells is the first step required in the action of CPE. This initial binding event is necessary for the

cytotoxicity associated with CPE seen both *in vivo* and *in vitro*. Binding and enterotoxicity has been demonstrated in a number of animal models including: rabbit, mouse, rat, chicken, monkey, dog, bovine, pig, and lambs. Binding was first described *in vitro* to be necessary for the cytopathic effects of CPE in a study where ^{125}I-labeled toxin was shown to bind to sensitive Vero cells while a cell line that was resistant to CPE-induced killing was not bound by the toxin (126). Early experiments demonstrated that CPE binding to isolated cells from rabbit intestine, kidney, and liver is specific (i.e. unlabeled toxin is able to compete away ^{125}I-CPE) and saturable (124). This study also showed that bound toxin did not dissociate upon treatment with chaotropic salts, suggesting a conformational change that locks the bound toxin in place, possibly due to insertion into the membrane. Additionally, pretreatment of cells with proteases inhibited the ability of CPE to bind these cells.

These initial observations suggested that a specific proteinaceous receptor is responsible for CPE binding. Early attempts to identify the CPE receptor utilized affinity chromatography immobilized with CPE. When isolated intestinal brush border membranes (BBMs) treated with CPE were lysed and run through the affinity column, two proteins of sizes 50 kDa and 70 kDa co-eluted with CPE, suggesting an association (216-217). However, whether these two proteins served as functional receptors was not proven. It was not until the late 1990's that Katahira et al. utilized expression cloning to identify the receptor for CPE, which they termed CPE-R (82). In this study, Katahira et al. cloned a cDNA library from the CPE-sensitive Vero cell line into a CPE-resistant cell line, L929 cells. A C-terminal binding fragment of CPE (discussed below) was biotinylated to identify L929 clones that successfully bound CPE. After purifying DNA from binding-capable L929 clones, sequence analysis identified an open reading frame of 630 bp encoding a 209 amino acid protein with a molecular mass of 22,029 Da with strong homology to

the androgen withdrawal apoptosis protein, RVP1. The *RVP1* gene is expressed in ventral prostate cells after withdrawal of androgen from the culture medium *in vitro* or castration *in vivo* (21). How this related to CPE action was somewhat confusing, but after further sequence analysis, the CPE-R was determined to be a member of the multi-gene family of four transmembrane proteins, named claudins, an integral component of the tight junction (199).

The tight junction (TJ) is an integral structure of epithelial and endothelial cells that serves to form a seal between adjacent cells and form a link to the actin cytoskeleton (11). TJs are the most apical structure in the junctional complex, forming a network of mesh-like intramembrane strands that encircle the entire cell. The first function of the TJ, referred to as its *gate* function, is to act as a selective barrier, regulating the paracellular transport of ions, solutes, and water. The second functional role of the TJ is to segregate the diffusion of proteins and lipids along the plasma membrane. This property, known as the *fence* function of TJs, gives rise to the distinct compartments of the apical and basolateral membranes. Both of these functions of the TJ serve to separate the lumen and its contents from the underlying tissue. In addition to these structural roles, recent research is now beginning to highlight the importance of TJ proteins in intracellular signaling pathways involved in cell proliferation and differentiation (11).

The main components important for forming the backbone of the TJ are the integral membrane proteins: claudins, occludin, tricellulin, and JAM (junctional adhesion molecule) (11). The claudin superfamily of proteins consists of 24 members with molecular weights of 20-27 kDa, and a predicted tetraspan structure containing a short N-terminal intracellular domain, two extracellular loop domains (the first being larger than the second), and a long cytoplasmic C-terminal tail (Fig. 1.2A). The C-terminal tail contains a PDZ domain which allows for the interaction of claudin with ZO-1, ZO-2, and ZO-3 (79), scaffolding proteins which bind actin,

thus, linking the tight junction to the actin cytoskeleton. The extracellular loops (ECLs) interact with the ECLs of the claudins present in adjacent cells. It is this interaction between ECLs that gives the charge selective (gate) properties of claudin strands. Examination of the first ECL reveals a high number of charged amino acids, which, when paired with an apposing ECL, forms an ion selective pore that regulates the paracellular pathway of ions, solutes, and water (204) (Fig. 1.2B). A functional role for the second ECL in the TJ has yet to be described.

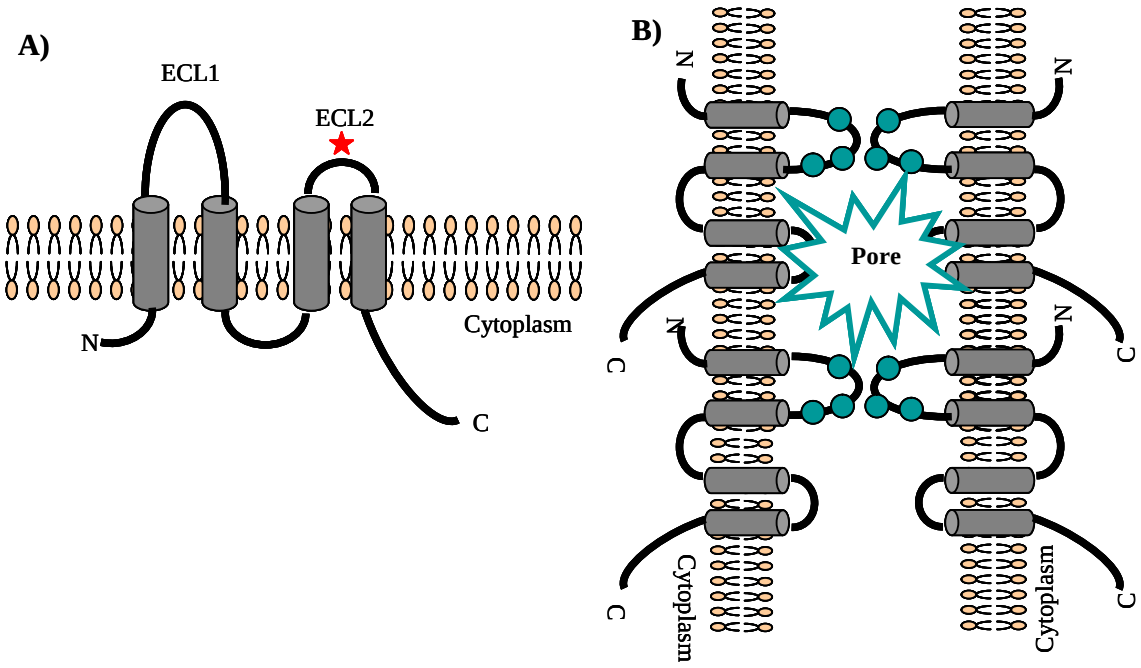

Figure 1.2 Proposed Claudin Structure.
A) Illustration shows the proposed 4 transmembrane-spanning structure of claudin, with short N-terminal and long C-terminal intracellular sequences and 2 extracellular loops (ECL1 and ECL2). The red star indicates the fproposed region of the ECL2 important for CPE binding. B) Charged residues of the ECL1 are represented by blue circles. Claudins form continuous strands with apposing cells, allowing for electrostatic interactions between ECL1s forming an ion-selective pore.

Upon further characterization, it was discovered that different affinities among CPE and the claudin (cldn) family members exists. For instance, CPE was shown to bind to claudin-3 and -4 with high affinity, but failed to bind claudin-1 or -2 (187). Question of the binding capabilities of the other claudin members was further addressed by examining the sensitivity of

transfecting a naturally CPE-insensitive cell line with different claudins, and revealed a group of binding capable claudins with varying degrees of affinity (cldn-6, -7, -8, and -14), and a group of non-binding claudins (cldn-5 and -10) (52). This same study also shed light onto the region of the claudin molecule which is responsible for binding of CPE. When chimeras containing the N-terminal half of cldn-1 and the C-terminal half of cldn-3 (and vice versa) were transfected into CPE-insensitive cells, only the cells expressing the construct with the C-terminal half of cldn-3 became sensitive to CPE treatment. Considering that the N-terminal half contains the first ECL while the C-terminal half contains the second ECL, it was concluded that the second ECL is the region most likely to be important for CPE binding.

Recent work has addressed the ability of the second ECL to bind CPE, and a more detailed analysis of the region important for binding has been investigated. When the amino acid sequences of binding-capable claudins and non-binding claudins are aligned (Fig. 1.3), a striking pattern is seen. Most of the residues in the second ECL are highly conserved, but at amino acid position 149 all of the binding-capable claudins contain an Asparagine (Asn, N) residue, whereas, non-binding claudins have either an Aspartic Acid (Asp, D) or Serine (Ser, S) at this residue. Robertson et al. investigated the significance of this difference by performing site-directed mutagenesis and changing the N to D in cldn-3 (binding) or the D to N in cldn-1 (non-binding) (157). After transfection of these mutated claudins into naturally CPE-insensitive rat fibroblast cells, cldn-3_{N149D} –expressing cells remained resistant to CPE treatment, while cldn-1_{D149N} –expressing cells displayed cytotoxic effects after CPE treatment. In addition, when CPE was pre-incubated with a peptide corresponding to the sequence of the second ECL of cldn-3, the ability of CPE to kill Caco-2 cells was inhibited. However, CPE cytotoxicity was not inhibited when CPE was pre-incubated with a peptide encoding the second ECL of cldn-2. The results

from this study confirm the importance of the second ECL in CPE binding, but more importantly identify one key residue (N149) that confers binding of claudin to CPE.

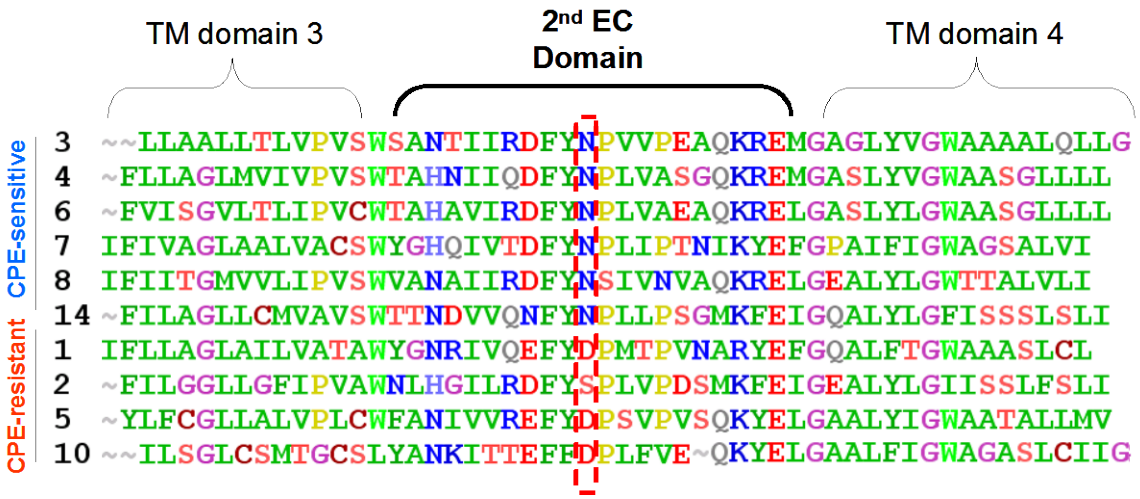

Figure 1.3 Alignment of CPE-sensitive and CPE-resistant Claudins.
Amino acid alignment of claudins capable of binding CPE (cldn-3, -4, -6, -7, -8, -14) vs. claudins unable to bind CPE (cldn-1, -2, -5, -10) reveals a pattern in which all CPE-sensitive claudins contain an asparagine (N) in the 2nd extracellular domain, while CPE-resistant claudins have either aspartic acid (D) or serine (S).

1.3.4.2 Formation of the Small Complex

After binding of CPE to its receptor, claudin, the toxin rapidly localizes into an SDS-sensitive complex of ~90 kDa on the surface of the target membrane (214). This complex, termed Small Complex (SC), readily forms at 4°C, but confers no cytotoxicity to CPE-treated cells (122). Although CPE becomes tightly associated with the SC, likely through a post-binding conformational change, this complex does not seem to insert into the membrane as it has been shown that the SC is sensitive treatment with proteases (213). The protein composition of the

SC has recently been investigated (158). Through immunoprecipitation (IP) and electroelution (EE) studies, cldn-4 was shown to be present within the SC. This was not a surprising finding given cldn-4 serves as a receptor for CPE. However, the IP and EE studies also found cldn-1 and -2 localized within the SC, an interesting result considering these claudins are not functional receptors. Prior experiments showed the presence of a 50 kDa protein in the SC (214), but it now seems that this probably represents aggregation of claudins which is an inherent characteristic of these proteins (133), however, the presence of a 50 kDa protein as a CPE co-receptor cannot be ruled out.

1.3.4.3 Formation of the Pre-Pore and Large Complexes

Although not sufficient for CPE-induced cytotoxicity, SC formation is the first step required for these effects. At 37°C, formation of the SC is a transitory step in which there is a rapid association with additional proteins to form a complex that is SDS-resistant and resolves with a higher molecular weight. Recent studies have demonstrated that after the formation of the SC there is a rapid olgimerization event where there is formation of a pre-pore complex on the surface of target membranes (158, 184). The pre-pore was shown to remain loosely attached to the membrane as it was highly susceptible to Pronase treatment. The pre-pore subsequently inserts into the membrane where it then forms a complex that is resistant to protease treatment with Pronase (213). Despite its insertion of the membrane, at least part of this complex remains exposed on the surface due to the fact that anti-CPE antibodies can recognize this complex (88). Initial studies using CHAPS to extract the complex from CPE-treated BBMs demonstrated that this larger complex was ~160 kDa in size, and its formation was dependent on temperature, e.g. this large complex forms at 24°C and 37°C, but not at 4°C (122, 217). This temperature dependence suggested the requirement of membrane fluidity for proper large complex formation.

Additionally, these studies revealed that the formation of the large complex coincided with the onset of CPE-induced cytotoxicity. Later experiments resolved the 160 kDa complex into two complexes of molecular weights of ~155 kDa and ~200 kDa on SDS-PAGE when extracted from the intestinal epithelial cell line, Caco-2 (179). Through EE and IP experiments, it was shown that the ~200 kDa complex contained the 65 kDa TJ protein occludin, possibly accounting for the increase in molecular weight of the ~155 kDa complex. This suggests that the ~155 kDa complex is possibly a precursor for the ~200 kDa complex (179). It should be noted, however, that the formation of the ~155 kDa complex is sufficient for CPE-induced cytotoxicity and can occur in the absence of the ~200 kDa complex (178). Additionally, claudin-deficient rat fibroblasts transfected to express occludin remain insensitive to CPE treatment, suggesting that occludin does not serve as a functional receptor for CPE action, and only becomes associated with the ~200 kDa through indirect associations (179). Up to this point, isolation of the ~200 kDa complex in the absence of ~155 kDa complex formation has not been achieved; therefore, the exact function of the ~200 kDa has yet to be determined. However, one consequence of the formation of this occludin-containing complex is the coincident removal from the TJ and internalization of occludin (179), which is most likely detrimental to the structure and function of the TJ barrier.

Just as was investigated for the SC, the presence of different claudins within the large complexes was examined. Similar to the findings for SC, both binding-proficient claudins (e.g. cldn-4) and non-receptor claudins (e.g. cldn-1 and -2) were found to be localized within the ~155 kDa and ~200 kDa complexes (158). As alluded to above, by using heteromeric gel shift analysis, this study also revealed that at least 6 copies of CPE were present within these complexes, suggestive of a hexamerization event. As a result, the nomenclature has been

updated where the ~155 kDa complex is now referred to as the CPE Hexamer-1 (CH-1) and the ~200 kDa complex is now termed the CPE Hexamer-2 (CH-2). When considering the number of CPE molecules and the varying number of receptor and non-receptor claudins present within these large complexes, a reassessment of the sizes of these complexes was prompted. Using gel filtration and Ferguson plot analysis, the sizes of the CH-1 and CH-2 were resized to be much larger than originally predicted with molecular weights of ~450 and ~600 kDa, respectively (158).

1.3.4.4 Mechanism of CPE-induced Cell Death

As mentioned above, concurrent with formation of the CH-1 complex, CPE-induced cytotoxicity is observed. Substantial evidence suggests the CH-1 complex serves as the functional pore of CPE action, corresponding to permeability alterations in target cells, leading to changes in water and ion fluxes. These membrane permeability alterations were characterized in Vero cells using radiolabeled markers of varying sizes (119). This study demonstrated that the CPE pores were large enough to allow molecules of up to 3000 Da to pass through, but not RNA (molecular size of 25000 Da). Additionally, the onset of the change in permeability occurred within 15 minutes of CPE treatment and was dose-dependent. Osmotic stabilizers such as sucrose, PEG, dextran, and BSA were able to protect against CPE-induced changes in cell permeability (121). The formation of functional pores in the membranes of Vero cells results in the complete inhibition of DNA, RNA, and macromolecule synthesis, as well as the reversal of glucose transport, within 30 minutes of CPE treatment (106, 120). This inhibition has been shown to be directly associated with the permeability alterations caused by CPE treatment (77).

Patch-clamp studies revealed the presence of ion-permeable channels within lipid bilayers treated with CPE (191). Multiple studies have investigated the importance of ions,

specifically Ca^{2+}, in the action of CPE (57, 76, 117, 190). Collectively, these studies determined that CPE binding, SC and large complex formation, small molecule membrane permeability alterations, and macromolecule synthesis inhibition are independent of the presence of extracellular Ca^{2+}. Conversely, morphologic damage, large molecule permeability alterations, cell lysis, villi tip desquamation, and fluid loss were shown to rely on the presence of extracellular Ca^{2+}.

Recently, the relationship between Ca^{2+} and CPE-induced cell death was further explored at the molecular level (31-32). Chakrabarti et al. investigated the dose-dependent effects of CPE treatment on the activation of cell death pathways (32). In this study, it was found that in the case of a low dose (1 μg/ml), CPE caused morphological and biochemical changes in Caco-2 cells characteristic of apoptosis. However, in the case of a high CPE dose (10 μg/ml), Caco-2 cells were killed in a morphological and caspase-independent mechanism characteristic of oncosis. This dose-dependent relationship of cell death was further explored, correlating these effects with the role of CPE-induced Ca^{2+} influx in Caco-2 cells (31). It was observed that the dose of CPE (low vs. high) correlated with the level of Ca^{2+} entering treated cells. For instance, low doses of CPE caused a mild influx of Ca^{2+}, while a high dose of CPE resulted in a strong influx of Ca^{2+}. The level of Ca^{2+} influx influenced the cell death pathway activated, and it was shown that the Ca^{2+}-dependent, cysteine protease, calpain, was differentially activated by the low and high CPE doses. Therefore, calpain is hypothesized to be implicated in determining which pathway, apoptosis or oncosis, is activated. The observed cell death characteristics are summarized in Table 1.2.

Table 1.2 Characteristics of CPE-induced Cell Death of Caco-2 Cells at Low (1 µg/ml) and High (10 µg/ml) Doses

Characteristic	CPE Dose	
	Low	High
Ca^{2+} Influx	Mild	Strong
Calpain Activation	Mild	Strong
Caspase 3/7 Activation	Yes[a]	No
Mitochondrial Depolarization	Yes[b]	No
Cytochrome *c* Release	Yes[b]	No
Cell Death Pathway	Apoptosis	Oncosis
Morphology	Cell rounding, membrane budding[a]	Cell swelling, membrane blebbing[c]
DNA Cleavage	Ladder-like[a]	Shearing[c]
Nuclear Condensation	Yes[a]	No

[a]Observation seen after 1 h of CPE treatment
[b]Observation seen after 15 min of CPE treatment
[c]Observation seen after 30 min of CPE treatment

1.3.5 CPE Structure/Function

1.3.5.1 N-terminal Activation Domain

Upon examination of the primary sequence encoded by the *cpe* gene, one can find multiple sites of protease cleavage, however, only two active cleavage sites are present. At amino acid position 25 there is a trypsin cleavage site, followed by a chymotrypsin site at amino acid position 36. Upon enzymatic cleavage with trypsin, purified CPE releases a peptide fragment of approximately 4000 Da. This results in a 3-fold increase in the activity of CPE, as first reported by Granum et al. (59). This result was subsequently confirmed in which trypsin-cleaved CPE showed 2-3 times more ^{86}Rb release than the native toxin, despite no change in the level of CPE binding (67). Chymotrypsin treatment results in the cleavage of 36 amino acids from the N-terminus, and this processing increases CPE activity on Vero cells by 3.2-fold (58). The role of the N-terminal activation domain is hypothesized to be important in the intestine of humans

during type A food poisoning, where trypsin and chymotrypsin, as well as other proteases, may serve to activate CPE, creating a more potent toxin.

1.3.5.2 N-terminal Cytotoxicity Domain

Initial studies indicating the importance of the N-terminal half of the CPE molecule in cytotoxicity were performed in which a CPE fragment encompassing amino acid residues 171-319 proved to be non-cytotoxic to Vero cells, yet retained binding activity (67). The role of the N-terminus was further explored in a study using deletion analysis to create recombinant N-terminal CPE fragments (87), as illustrated in Fig. 1.4. Findings from this study demonstrated that the first 44 amino acids can be removed without any deleterious effect on cytotoxicity; however, removal of the first 52 amino acids produces a non-cytotoxic fragment. Both constructs had full binding capability, however, the fragment lacking amino acids 1-52 could not form large complex. These findings suggested an essential role of the region between residues 45 and 53 required for CPE cytotoxicity. Random mutagenesis of the *cpe* gene provided additional insight into the role of the N-terminus in large complex formation and CPE-induced cytotoxicity (86). Two point mutations, G49D and S59L, resulted in the complete attenuation of cytotoxicity on BBMs, despite being fully binding capable. Additionally, these mutations were able form SC, but could not form large complex, further supporting the role of the N-terminal region in formation of the large complex.

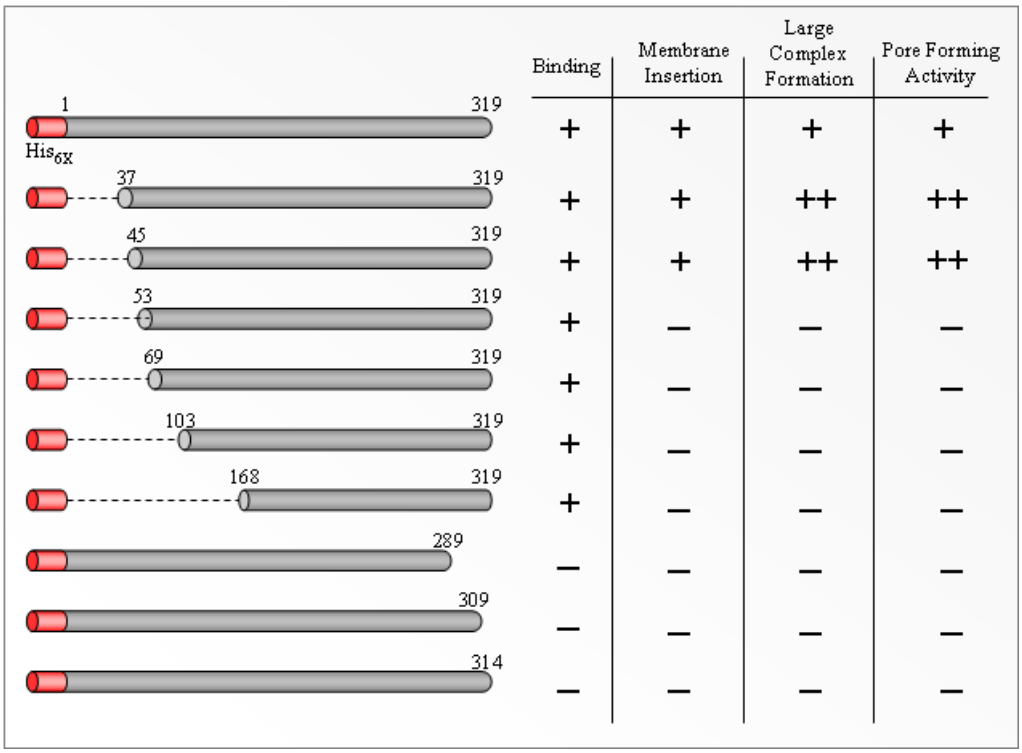

Figure 1.4 Deletion Analysis of rCPE constructs

Further investigation of the N-terminal cytotoxicity region employed site-directed mutagenesis to fine-map this region and its amino acid residues (182). Each of the residues within the 45-53 region was replaced individually by alanine-scanning mutagenesis, and the effect on binding, complex formation, and cytotoxicity was measured. One point mutant, D48A, showed a complete defect in the ability to form large complex and induce cytotoxicity, as quantified by ^{86}Rb release. The D48A mutant, however, still retained full binding and SC formation ability. When the D48 residue was replaced by either an E or N, these variants still had the characteristics of the D48A variant, indicating both size and charge are important for this residue's ability to confer cytotoxicity and large complex formation. A second variant, I51A, also proved to be deficient in large complex and cytotoxicity. Other mutants, G47, G49, and W50, displayed atypical large complex formation, yet retained the ability to be toxic. These

results indicated the region 47-51 to be particular important for large complex formation and cytotoxicity. Additionally, it is hypothesized that this region serves as a latch domain to allow the interaction of CPE molecules during oligomerization, a structural domain similarly seen in the pore-forming alpha-hemolysin from *Staphylococcus aureus* (184-185).

1.3.5.3 C-terminal Binding Domain

The first step required for CPE action is binding to the membrane surface of target cells. The $CPE_{171-319}$ variant used in the study by Hanna et al., as mentioned above, not only revealed the importance of the N-terminal domain for cytotoxicity, but also demonstrated the importance of the C-terminal half of the CPE molecule for binding (67). Further mapping of the C-terminal region important for binding, showed that a short fragment of $CPE_{290-319}$ recombinantly expressed in *E. coli* was able to compete for binding against native CPE on BBMs as well as inhibit CPE-induced cytotoxicity of Vero cells (66). Moreover, a synthetic peptide corresponding to amino acids 290-319 of CPE was also able to specifically block CPE binding and competitively inhibit cytotoxicity. Additionally, when mice were immunized with the $CPE_{290-319}$ synthetic peptide, neutralizing antibodies were produced, adding more support for this region's importance in CPE binding (132). Further deletion mutagenesis revealed that even when only the last 5 amino acids of CPE are removed, toxin binding is inhibited (87).

Several recent studies have investigated the use of C-terminal CPE (C-CPE) derivatives as modulators of claudins, which have given further insight into the amino acids of the C-terminal domain essential for binding. The first of these studies showed that treatment of Caco-2 cells with C-CPE ($CPE_{184-319}$) decreased transepithelial electrical resistance (TEER), but deletion of the C-terminal 16 amino acids of C-CPE reversed this decrease in TEER (193). Alanine-scanning mutagenesis of the three tyrosines in this 16 residue region (Y306, Y310, and Y312)

revealed these to be important for binding, TEER, and intestinal absorption, with Y306 being most crucial (68). Upon further analysis of Y306, replacing Y with W or F had no reduced effects on binding, however, a Y306K mutant greatly reduced binding and TEER (41). This finding indicated aromatic and hydrophobic properties, but not hydrogen bonding potential, influence the binding of C-CPE to claudin. An additional L315A substitution was found to decrease modulation of the TJ as compared to C-CPE, and when coupled with the Y360A variant, the ability to bind claudin, modulate TEER, and enhance intestinal absorption was fully lost (192). Collectively, these results confirm the importance of the C-terminus in CPE binding, and narrow down the important residues to Y306 and L315. Information from these studies can aid in the development and design of claudin modulators useful for increasing drug absorption in the intestine (see below).

Another recent endeavor was undertaken to solve the crystal structure of CPE (205). A C-CPE fragment representing a 14 kDa peptide corresponding to residues 194-319 was used for crystallization. At a resolution of 1.75 Å, the solved C-terminal structure reveals a nine-stranded β sandwich with anti-parallel strands, as shown in Fig. 1.5. Interestingly, a loop spanning residues K304-Y312 lies outside of the β sandwich, and contains the three tyrosine residues, described above, important for CPE binding. As mentioned previously, CPE lacks nucleotide or amino acid homology with any other known proteins. However, when this C-CPE structure is compared to other known protein structures, an unappreciated similarity is seen with the collagenase, ColG, from *C. histolyticum* and from members of the Cry family of insecticidal toxins from *Bacillus thuringiensis*. In both cases, as is for CPE, these structures represent the regions that play a role in binding. This CPE structure can aid in designing future mutagenesis

studies to determine important CPE:claudin interactions. Current research is aimed at solving the full-length CPE protein, as well as the crystal structure of CPE bound to its receptor, claudin.

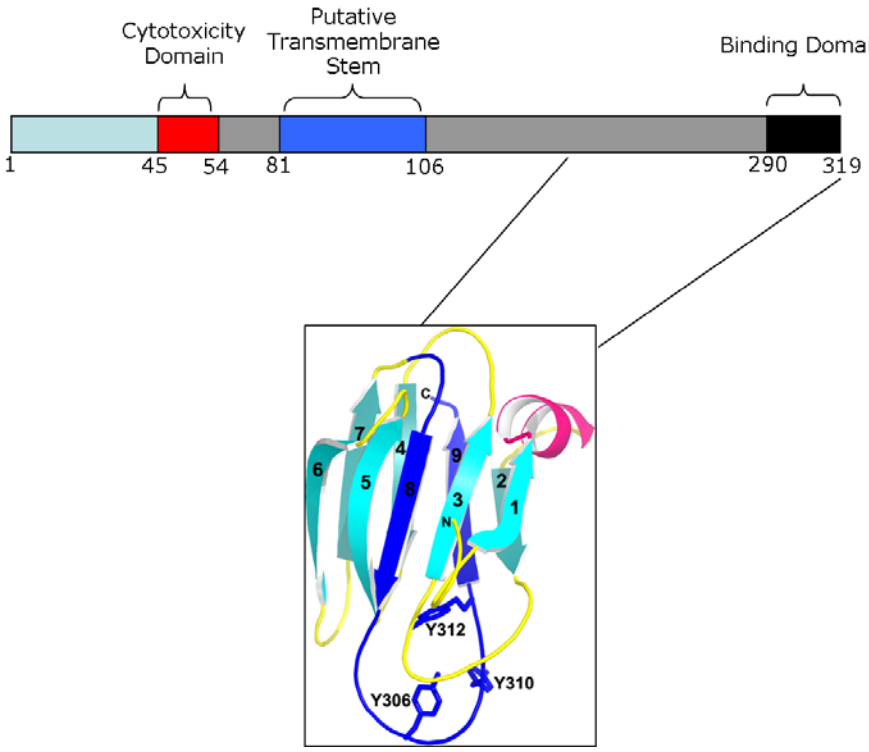

Figure 1.5 Functional Domain Mapping and C-CPE$_{194-319}$ Structure
Map illustrates positions of the N-terminal Cytotoxicity Domain, Putative Transmembrane Stem Domain, and C-terminal Binding Domain. Structure shows β sandwich with anti-parallel strands. Binding loop (dark blue) protrudes from the β sandwich, exposing tyrosines previously shown to be important for binding. Modified from (205).

1.3.5.4 Putative Transmembrane Stem Domain

Examination of the primary sequence of the CPE protein reveals a region (residues 81-106) with a striking pattern of alternating residues of side chain polarity. This alternating pattern is reminiscent of the transmembrane domains of the β-barrel family of pore-forming toxins in which β-hairpins from toxin monomers insert into the membrane after oligomerization to form a functional pore (196, 200). When amino acids 81-106 are deleted from CPE, this variant (TM1)

cannot form functional pores within the membrane and cannot elicit cytotoxicity of Caco-2 cells (184). Interestingly, however, the TM1 mutant can still form the CH-1 complex (but not CH-2), but the CH-1 complex formed appears to be significantly more sensitive to proteases and dissociation from the membrane, suggesting it is in an unstable, exposed, and uninserted state. These findings suggest the TM1 domain is a putative transmembrane stem domain important for insertion into the membrane, and deletion of this domain results in the stalling of the CPE prepore on the exposed plasma membrane.

1.3.6 Practical Applications of CPE and CPE Derivatives

1.3.6.1 CPE as a Cancer Therapeutic

The ability of CPE to bind certain claudins, but not others, has sparked significance interest in the cancer field since the observation that cldn-3 and-4 (CPE receptors) are overexpressed in a number of different cancers. Specifically, claudins have been shown to be dysregulated in many pancreatic, prostrate, breast, ovarian, and uterine cancers (108, 111, 131, 143, 163) (see Table 1.3 for a more extensive list). The role of claudins and how their expression in related to cancer progression is an area of active research. One study investigated the mechanism of this dysregulation in ovarian cancer, and found a possible link between the overexpression of cldn-4 and a decreased methylation state of the protein (108). Gene regulation by growth factors such as hepatocyte growth factor and epidermal growth factor have been implicated as additional mechanisms of differential claudin expression in cancer (90, 177), as well as exposure to various cytokines (65, 83). Clinically speaking, aberrant expression of claudins may lead to cancer progression and metastasis by reducing cell adhesion and increasing tumor motility (3).

Table 1.3 Differential Expression of Claudins in Cancers

Claudins Upregulated in Cancers		Claudins Downregulated in Cancers	
Cancer Type	**Claudins Dysregulated**	**Cancer Type**	**Claudins Dysregulated**
Breast	3, 4	Breast	1, 2, 4, 7
Prostate	1, 3, 4, 7	Prostrate	2, 5
Ovarian	1, 3, 4, 5, 7, 16	Head and Neck	7
Pancreatic	1, 4	Glioblastoma	1
Colon	1, 12	Colon	8
Gastric	1,3, 4, 5, 7	Gastric	4, 18
Thyroid	1, 4, 7, 10	Thyroid	1
Hepatocellular	1, 2, 7, 10	Hepatocellular	3, 4, 7
Cervical	1, 7	Melanoma	1
Renal	1, 3, 4, 7, 8	Renal	7
Lung	1, 3, 4, 5	Lung	1, 5

Information compiled from (148) and (89).

In 2001, Michl et al. first investigated the potential of CPE as a tumor-targeting therapeutic (131). The authors demonstrated a significant overexpression of cldn-4 in many pancreatic and colon carcinoma tissues and a dose-dependent killing of a pancreatic cancer cell line when treated with CPE. Additionally, when injected directly into a xenograft tumor in nude mice, it was observed that CPE caused the inhibition of tumor growth and the induction of tumor necrosis. Despite claudin expression in various other tissues, it was important to note that mice harboring tumors that were injected with CPE did not experience any signs of toxicity. Similar studies have been performed with breast and uterine cancer tissues and cell lines, as well as chemotherapy-resistant ovarian cancer, and in all cases, CPE was shown to either halt tumor growth or actually, significantly decrease tumor size (92, 163-164).

One particularly intriguing use of CPE was a study in which CPE was used as a targeted therapeutic for brain metastasis (91). By immunohistochemical analysis, it was observed that expression of cldn-3 and -4 were highly expressed in brain metastases originating from breast,

lung, and colon carcinomas. However, cldn-3 and -4 expression was absent from the surrounding normal brain tissue, as well as all regions of the CNS. Visualized by bioluminescent imaging, intracranial administration of CPE significantly inhibited tumor growth by 10-fold and increased mouse survival. Amazingly, there was no noticeable local or systemic toxicity associated with the intracranial CPE delivery method.

Recent research has focused on use of CPE fusion constructs as cancer-targeting molecules. One such study fused tumor necrosis factor (TNF) to C-$CPE_{290-319}$ and tested its effect on ovarian cancers expressing high levels of cldn-3 and -4 (224). TNF was successfully delivered to the cytosol, and cytotoxicity was observed and correlated with the level of claudin expression, as shown by shRNA knockdown of cldn-3 or -4 which inhibited CPE-TNF killing. The investigators, however, did not show the delivery or cytolysis by their construct in a tumor experimental model. Saeki et al. constructed a C-CPE fusion with the protein synthesis inhibitory factor (PSIF) from *Pseudomonas aeruginosa*, and demonstrated that intratumoral injection of C-CPE-PSIF significantly suppressed tumor growth, resulting in 36% of the tumor volume (161).

These studies described illustrate the promising potential for CPE and CPE derivatives use in cancer therapeutics. Most, if not all, of these studies are using a tumor model in which CPE is injected directly into the tumor, however. In many cases, this would not be plausible in a clinical setting, and therefore, additional research is needed to develop a tumor-targeting CPE molecule for these purposes.

1.3.6.2 CPE Derivatives in Drug Delivery

As described in detail above, it is well recognized that the C-terminus of CPE is responsible for binding of the toxin to receptor claudins. Additionally, numerous reports have shown that C-

terminal CPE fragments are still capable of binding target cells, yet do not induce cytopathic effects. However, C-CPE binding to cells does have some significant effects. For one, it has been shown that C-CPE binding to MDCK cells results in the removal of cldn-4, but not cldn-1, from the TJ, and its possible internalization and degredation (187). As a result, TEER is drastically reduced in MDCK cells, a result also confirmed in Caco-2 cells (193). These results indicate that C-CPE has the ability to alter the overall structure and function of the TJ, loosening the contacts between adjacent cells and allowing larger molecules to pass from apical to basolateral sides of cells. This observation has led to an exciting area of CPE research in which CPE derivatives are being used as methods to increase drug delivery across the epithelial barrier.

An initial study examined the use of C-CPE as a claudin modulator allowing the movement of large molecules across the epithelial barrier as a means of enhanced drug absorption (93). This study used an *in vivo* rat loop assay to study the effects of C-CPE on the absorption of dextrans. In a dose-dependent manner, C-CPE was shown to enhance the absorption of dextrans of up to 20 kDa in size. Importantly, C-CPE was shown to be 400 times more potent at enhancing dextran absorption than capric acid, a clinically used enhancer of absorption. Additionally, no intestinal damaged in the rats was observed with C-CPE treatment. The enhanced absorption was related to the removal of claudin from the TJ and required binding to claudin (93), however, binding was not sufficient for this effect. When the N-terminal 36 amino acids of C-CPE were deleted, the enhanced dextran absorption effect was greatly reduced (116).

1.4 SPECIFIC AIMS

1.4.1 Specific Aim 1

The first aim of this project is to explore the role of the cholesterol/sphingolipid-rich membrane microdomains, known as lipid rafts, in the mechanism of action of CPE. The role of lipid rafts has been well established in the action of many bacterial pore-forming toxins, as well as many clostridial toxins. These membrane raft domains serve as a platform for toxin binding, oligomerization, and insertion of toxin complexes in target cell membranes. Therefore, considering the pore-forming activity of CPE, it is hypothesized that CPE may interact with lipid rafts. To test this hypothesis lipid rafts will be disrupted by perturbing cholesterol levels in cells and assessing the effect on CPE complex formation and cytotoxicity.

1.4.2 Specific Aim 2

Claudins serve as receptors for CPE; however, CPE cannot bind to all members of the claudin family. Recently, it has been discovered that even non-receptor claudins can become associated with CPE complexes. Through immunoprecipitation experiments, CPE has been shown to also interact with the tight junction protein, occludin; and occludin has also been shown to be directly located within the CH-2 complex. When one considers the complex architecture of the TJ and the close interactions between TJ proteins, one can hypothesize that these are most likely not the only cellular proteins making up the toxin complexes. It is the second aim of this project, therefore, to determine what cellular components, in addition to claudin and occludin, make up the CPE complexes. This aim will be accomplished by isolating toxin complexes and utilizing

mass spectrometry to identify cellular proteins located within each complex. Electroelution and immunoprecipitation will be employed to confirm identified proteins.

1.4.3 Specific Aim 3

Upon histological assessment of CPE damage of the intestinal epithelia in animal models, one can visualize the infiltration of inflammatory cells, suggesting inflammatory events are occurring. Additionally, *in vitro* data suggests that CPE can activate cell death pathways that are pro-inflammatory (e.g. oncosis). Previous studies have indicated CPE can cause the systemic induction of inflammatory cytokines in animal models, but the role of cytokines in the area of local CPE damage (i.e. in the intestine) has not been investigated. Despite the numerous reports detailing the need for CPE complex formation, the formation of CPE complexes has never been demonstrated as a contributor to CPE action *in vivo*. Moreover, recent epidemiological studies have implicated type A food poisoning in the deaths of a high rate of individuals in mental health care facilities. It was concluded that these deaths were attributed to the ability of CPE to gain access to the circulation. The goal of Aim 3, therefore, is to develop a mouse model that enables us to mimic CPE-induced lethality where CPE complex formation in the intestine induces damage that allows CPE to gain access to the circulation. Furthermore, the development of this mouse model will allow us to measure the local cytokine production profile within the intestine during CPE challenge.

2.0 THE ROLE OF LIPID RAFTS IN THE ACTION OF *C. PERFRINGENS* ENTEROTOXIN

The data presented in this Chapter has been published as original work in **Caserta JA, Hale ML, Popoff MR, Stiles BG, McClane BA**. 2008. Evidence that membrane rafts are not required for the action of *Clostridium perfringens* enterotoxin. Infect Immun. 76:5677-85.

2.1 INTRODUCTION AND RATIONALE

2.1.1 Bacterial Pore-Forming Toxins

Despite the evident lack of sequence homology of CPE with other known bacterial toxins, there does exist significant structural homology with the family of pore-forming toxins. The plasma membrane is a dynamic and complex structure that serves multiple functions in the eukaryotic cell. Thus, the plasma membrane has proven to be an attractive target for bacteria and their products and toxins. Of the many toxins produced by bacteria, pore-forming toxins (PFTs) are the most numerous group of toxins, compromising 30% of all bacterial toxins described. PFTs are classified into two groups based on the structural components responsible for causing pore formation (78). The first class of PFTs, α-PFTs, employ alpha helices to span the lipid bilayer, and include examples such as *E. coli* colicins (29), actinoporins produced by sea anemones (95),

and the insecticidal Cry family from *Bacillus* (151). The other class of PFTs is the β-barrel PFTs (β-PFTs) which contain amphipathic β-strands that combine in multiprotein complexes to form a β-barrel pore. Well known examples of β-PFTs include *Staphylococcus aureus* α-toxin (185), aerolysin (48), protective antigen from Anthrax toxin (222), and the large family of cholesterol-dependent cytolysins (CDCs) (200). Despite the structural differences between various PFTs, most have a common mechanism of action (Fig. 2.1). The first step is secretion of the toxin in a monomer form and diffusion towards the target membrane. Step 2 involves binding of the toxin monomer to a specific receptor on the surface of the membrane of target cells. Third, monomers associate with one another to form an oligomeric prepore on the surface of the membrane, commonly mediated through a latch domain. Lastly, the prepore inserts into the membrane forming the functional pore.

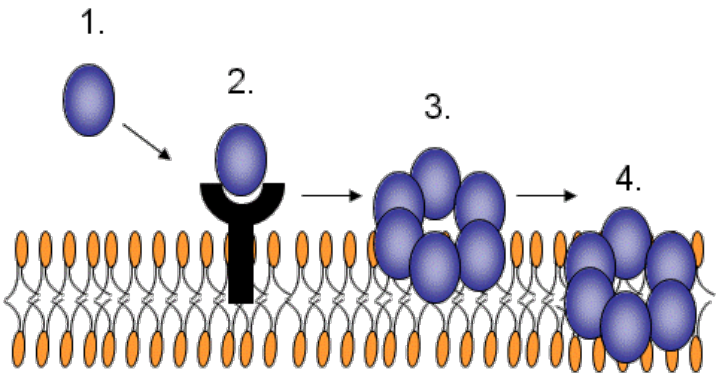

Figure 2.1 Mode of Action by Pore-forming Toxins

2.1.2 Lipid Rafts and Their Role in Bacterial Pathogenesis

When one thinks about the mechanism of pore formation by PFTs, it is apparent that the key, rate-limiting step is that of oligomerization, or the aggregation of multiple monomers and their associated receptors. Bacteria are constantly evolving in order to take advantage of eukaryotic

cells to aid in the action of their products. In the case of bacterial toxins, bacterial have evolved mechanisms to make the oligomerization process more efficient. Many bacteria and their toxins have been shown to utilize host cell lipid rafts as a means to aid in their pathogenesis, relying of these domains for binding, internalization/invasion, and evasion (70, 98, 115, 208).

Lipid rafts, also known as detergent-resistant membranes (DRMs), and recently redefined as membrane rafts, are small (10-200 nm), highly specialized and dynamic domains within the lipid bilayer that are rich in cholesterol, sphingolipids and serve to compartmentalize cellular processes (152). Although small, these raft domains have the ability to coalesce into larger domains allowing for the clustering of similar proteins within the microdomain, while excluding other non-raft-associated proteins. This clustering serves as a platform for compartmentalizing cellular processes such as signal transduction, protein sorting, and membrane trafficking (23).

Glycerophospholipids with long, fully saturated acyl chains make up the composition of raft domains, allowing tight packing of these lipids. Additionally, rafts are highly enriched in sphingolipids which laterally associate with one another through hydrogen bonding of head groups. The large head groups of sphingolipids and glycosphingolipids results in a void that allows cholesterol to preferentially interdigitate within the spaces of the fatty acid chains serving as a glue to maintain the structure and function of these domains (175). Enrichment of cholesterol within lipid rafts results in a liquid-ordered (L_o) state with decreased fluidity. The result is a condensed assemblage separated from the surrounding disordered unsaturated glycerophospholipid environment (i.e. non-rafts). Additionally, an early observation was made that membrane rafts are resistant to non-ionic (Triton X-100) detergent extraction at 4°C. With this detergent insolubility and the high lipid content, which allows these domains to float on sucrose density gradients, a method of lipid raft isolation was established (24). Much of the

criticism of the lipid raft theory argues that DRMs extracted at 4°C are just artifacts and are not isolations of pre-existing structures (22). However, it has been shown recently that membranes have the capacity to partition into raft domains at physiologic temperature (107).

2.1.3 Rationale

Many pore-forming toxins hijack lipid rafts to aid in toxin binding, oligomerization, and/or pore insertion into membranes of target cells. Similarly, *C. perfringens* toxins, such as β, ε, ι, and PFO (64, 137, 141-142, 209), have all been shown to require lipid rafts for their action. Because CPE shares structural and functional aspects of these toxins, it is hypothesized that CPE may also require lipid raft domains for its action.

2.2 MATERIALS AND METHODS

2.2.1 Materials

CPE was purified to homogeneity from strain NCTC 8239, as described previously (127). Methyl-β-cyclodextrin (MβCD) was purchased from Sigma-Aldrich (St. Louis, MO). Claudin-4 and occludin antibodies were purchased from Invitrogen (Carlsbad, CA). Flotillin-1 antibody was purchased from Santa Cruz Biotechnology (Santa Cruz, CA) and Na^+K^+-ATPase antibody was obtained from Affinity Bioreagents (Golden, CO).

2.2.2 Cell Culture

Caco-2 cells were maintained in Eagle minimal essential medium (Sigma, St. Louis, MO) supplemented with 10% fetal bovine serum (Mediatech, Herndon, Va.), 1% nonessential amino acids (Sigma, St. Louis, MO), 100 U/ml of ampicillin, and 100 μg/ml of streptomycin. All cultures were grown at 37°C with 5% atmospheric CO_2.

2.2.3 Small Complex Formation

Caco-2 cells were seeded into 100 mm dishes (Corning, Corning, NY) and grown to confluency (4-5 days). After treatment with CPE (2.5 μg/ml) in cold (4°C) Hanks' Balanced Salt Solution without Ca^{2+} and Mg^{2+} (iHBSS) for 15 min, the toxin was removed and cells were then washed twice with 10 ml iHBSS. Cells were then gently scraped and centrifuged for 3 min at 1000 x g. Cell pellets were resuspended in 950 μl of TX-100 extraction buffer (see below) and loaded onto sucrose density gradients as described later. Visualization of the SC was acquired by immunoblotting with an anti-CPE antibody, as described below.

2.2.4 CH-1 and CH-2 Complex Formation

Caco-2 cells were seeded into 100 mm dishes (Corning, Corning, NY) at a density of 2.5 x 10^5 cells/ml in 10 ml. Those cultures were then grown to confluency (4-5 days) and treated with 2.5 μg/ml of CPE in warm iHBSS for 60 min at 37°C. After this treatment, cells were washed twice with 10 ml iHBSS, harvested by gentle scraping and centrifuged for 3 min at 1000 x g to pellet material. Cell pellets were washed with 10 ml iHBSS, centrifuged, and resuspended with 950 μl of TX-100 extraction buffer and loaded onto sucrose gradients (see below). Visualization of CH-1 and CH-2 was acquired by Western blot with an anti-CPE antibody, as described below.

2.2.5 Ib Treatment

Caco-2 cells were seeded into 100 mm dishes (Corning, Corning, NY) at a density of 2.5 x 10^5 cells/ml in 10 ml. Cultures were grown to confluency (4-5 days) and treated with 2.0 µg/ml of Ib for 15 min at 37°C.

2.2.6 Cholesterol Depletion

For experiments involving cholesterol depletion, Caco-2 cells were pre-treated with 10 mM MβCD in iHBSS at 37°C. After 60 min of treatment, MβCD was removed and cells washed twice with iHBSS.

2.2.7 Cholesterol Quantitation

The cholesterol content of Caco-2 cells was determined before and after depletion of cholesterol by MβCD treatment using the Amplex Red Cholesterol Assay kit (Invitrogen, Carlsbad, CA), with modifications. Briefly, Caco-2 cell monolayers with or without MβCD treatment (60 min) were washed 2 times, scraped and lysed in 750 µl of the Amplex Red 1X Reaction Buffer. Cells were lysed for 15 min at room temperature and insoluble material was pelleted by centrifugation for 1 min at 13,000 x g. A 50 µl aliquot of supernatant for each sample was transferred to wells of a clear 96-well microtiter plate. A 50 µl aliquot of Amplex Red working solution (cholesterol esterase omitted) was then added to each sample well. Samples were covered and incubated for 30 min at 37°C in the dark. Following this incubation, samples were read using Revelation 4.21 Software (Dynax Technologies) by measuring OD absorbance at 570 nm.

2.2.8 TX-100 Extraction of Caco-2 cells and Sucrose Density Gradient Centifugation

Caco-2 cells treated under the varying conditions explained above were extracted with 950 µl of TX-100 extraction buffer (1% TX-100, 10mM NaF, 25 mM Tris-HCl pH 7.6, 150 mM NaCl, 5 mM EDTA, 30 mM Na-pyrophosphate, 10 mM β-glycerophosphate, 1X Complete Protease Inhibitor Cocktail (Roche)) for 1 h at 4°C. Following this cold TX-100 extraction, lysates were overlayed with 950 µl of an 80% sucrose solution (80% sucrose in 25 mM Tris-HCl pH 7.6, 150 mM NaCl, 5 mM EDTA, 30 mM Na-pyrophosphate, 10 mM β-glycerophosphate). Subsequently, 1.9 ml of a 30% sucrose solution was overlayed on this sample, followed by 950 µl of a 5% sucrose solution. Samples were then spun at 200,000 x g for 18 h in a Beckman XL-90 ultracentrifuge. After centrifugation, twelve 400 µl fractions were collected from the top of the gradient.

2.2.9 Western Blotting

For detection of claudin-4, occludin, flotillin-1, and Na^+K^+-ATPase, each of the twelve gradient fractions were concentrated by TCA precipitation. One-fourth volume (100 µl) of 100% TCA was added to each fraction and incubated on ice for 1 h. Samples were then centrifuged (14,000 x g) for 15 min at 4°C. Pellets were washed twice with 200 µl of ice cold acetone. Those pellets were resuspended in 50 µl of 1X Laemmli Buffer and analyzed by SDS-PAGE, using 10% (for occludin, NaK ATPase) or 12% (for claudin-4, flotillin-1) acrylamide gels. Those separated proteins were transferred to nitrocellulose, and probed with appropriate primary (rabbit anti-claudin-4, mouse anti-occludin, rabbit anti-flotillin-1, or mouse anti-Na^+K^+-ATPase) and secondary antibodies (mouse or rabbit) conjugated with horseradish peroxidase (HRP) (Sigma, St. Louis, MO).

For experiments determining the localization of CPE complexes on sucrose gradients, 50 µl aliquots of each fraction were run on native 6% PAGE gels (for SC) or mixed with 10 µl of 5X Laemmli Buffer were analyzed by SDS-PAGE using 4% acrylamide gels (for CH-1 and CH-2). After electrophoresis, separated proteins were transferred to nitrocellulose, and probed with a rabbit anti-CPE antibody followed by incubation with a goat anti-rabbit antibody conjugated to HRP (Sigma, St. Louis, MO). Densitometry of Western blots was performed using the program Quantity One (BioRad, version 4.6.3).

2.2.10 Trypan Blue Staining

Caco-2 cells were seeded into 35 mm dishes at a density of 5 x 10^4 cells/ml in 2 ml and grown to confluency (4 days). Control and MβCD-treated cells were washed and treated with CPE (2.5µg/ml) for various times. After CPE treatment, cells were harvested by gentle scraping and centrifugation, pellets were then resuspended in 500 µl of 0.4% Trypan Blue Stain (Sigma). Live and dead cells were counted microscopically using a hemocytometer. % Viability was calculated as expressing the number of non-blue (alive) cells over the total number of cells (blue and non-blue).

2.2.11 Formation of CH-1 in Absence of CH-2

For experiments requiring the formation of CH-1 in the absence of appreciable CH-2 complex, a previously described technique was used (158, 178). Caco-2 cells were seeded at a density of 2 x 10^5 cells/ml into two 75 mm Transwell permeable supports (Corning) for each experimental condition (Untreated or CPE-treated). After confluency (5 days), cells were treated apically with

CPE (1.0 μg/ml) for 30 min. After CPE treatment, cells were extracted and subjected to sucrose density gradient centrifugation as described above.

2.3 RESULTS

2.3.1 Detergent Solubility and Raft Localization of CPE Small Complex

To evaluate the involvement of membrane rafts in CPE action, we first investigated whether CPE complexes localize within DRMs. Since rafts are characteristically insoluble in TX-100 when extracted at 4°C (23), a series of sucrose density gradient experiments were performed using cold TX-100 extracts of Caco-2 cells treated with CPE (2.5 μg/ml) for 15 min at 4°C, conditions that allow formation of the ~90 kDa SC without appreciable formation of the CH-1 or CH-2 complexes (122). The formation of the ~90 kDa complex likely represents the interaction of CPE with its receptor, claudin (214, 216). When fractions from the gradient were collected, subjected to Native-PAGE, and Western blotted with an anti-CPE antibody, the CPE SC was localized exclusively within the detergent-soluble fractions (8-12) of the gradient (Fig. 2.2A). The marker protein flotillin-1 was used as a control for raft-associated proteins and, as expected, it predominately migrated towards the top of the gradient, mostly within fractions 2-5 (Fig. 2.2B). In contrast, Na^+K^+-ATPase, a non-raft protein marker (137), was present within the detergent-soluble fractions at the bottom of the gradient (fractions 9-12) (Fig. 2.2B). CPE treatment had no observable effect on the localization of either marker proteins (data not shown).

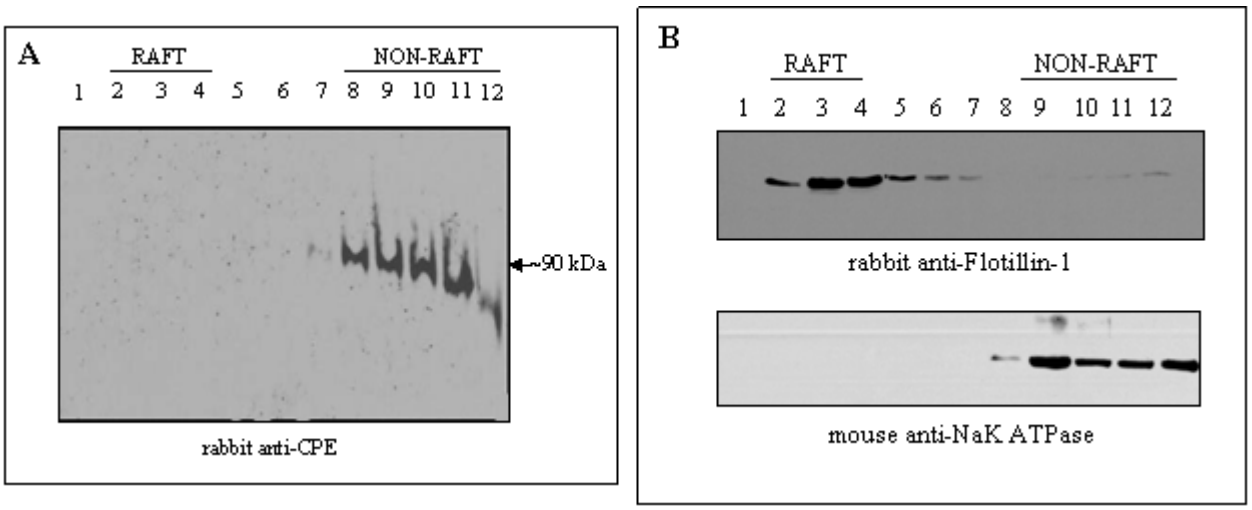

Figure 2.2 The CPE Small Complex (SC) is not localized within lipid rafts.
A) CPE Western blot of sucrose gradient fractions from Caco-2 cells containing SC. After treatment with CPE (2.5 μg/ml) for 15 min at 4°C, Caco-2 cells were cold extracted with TX-100 and subjected to sucrose gradient centrifugation. Gradient fractions were loaded on a 6% Native-PAGE gel, transferred to nitrocellulose, and Western blotted with an anti-CPE antibody. Sucrose gradient fractions are numbered 1-12 at the top of the blot, with fraction 1 being the gradient top and fraction 12 representing the gradient bottom. "Raft" and "Non-Raft" labels reflect localization of raft-associated or non-raft-associated proteins, respectively. Arrow depicts SC migration. Shown is a representative blot for 3 independent experiments. B) Western blotting of gradient fractions from Caco-2 cells to determine raft vs. non-raft fractions. *Top panel*, Gradient fractions were concentrated using TCA (see Materials and Methods), loaded onto a 12% SDS-PAGE gel, and Western blotted with a rabbit anti-flotillin-1 antibody. *Bottom panel*, same fractions were loaded onto a 10% SDS-PAGE gel and Western blotted with a mouse anti-Na^+K^+-ATPase antibody. Shown are representative blots from 3 independent experiments.

2.3.2 Detergent Solubility and Raft Localization of CH-1 and CH-2 Complexes

The Fig. 2.2 results indicated that SC formation, which corresponds to the initial binding of CPE to its receptor (214), does not occur within membrane rafts. However, rafts might still contribute to CPE oligomerization. To explore this possibility, experimental conditions were used that allow formation of both the CH-1 and CH-2 SDS-resistant complexes in Caco-2 cells. In this case, Caco-2 monolayers were treated with CPE (2.5 μg/ml) for 60 min at 37°C, followed by a cold TX-100 extraction and sucrose density gradient centrifugation. Western blot analysis (Fig. 2.3A) of those gradient fractions indicated that the CH-1 complex localized exclusively within

the detergent-soluble fractions (fractions 8-12) at the bottom of the gradient. The CH-2 complex also predominately localized within those detergent-soluble fractions (Fig 2.3A), although a small pool of CH-2 complex was detected within the detergent-insoluble fractions (fractions 3-5).

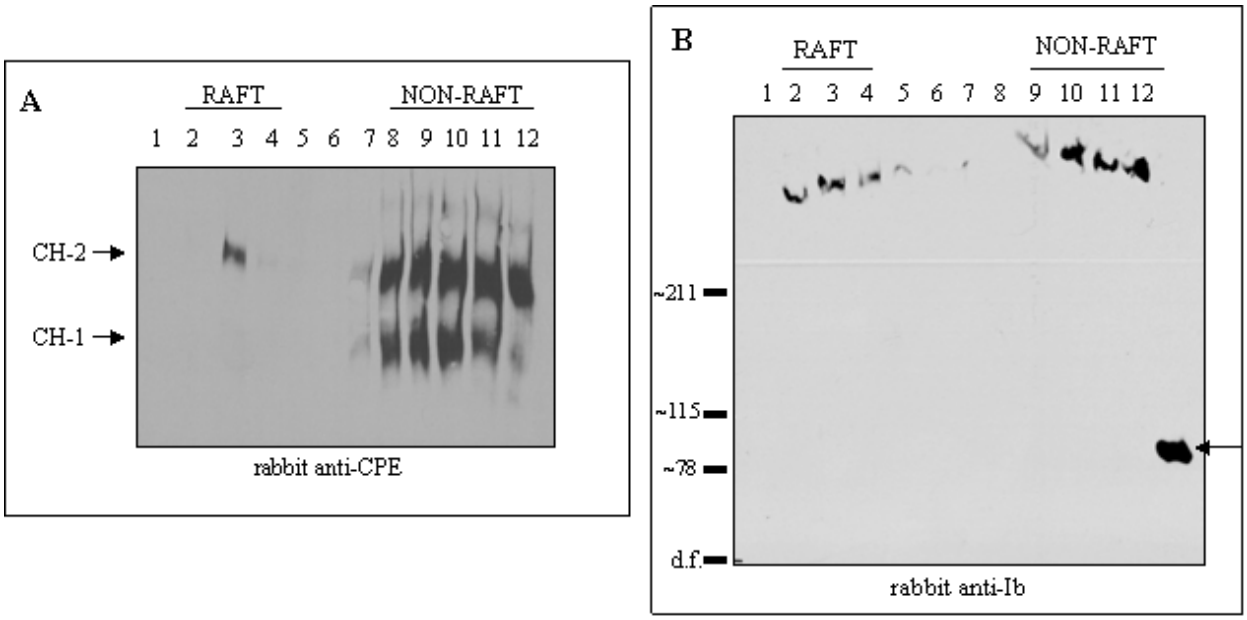

Figure 2.3 Localization of the CH-1 and CH-2 Complexes.
A) CPE Western blots of sucrose gradient fractions from Caco-2 cells containing CH-1 and CH-2. After treatment with CPE (2.5 μg/ml) for 60 min at 37°C, Caco-2 cells were cold extracted with TX-100 and subjected to sucrose gradient centrifugation. Gradient fractions were loaded on a 4% SDS-PAGE gel, followed by Western blotting with a rabbit anti-CPE antibody. Sucrose gradient fractions are numbered 1-12 at the top of the blot, with fraction 1 representing the gradient top and fraction 12 the gradient bottom. "Raft" and "Non-Raft" labels depict localization of raft-associated and non-raft-associated proteins, respectively. Arrows indicate migration of the CH-1 and CH-2 complexes. Shown is a representative blot for 3 independent experiments. B) Ib Western blots of sucrose gradient fractions from Caco-2 cells containing Ib oligomers. Caco-2 cells were treated with 2.0 μg/ml of Ib for 15 min at 37°C, followed by cold TX-100 extraction and sucrose gradient centrifugation. Fractions were visualized by Western blot of a 4% SDS-PAGE gel with a rabbit anti-Ib. Single arrow indicates 20 ng of purified free Ib. Shown is a representative blot from 2 independent experiments.

Since the data from Fig. 2.3 suggested that, except for a small fraction of CH-2, both the CH-1 and CH-2 complexes are non-raft-associated, a control was run to demonstrate that our methods could detect raft-associated toxin oligomers. Caco-2 cells were treated with Ib, the binding subunit of *C. perfringens* iota toxin, whose oligomers are localized, at least partially, in

membrane rafts (64, 142). In agreement with those previous findings, Ib oligomers were detected (Fig. 2.3B) within raft fractions.

2.3.3 Effect of Cholesterol Depletion on CPE Complexes

To evaluate whether membrane rafts are needed for CPE complex formation, these microdomains were disrupted by depleting cells of cholesterol using the compound methyl-β-cyclodextrin (MβCD), which extracts cholesterol directly from the plasma membrane of cells. When the total cholesterol content of Caco-2 cells was measured before and after MβCD treatment, MβCD had removed ~70% of the cholesterol from Caco-2 cell monolayers (see Materials and Methods).

Depletion of cholesterol in Caco-2 cells by MβCD pre-treatment prior to the addition of CPE had no major effect on CH-1 complex formation (Fig. 2.4A). Additionally, MβCD pre-treatment did not affect localization of the CH-1 complex in detergent-soluble fractions. Similarly, MβCD pre-treatment had little or no effect on the formation or localization of the CH-2 complex pool that is non-raft-associated (Fig. 2.4A). However, the small raft-associated pool of CH-2 complex (Fig. 2.3A) in CPE-treated Caco-2 cells was absent from cells depleted of cholesterol with MβCD treatment prior to CPE treatment, thus, confirming that this small pool is in fact raft-associated as it is sensitive to cholesterol depletion.

As a control to show the effectiveness of MβCD in disrupting the localization of normally raft-associated oligomers, Caco-2 cells were pre-treated with MβCD prior to treatment with Ib. Fig. 2.4B shows that cholesterol depletion effectively prevented the ability of Ib oligomers to form in raft domains, confirming that MβCD treatment affects the presence of toxin complexes in membrane microdomains.

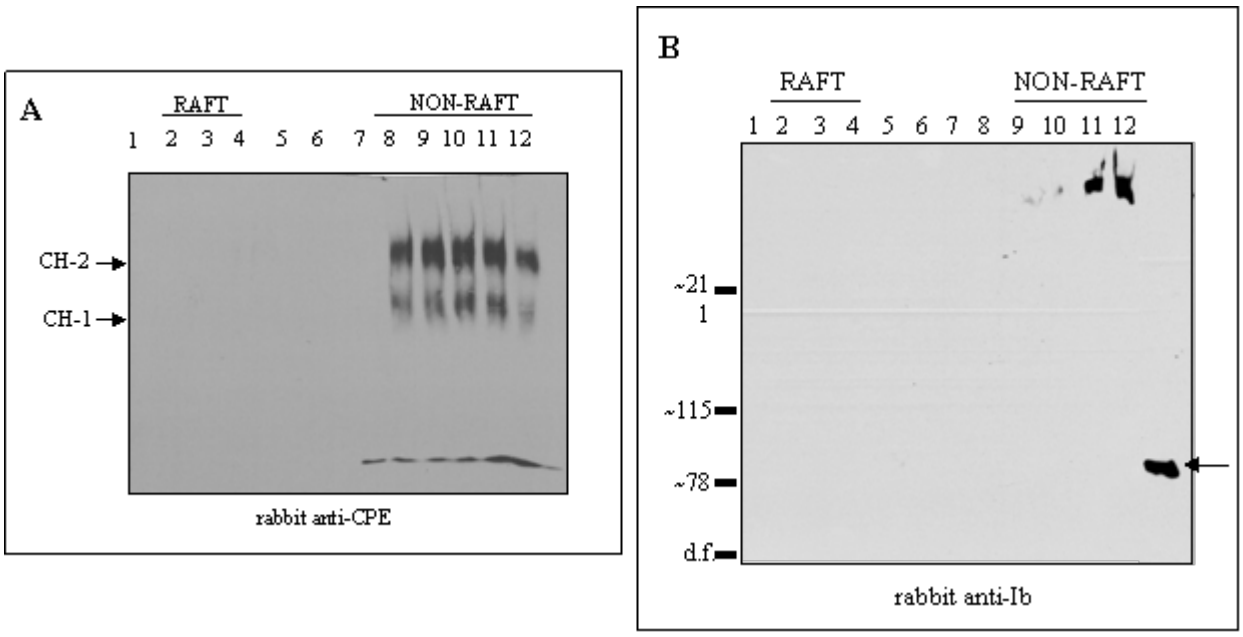

Figure 2.4 Effect of Cholesterol Depletion on CH-1 and CH-2 Formation.
A) CPE Western blot of sucrose gradient fractions from CPE-treated Caco-2 cells with reduced cholesterol levels. Caco-2 cells were pretreated with 10 mM MβCD for 60 min, followed by treatment with CPE (2.5 μg/ml) for 60 min. Those Caco-2 cells were then cold extracted with TX-100 and subjected to sucrose gradient centrifugation. Gradient fractions were loaded on a 4% SDS-PAGE gel and Western blotted with a rabbit anti-CPE antibody. Arrows indicate migration of the CH-1 and CH-2 complexes. Shown is a representative blot from 3 independent experiments. B) Ib Western blots of sucrose gradient fraction from Ib-treated Caco-2 cells with reduced cholesterol levels. Caco-2 cells were pretreated with 10 mM MβCD for 60 min followed by treatment with 2.0 μg/ml Ib for 15 min at 37°C. Fractions were visualized by Western blotting of a 4% SDS-PAGE gel with a rabbit anti-Ib antibody. Arrow indicates migration of 20 ng free purified Ib. Shown is a representative blot from 2 independent experiments.

2.3.4 Effect of Cholesterol Depletion on CPE Cytotoxicity

Since the CH-1 complex is sufficient to obtain CPE-induced cytotoxicity (122), Fig. 2.4 results suggested that membrane rafts do not play a major role in the cytotoxic effect of CPE action. To further address this question, we directly examined whether MβCD pre-treatment can protect Caco-2 cell cultures from CPE by quantitatively measuring cell viability using trypan blue staining.

In these studies, Caco-2 cell monolayers were pre-treated with 10 mM MβCD for 60 min, or left untreated, followed by treatment with CPE (2.5 µg/ml) for varying times (10, 20, 30, and 45 min). Fig. 2.5 shows no significant effect of cholesterol depletion on the viability of Caco-2 cells in the absence of CPE (see time 0). Likewise, there was no inhibition of CPE-induced cytotoxicity with pre-treatment of Caco-2 cells with MβCD. There was, in fact, a slight increase in Caco-2 cell sensitivity to CPE after MβCD pre-treatment. These data are consistent with the above Western blot analysis of CPE complex formation in which membrane rafts are not required for formation of the CH-1 complex that triggers cytotoxicity.

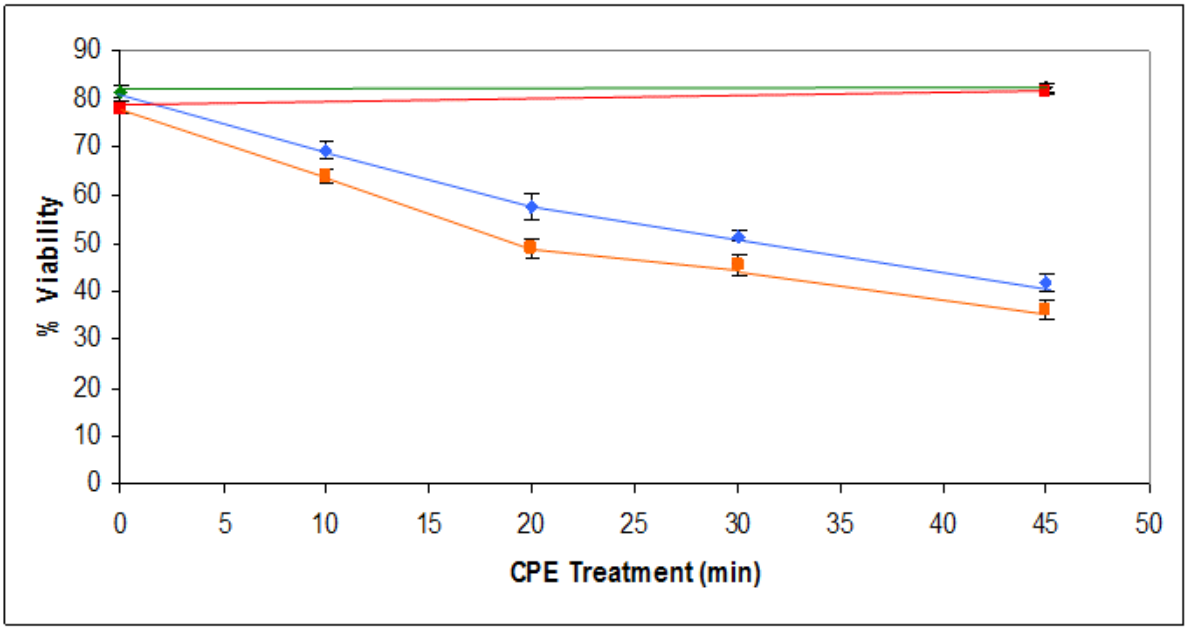

Figure 2.5 Effect of Cholesterol Depletion on CPE-induced Cytotoxicty.
Caco-2 monolayers were left untreated (♦) or pre-treated for 60 min with 10 mM MβCD (■). Cells were then treated for varying times (10, 20, 30, or 45 min) with 2.5 µg/ml of CPE, or left untreated (time 0). Trypan blue staining was performed as described in Material and Methods to obtain % Viability at each time point. Data points (♦) and (■) represent % viability of untreated or MβCD-treated, respectively, with buffer only during the course of 45 min. Error bars represent standard deviation of the mean of 3 independent experiments performed in triplicate.

2.3.5 Detergent Solubility and Raft Localization of Claudin-4

One possible contributor to CPE complexes not being associated with membrane rafts would be for the toxin receptor to reside outside of raft domains in control (no CPE treatment) Caco-2 cells. The presence of claudins within raft domains has been somewhat controversial (99-100, 114); therefore, we investigated whether the CPE receptor, claudin-4, is associated with DRMs in our experimental system. Sucrose density gradient experiments followed by claudin-4 Western blots (Fig. 2.6A) showed that, when extracted from control Caco-2 cell monolayers, claudin-4 is normally localized to the detergent-soluble, non-raft fractions at the bottom of the gradient. CPE-treatment of Caco-2 cell monolayers did not affect localization of claudin-4 into non-raft domains (Fig. 2.6B). Similarly, MβCD-treatment had no significant effect on the detergent solubility of claudin-4 in Caco-2 cells (Fig. 2.6C).

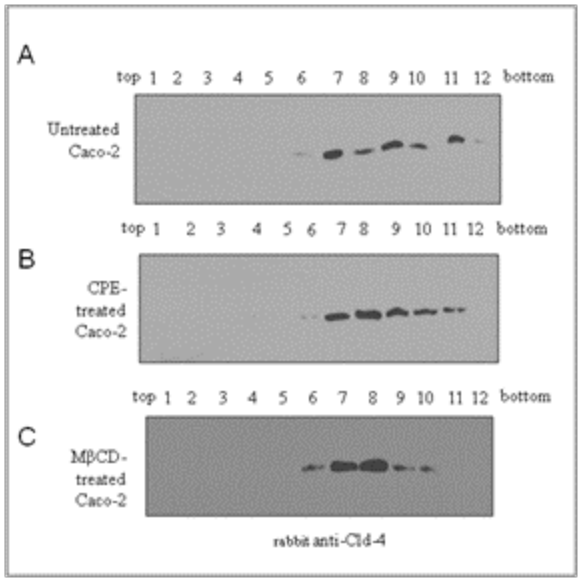

Figure 2.6 Raft Localization of Claudin-4.
Caco-2 cells were untreated (A), treated with 2.5 µg/ml of CPE for 60 min (B), or treated for 60 min with 10 mM MβCD (C) followed by cold TX-100 extraction and sucrose density gradient centrifugation. Each fraction was concentrated using TCA (see Materials and Methods) and loaded onto a 12% SDS-PAGE gel. Those gels were then Western blotted with a rabbit anti-claudin-4 primary antibody.

2.3.6 Detergent Solubility and Raft Localization of Occludin

In addition to claudins, a second TJ protein named occludin is also present within the CH-2 complex (179). Existing literature is contradictory concerning the presence of occludin in membrane rafts, so we similarly assessed occludin localization in our experimental system. After sucrose gradient centrifugation of control Caco-2 cell TX-100 extracts and Western blot analysis using an anti-occludin antibody, occludin localized mostly in gradient fractions 3-5, suggesting that this TJ protein is mainly raft-associated (Fig. 2.7A). In contrast, similar analysis of Caco-2 cells treated with CPE for 60 min revealed that most of the raft-associated occludin extracted from those cells had shifted to non-raft fractions in the sucrose gradient (Fig. 2.7B). However, a small pool of occludin remained raft-associated in CPE-treated cells. This CPE-induced shift in occludin to non-raft fractions was similar to that observed when Caco-2 cells were treated with MβCD alone, i.e. without CPE treatment (Fig. 2.7C). The CPE-induced shift of occludin to non-raft fraction was not a consequence of generalized membrane raft dissolution since flotillin-1 remained raft-associated in these cells (data not shown).

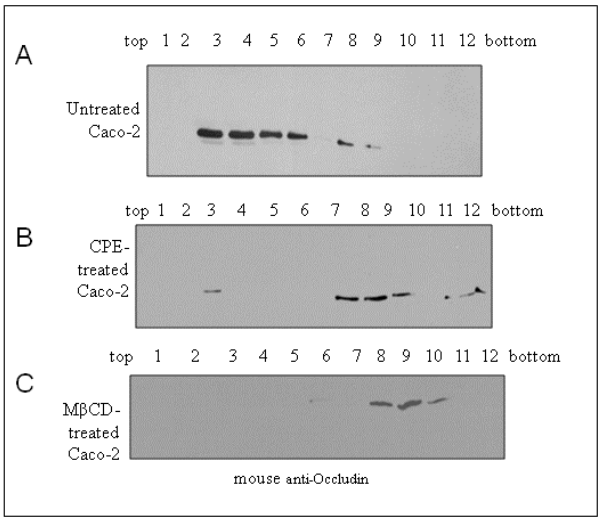

Figure 2.7 Raft Localization of Occludin.
Caco-2 cells were untreated (A), treated with CPE (2.5 μg/ml) for 60 min (B), or treated for 60 min with 10 mM MβCD (C) followed by cold TX-100 extraction and sucrose density gradient centrifugation. Each fraction was concentrated using TCA (see Materials and Methods) and loaded onto a 10% SDS-PAGE gel. Those gels were then Western blotted with a mouse anti-occludin primary antibody.

2.3.7 Kinetics of CPE-induced Occludin Redistribution

The CPE-induced shift of occludin from raft to non-raft fractions was further investigated by kinetic analysis. Densitometric scanning of occludin Western blots of pooled raft fractions (gradient fractions 2-4) or non-raft fractions (gradient fractions 9-12) from Caco-2 cells treated with CPE for varying times showed that the shift of occludin from insoluble to soluble gradient fractions begins relatively quickly upon CPE treatment and increases with time thereafter up to 30 min (Fig. 2.8A). Specifically, after only 10 min of CPE treatment, most occludin remained raft-associated, as in untreated Caco-2 cells (Fig. 2.7A). However, by 30 min of CPE treatment the majority of occludin had shifted to non-raft fractions (Fig. 2.8A). Additionally, CPE treatment caused an apparent decrease in the total cellular levels of occludin, similar to that observed with MβCD treatment alone (Fig. 2.7C).

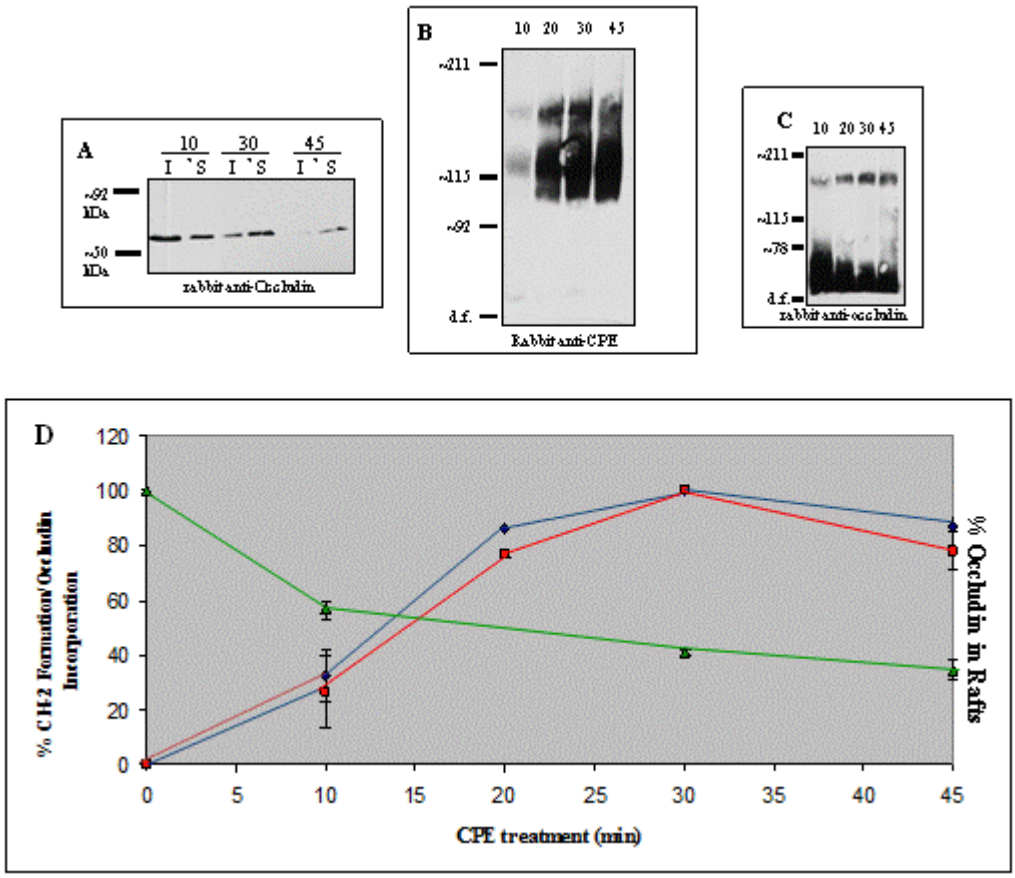

Figure 2.8 Kinetics of CPE Complex Formation and Occludin Distribution.
A) Caco-2 monolayers were treated with 2.5 µg/ml of CPE for the indicated times (10, 30, and 45 min) and sucrose gradients were then performed for TX-100 lysates of each time. Gradient fractions 2-5 were pooled and concentrated for each time point to give detergent-insoluble raft fractions (I). Gradient fractions 9-12 were pooled and concentrated to give detergent-soluble non-raft fractions (S). Pooled samples were run on a 10% SDS-PAGE gel and Western blotted using a rabbit anti-occludin antibody. Caco-2 monolayers were treated with 2.5 µg/ml of CPE for the indicated times (10, 20, 30, and 45 min), lysed in SDS buffer and subject to SDS-PAGE and Western blotted with B) rabbit anti-CPE antibody or C) rabbit anti-occludin antibody. D) Densitometry analysis of Western blot data from A-C) (▲) depicting % occludin within detergent-insoluble rafts at each time point. Data were calculated by comparing band intensity of raft-associated occludin over non-raft-associated occludin. Data points (♦) and (■) represent densitometry analysis of Western blots of % CH-2 formation and % occludin incorporation into CH-2, respectively. To calculate the % CH-2 formation and % occludin incorporation into CH-2, each time point was taken as a percentage of 100% normalized to highest band intensity at 30 min of CPE treatment. Error bars represent the standard deviation of the mean for 3 independent experiments.

Since occludin is associated with the CH-2 complex (179), which mainly forms outside of raft microdomains (Fig. 2.3), densitometry analysis was performed on Western blots data to quantitatively determine the fold increase in CH-2 formation over time in order to test whether

the kinetics of CH-2 complex formation could be a contributor to the CPE-induced shift of occludin from membrane rafts. As reported previously (179), this kinetic experiment demonstrated (Fig. 2.8B and 2.8D, diamonds) CH-2 complex formation begins within 10 min of CPE toxin challenge. By 30 min of toxin treatment, significant amounts of the CH-2 had formed in Caco-2 cells under the experimental condition used in these studies. Densitometry of occludin Western blots also revealed (Fig. 2.8C and 2.8D, squares) a time-dependent incorporation of occludin into the CH-2 complex, as reported previously (179). However, these analyses also suggested that not all occludin within Caco-2 cells may be associated with the CH-2 complex since considerable amounts of occludin was present at the gel dye front (Fig. 2.8C). Coincident with CH-2 formation, the amount of occludin present at the gel dye front decreased with time of CPE treatment under the experimental conditions used. These CPE blots showing the presence CH-2 were stripped and reprobed with an occludin antibody to confirm the presence of occludin within CH-2 (data not shown). The data presented in Fig. 2.8D are consistent with a relationship between CH-2 formation, occludin incorporation into CH-2, and removal of occludin from lipid rafts (Fig 2.8A-D, triangles).

To distinguish whether the shift of occludin from raft to non-raft domains seen in Figs. 2.7 and 2.8 is correlated with CH-2 complex formation or is merely a by-product of CPE challenge, additional experiments were performed that investigated the effects of SC and CH-1 on occludin distribution. To assess the effect of SC formation on occludin distribution, the gradient fractions from Fig. 2.2 were pooled, concentrated into raft and non-raft fractions, and Western blot analysis was performed using an anti-occludin antibody. When compared to untreated Caco-2 cells, results from this experiment (Fig. 2.9A) showed that occludin remains in

the insoluble raft fractions upon CPE treatment at 4°C, strongly suggesting that SC formation has no major effect on the localization of occludin in raft domains.

A second experiment was then performed to address whether CH-1 complex formation is sufficient to cause the redistribution of occludin observed after CPE treatment (Figs. 2.7 and 2.8). This experiment used Caco-2 cells grown on Transwell supports, which produces polarized monolayers (158, 178) with fully formed tight junctions, e.g. 4-70 kDa fluorescently-labeled dextrans are impermeable to these monolayers (data not shown). As described previously (158, 178), formation of the CH-1 complex in the absence of any CH-2 formation was obtained by treating these cells apically with CPE (1.0 µg/ml) for 30 min.

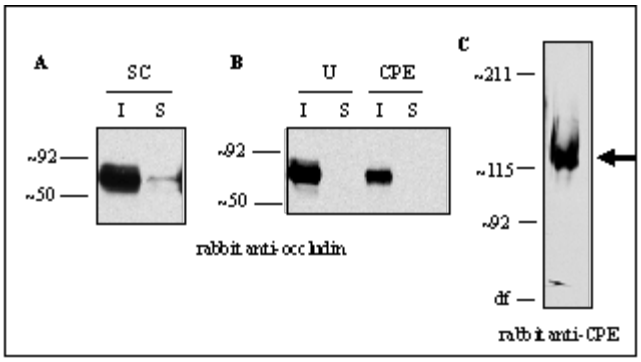

Figure 2.9 Effects of SC and CH-1 on Occludin Distribution.
A) After treatment with CPE (2.5 µg/ml) for 15 min at 4°C, Caco-2 cells were extracted with cold TX-100 and subjected to sucrose gradient centrifugation. Gradient fractions 2-5 and 9-12 were pooled and concentrated to give detergent-insoluble raft fractions (I) or detergent-soluble non-raft fractions (S), respectively. Pooled samples were run on a 10% SDS-PAGE gel and Western blotted using a rabbit anti-occludin antibody. B) Caco-2 cells were grown in Transwell permeable supports until confluency to form CH-1 in the absence of CH-2, and either left untreated or treated with CPE (1.0 µg/ml) for 30 min at 37°C. TX-100 extraction and sucrose gradients were performed as before, followed by pooling of fractions to obtain detergent-insoluble (I) and detergent-soluble (S) samples. Pooled samples were run on a 10% SDS-PAGE gel and Western blotted using a rabbit anti-occludin antibody. C) CPE Western blot of CPE-treated Caco-2 TX-100 extractions from B) confirming the presence of CH-1 without CH-2. Arrow indicates CH-1 complex formation, in the absence of CH-2 complex. Representative blots are shown for 2 independent experiments.

Sucrose gradients and CPE Western blots were performed as above, which confirmed the presence of CH-1 in non-raft fractions (data not shown), along with the absence of the CH-2 complex from these cells (Fig. 2.9C). Western blots of these polarized Transwell cultures

containing tight junctions also confirmed the data in Fig. 2.6 with the presence of claudin-4 in non-raft fractions (data not shown). Additionally, occludin Western blots (Fig. 2.9B) of those same gradient samples revealed that, with or without CPE treatment, occludin remains raft-associated in these CH-1-containing Transwell cultures, indicating that CH-1 formation and CPE cytotoxicity from pore formation are not sufficient for the redistribution of occludin to non-raft fractions observed in the presence of CH-2.

2.4 DISCUSSION

Membrane rafts are now well-established in contributing to the action of many bacterial toxins. With respect to PFTs, raft domains can promote toxin receptor binding, oligomerization, and oligomer insertion into membranes for pore formation. The involvement of membrane rafts in PFT oligomerization is largely attributable to their dynamic ability to coalesce into larger domains, serving as platforms that allow for protein clustering.

Since membrane rafts are involved in the action of many PFTs, the current study investigated whether these microdomains also contribute to the action of CPE, another PFT, whose action involves sequential formation of three CPE-containing complexes, i.e. SC, CH-1, and CH-2 (158, 179, 214). Experiments assessing whether each of those CPE complexes is localized within membrane rafts showed that both the SC and CH-1 are found exclusively outside rafts in non-polarized and polarized Caco-2 cells. In our Caco-2 model, we were capable of detecting toxin oligomers localized to membrane rafts since Ib oligomers were, as reported previously (64, 142), detected in raft fractions.

Localization of the CH-1 complex outside lipid rafts of polarized and non-polarized cells was interesting since formation of this complex, which appears to be sufficient for causing CPE-induced cytotoxicity, is thought to correspond to the CPE pore (118, 158, 178). Therefore, Caco-2 cells were pre-treated with MβCD to deplete cells of their cholesterol and disrupt rafts to determine if these domains are required for CH-1 formation. This pre-treatment had no detectable effect on the formation of CH-1 (Fig. 2.4) or on its presence within non-raft fractions. In contrast, MβCD pre-treatment effectively shifted raft-associated Ib oligomers from raft into non-raft membrane domains in Caco-2 cells, confirming that this pre-treatment was sufficient to disrupt membrane rafts in Caco-2 cells.

The inability of cholesterol depletion to affect CH-1 formation suggested that rafts are not required for CPE action. Further support for this suggestion was then provided by the inability of MβCD treatment to delay the onset of CPE-induced cytotoxicity in Caco-2 cells (Fig. 2.5). In fact, pre-treatment of cells with MβCD before CPE addition slightly increased CPE-induced damage to Caco-2 cell monolayers even though MβCD itself caused no cytotoxic effects in our system. One possible explanation for this increased CPE sensitivity is that cholesterol depletion might loosen the TJ, so that CPE gains access to the basolateral side of the cell, where more CPE receptors are located (178). This possibility is supported by previous studies showing that MβCD treatment decreases transepithelial resistance in Caco-2 and MDCK cells (50, 99). It is also possible that removing an important structural component of the plasma membrane (i.e. cholesterol) compromises the overall integrity of the plasma membrane, increasing susceptibility of the cell to CPE.

While there is less certainty regarding its contribution to CPE action, the CH-2 complex is clearly not required for CPE-induced cytotoxicity and only forms in damaged, dying cells

(179). CH-2 may represent a second CPE pore that further contributes to increased membrane permeabilty alterations; it also appears to facilitate the observed removal of occludin from TJs of CPE-treated cells, with subsequent internalization into the cytoplasm (178). In the current study, most of the CH-2 complex formed by CPE-treated Caco-2 cells localized outside rafts, although a small pool of CH-2 in Caco-2 cells was raft-associated (Fig. 2.2). MβCD-pre-treated cells did not contain this small pool of raft-associated CH-2 (Fig. 2.4), supporting its association with raft microdomains.

CPE is an unusual PFT in that eukaryotic proteins are closely associated with the CPE oligomer (158). Therefore, we investigated whether the observed CPE oligomerization outside membrane rafts might involve CPE complex-associated eukaryotic proteins (especially receptor claudins) residing in non-raft membrane domains prior to CPE treatment. We first determined whether a TJ protein, claudin-4, is raft-associated in our cell culture model system since i) this CPE receptor is present in SC, CH-1 and CH-2 (158), and ii) there are conflicting reports regarding the association of claudins with lipid rafts (99-100, 114). The methods used in our study localized claudin-4 of Caco-2 cells exclusively within non-raft-associated fractions. Since claudin-4 is a CPE receptor and the SC forms immediately upon CPE binding, the presence of claudin-4 CPE receptors in non-raft lipid domains offers an explanation for the localization of SC to non-raft fractions.

The exclusive localization of CH-1 and claudin-4 in non-raft fractions of non-polarized or polarized Caco-2 cells and the formation of CH-1 in MβCD-treated cells also indicates that, unlike most PFTs, CPE does not require rafts to promote its oligomerization. For CPE, raft-mediated clustering of receptors may be unnecessary since claudins already lie in close proximity to one another due to their presence in TJs as polymerized strands (53, 199).

Furthermore, those strands also closely associate with similar claudin strands in the same and on apposing cells. However, membrane fluidity does appear to play some role in CH-1 formation since CPE binds and forms SC at 4°C, yet CH-1 and CH-2 formation are inhibited at this low temperature (179).

Although most PFTs oligomerize within rafts, CPE in not a unique PFT with respect to its ability to bind and oligomerize outside lipid rafts. Protective antigen (PA) of anthrax toxin also binds to receptors and oligomerizes outside of a raft. However, unlike CPE, oligomerization triggers the association of the PA pre-pore with membrane rafts (1). The presence of PA oligomers in rafts appears important for the eventual translocation of lethal and edema factors through the PA pore (222), i.e. for cytotoxicity, since MβCD inhibits this process. Thus, our results distinguish CPE from PA (and other PFTs) in that CPE not only binds and oligomerizes independently of raft domains, but also forms active pores outside of these microdomains. The lack of movement of CPE oligomers into rafts might be attributable to claudin CPE receptors being localized in strands where movement is relatively restricted inside TJs.

The association of occludin with membrane rafts has also been controversial (40, 85, 100, 145). In contrast to the exclusive association of claudin-4 with non-raft fractions, our study found that most occludin localizes in raft fractions of control (no CPE treatment) non-polarized or polarized Caco-2 cells. As expected, MβCD treatment of Caco-2 cells completely shifted occludin to non-raft membrane fractions. CPE treatment similarly shifted most of the occludin in polarized or non-polarized Caco-2 cells from raft to non-raft membrane domains. This effect was time-dependent (Fig. 2.8) and paralleled the appearance of most occludin-containing CH-2 in non-raft microdomains of CPE-treated Caco-2 cells. Establishing this correlation is consistent with the possibility that occludin is pulled from lipid rafts as it becomes associated with CH-2.

Also consistent with CH-2 complex formation specifically contributing to the redistribution of occludin into non-raft domains, our results showed that the presence of the SC or CH-1 complexes (in the absence of CH-2) is not sufficient to shift occludin from rafts. This result also indicates that removal of occludin from rafts is not merely a nonspecific consequence of CPE-induced cytotoxicity. Nor is removal of occludin from rafts due to nonspecific occludin internalization since our previous studies showed occludin internalization only occurs in the presence of CH-2 (178). Additionally, the CPE-associated removal of occludin from raft domains is not a non-specific consquence of raft breakdown as we observed that CPE treatment does not remove the raft marker, flotillin-1, from rafts.

However, sequestration of occludin in CH-2 may not fully explain CPE effects on occludin membrane distribution since not all occludin present in CPE-treated Caco-2 cells is localized in the CH-2 complex, at least as assessed by Western blotting. CPE treatment also had other effects on occludin in Caco-2 cells. In particular, total occludin levels appeared to slightly decrease in CPE-treated cells. This effect was noticed in cells containing CH-1 in the absence of CH-2, but appeared to be stronger when both CH-1 and CH-2 complexes were present, possibly because cells containing both complexes together enhance cell death. The observed CPE-induced decrease in occludin could be a general response to cell death and also might involve, at least in part, the previously described CPE-induced removal of occludin from the TJ into the cytoplasm of Caco-2 cells, an effect that seemingly correlates with CH-2 formation (178). A recent study (13) has shown that removal of occludin from the tight junction by addition of an exogenous peptide activates the extrinsic pathway of apoptosis which is mediated by the formation of a complex between occludin and Fas and FADD, a death receptor adaptor molecule of the death inducing signaling complex (DISC). It is plausible that CPE-dependent removal of

occludin from the tight junction may be triggering apoptosis, a process that has been previously described in CPE-treated cells (32). Experiments are needed to examine whether CPE treatment results in the interaction of occludin with FADD and the DISC, and is activating apoptosis through the extrinsic pathway. In addition to the gate and fence functions of the tight junction, this junctional complex of the cell can serve as an intracellular signaling platform (60) and occludin has been shown to serve as a signaling molecule (223). This opens many pursuable avenues for signaling studies investigating the intracellular signaling effects of CPE treatment in the context of tight junction disruption.

It is also notable that even CPE-treated Caco-2 cells still contained a small pool of raft-associated CH-2 and occludin. This small amount of raft-associated CH-2 could represent interactions between SC or CH-1 with a distinct occludin pool. Different occludin pools could correspond to differences in occludin phosphorylation (114, 145, 219), polymerization (53), internalization (178), or an occludin splice variant (61). Further studies will be needed to clarify the complicated relationship between occludin, rafts, and CH-2 formation.

In summary, the current study strongly suggests that CPE is a novel PFT that does not require lipid rafts for binding, oligomerization, or cytotoxicity. The presence of claudin receptors in polymerized strands may restrict the subsequent movement of receptor-bound CPE or CPE oligmers into rafts. Furthermore, CPE treatment causes a dramatic shift of most occludin in Caco-2 cells, from raft to non-raft domains. This effect may be mediated, at least in part, by the sequestration of occludin in the CH-2 complex.

3.0 DEVELOPMENT OF A CPE COMPLEX ISOLATION METHOD FOR COMPOSITIONAL ANALYSIS BY MASS SPECTROMETRY

3.1 INTRODUCTION AND RATIONALE

3.1.1 CPE Complex Formation

Oligomerization of pore-forming toxins results in the formation of high molecular weight complexes on target cell membranes (56, 136, 228). The formation of CPE-containing protein complexes on the surface of target cell membranes is crucial to the pore-forming action of the toxin. For example, CPE-induced pore-formation and cytotoxicity requires, and occurs concomitantly, with the formation of the CH-1 complex (86, 122). Additionally, formation of the CPE Small Complex (SC), although not sufficient for cytotoxicity, is still a necessary first step prior to observing CPE-induced pore-formation (122).

Recent studies have reassessed both the size and composition of the three CPE complexes (SC, CH-1, and CH-2) (158). When the CPE receptor, claudin-4, was first identified, it was suggested this protein is present within the high molecular weight CPE complexes (82). However, it was not until recently that direct evidence for the presence of receptor claudins within the CPE complexes was available (158). Analysis by electroelution of the three CPE complexes directly revealed the presence of claudin-4, as well as another functional CPE

receptor, claudin-3, within these complexes. This was the first report of the presence of a toxin receptor within a high molecular weight toxin complex. Interestingly, however, immunoprecipitation showed that despite lacking the ability to bind to CPE, claudin-1 was found to interact with CPE. Furthermore, electroelution of the SC, CH-1, and CH-2 complexes revealed the presence of claudin-1 within these complexes. These studies showed that not only do receptor claudins become associated with the CPE-containing complexes, but non-receptor claudins can also associate with these complexes.

Additionally, it was not until recently that the stoichiometry of the CPE complexes was addressed. Before the identification of claudin as the CPE receptor, it was originally hypothesized that one CPE monomer bound to one ~50 kDa unidentified protein and one ~70 kDa unidentified protein to make up the "~155 kDa Large Complex" (122). The identification of the presence of the 65 kDa protein, occludin, in a second large CPE complexes led to the naming of the "~200 kDa Large Complex" (179). Knowledge of claudin, a protein of only ~20 kDa, as the CPE receptor led to the questioning of the original model of the composition of CPE complexes. Therefore, the number of CPE molecules within the Large Complexes was assessed by molecular weight variants of CPE and heteromeric gel shift analysis, which revealed the presence of six copies of CPE (158). In turn, now knowing that six copies of CPE and both receptor and non-receptor claudins can be present in the complexes, the sizes of the CH-1 and CH-2 complexes were reassessed by gel filtration and Ferguson plot analysis (158). The molecular weights of the CH-1 and CH-2 complexes were resized to be ~450 kDa and ~600 kDa, respectively. Taking into consideration i) the presence of both receptor and non-receptor claudins, ii) the stoichiometry of 6 CPE molecules, and iii) the larger molecular weights, the composition of the CPE complexes are is more heterogeneous than originally thought.

3.1.2 The Complexity of the Tight Junction

As described, the tight junction (TJ) is an important structure of epithelial cells for forming a continuous intercellular barrier between adjacent cells, separating apical vs. basolateral compartments, and regulating the transport of solutes across the epithelium (6). The claudin family of proteins has emerged as the most critical TJ proteins for maintaining TJ functions such as regulating permeability selectivity (6). Although claudins are likely the most important TJ proteins for function, they are far from the only TJ-associated proteins. Proteomic analysis of enriched junctional membrane proteins identified >40 proteins that are associated with this membrane fraction (221). The schematic in Figure 3.1 illustrates the complexity of the TJ, highlighting both the transmembrane and cytosolic structural components, as well as the intracellular signaling elements that are transiently associated with the TJ.

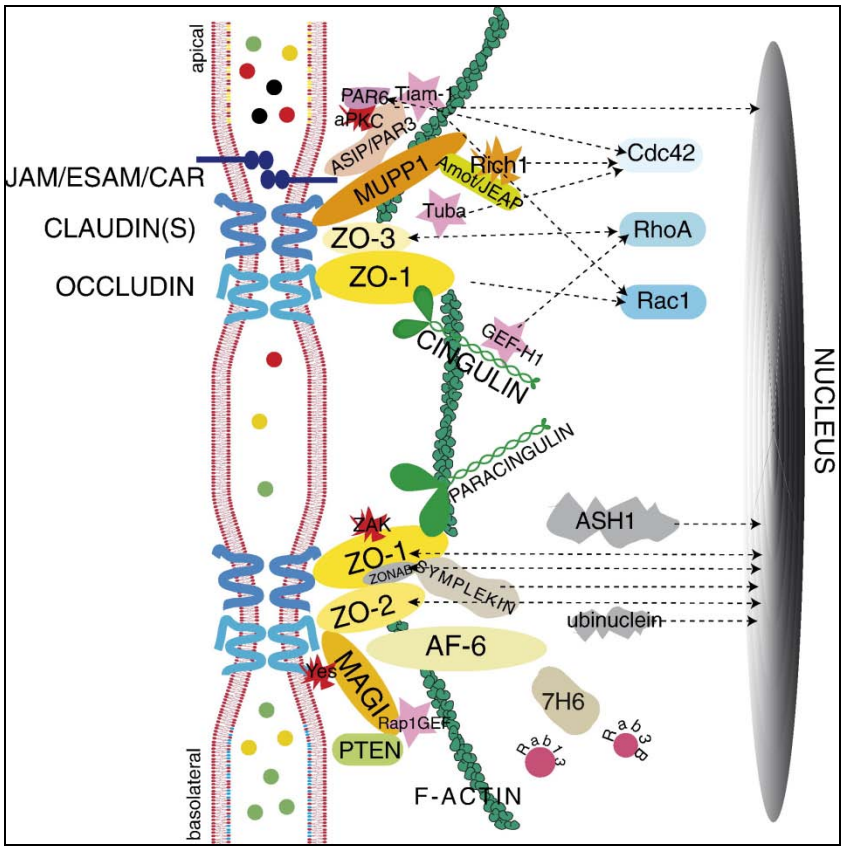

Figure 3.1 Schematic Representation of the Tight Junction and its Associated Proteins.
This diagram illustrates the structural transmembrane components of the TJ, such as Claudin, Occludin, and JAM, which traverse the plasma membrane to interact with adjacent cells. Intracellular scaffolding proteins, such as ZO-1, -2, and -3, PAR-3, PAR-6, MUPP1, MAGIs and AF-6, contain PDZ domains that serve to link the TJ to the actin cytoskeleton. Kinases (aPKC, ZAK, c-Yes), GEFs (Tiam1, GEF-H1, Tuba, Rap1GEF), membrane traffic regulators (Rab3B and Rab13), and signaling proteins (Cdc42, RhoA and Rac1) transiently associate with the TJ plaque and serving functions necessary for assembly, stabilization, and maintenance of the junction, and regulating proliferation and differentiation. Taken from (62).

3.1.3 Rationale

Considering the recent findings of the large CPE-containing complexes containing both claudin receptors and non-receptors, it seems that the CPE complexes on the membrane have the ability to associate with proteins that may not necessarily have the ability to directly bind to CPE. Therefore, it is plausible that the CPE complexes are capable of pulling proteins that associate

with receptor claudins into the protein complex. When one considers the complex architecture of the TJ and the numerous proteins that are closely or transiently associated with claudin, many other TJ proteins besides claudin and occludin could be present within the CH-1 and CH-2 complexes. Antibody studies aimed at identifying likely constituents of the complexes would be nothing less than a fishing expedition, and would not be an economical strategy. We, therefore, wish to develop a method to isolate the CPE complexes individually to analyze their protein components by mass spectrometry.

3.2 MATERIALS AND METHODS

3.2.1 Affinity Purification of rCPE

E. coli strain pJK9 (full length wild type CPE cloned into the pTrcHisA vector) was inoculated into 50 ml of LB Broth containing 100 μg/ml ampicillin (LB Amp), and grown overnight by shaking at 37°C. The following day, 20 ml of the overnight culture was inoculated into 1L of LB Amp and shaken for 3 h. The production of rCPE was induced by the addition of IPTG (final concentration of 1 mM) with shaking for 4 more hours. Cultures were harvested by centrifugation for 15 min at 7500 rpm in a GS-3 rotor. Pelleted cells were frozen overnight at -20°C. After thawing, pellets were resuspended in 20 ml of HisTrap Binding Buffer (20 mM sodium phosphate, 0.5 M NaCl, 20 mM imidazole, pH 7.4). Cells were lysed by 8 X 1 min blasts of sonication using the Misonix Sonicator 3000 (output of 7.0). Cell debris was removed by centrifugation for 15 min at 7500 rpm in a SS-34 rotor. Supernatant was then filtered using a 0.45 μm syringe filter.

A 1 ml HisTrap Fast Flow Ni^{2+}-affinity column (GE Lifesciences) was prepared by manually equilibrating the column with 10 column volumes (10 ml) of Binding Buffer using a Luer-Lok syringe system. The filtered supernatant was added to the column using a syringe at a flow rate of 1 ml/min. The column was washed twice with 5 ml of Binding Buffer. Elution was performed by adding 5 ml of HisTrap Binding Buffer (20 mM sodium phosphate, 0.5 M NaCl, 500 mM imidazole, pH 7.4) to the column and collected 5 X 1 ml fractions. Column flow-throughs were collected for each step for analysis by SDS-PAGE, where 10 µl of each fraction was loaded onto a 12% SDS-PAGE gel followed by staining with Coomassie blue. Purified fractions were combined (Fractions 2 and 3) and a Lowry was performed to determine the protein concentration.

3.2.2 Affinity Purification of rCPE Complexes

Ten 100 mm cell culture plates were seeded with Caco-2 cells at a density of 1 x 10^5 cells/ml. When confluent (4-5 days), monolayers were treated with 2.5 µg/ml of rCPE for 45 min. Cells were harvested by gentle scrapping and centrifugation. Pellets were washed and lysed in 1% TX-100. Lysates were spun down and filtered with a 0.45 µm syringe filter and added to the HisTrap column. Purification was performed similar to that for purification of rCPE (above). 25 µl aliquots of each fraction were run on 4% SDS-PAGE, transferred to nitrocellulose and Western blotted with a rabbit anti-CPE antibody.

3.2.3 AlexaFluor488 Labeling

Alexa labeling was performed as described by the manufacturer for the AlexaFluor 488 Protein Labeling Kit (Invitrogen). Native CPE (nCPE) was reconstituted in PBS to a final concentration

of 2 mg/ml. 500 µl of nCPE (2 mg/ml) was used for labeling; 50 µl of 1M Sodium Bicarbonate was added to the 500 µl of CPE. This solution was added to a vial of reactive dye and stirred for 1 h at RT. After the labeling reaction, the solution was added to a gel filtration column (supplied with kit) and 1 ml fractions were collected after eluting with Elution Buffer (10 mM potassium phosphate, 150 mM NaCl, 0.2 mM sodium azide, pH 7.2). Ten µl of each fraction was analyzed by running on 12% SDS-PAGE and visualizing bands by scanning on a Typhoon 9400 Scanner (Amersham).

3.2.4 Affinity Purification of Rabbit α-CPE Antibody

Serum from rabbits immunized with purified nCPE was affinity purified by using a Protein A-agarose column (Pierce). Five milliliters of rabbit serum was diluted 1:1 with Binding Buffer (100 mM sodium phosphate, 150 mM NaCl, pH 7.2). To avoid clogging of the purification column, diluted serum was filtered using 0.45 µm syringe filters. Using the Luer-Lok adapter system, a syringe filled with 10 column volumes (10 ml) of Binding Buffer was attached to the column, and to equilibrate the column Binding Buffer was flowed through the column at a rate of ~1 ml/min. After equilibration, diluted serum was added through the column at a rate of ~1 ml/min. The column was then washed with 10 ml of Binding Buffer. Bound antibody was eluted from the column using 5 ml of Elution Buffer (0.1M Glycine, pH 2.0). Prior to elution, 500 µl of 1M Tris, pH 8.0 was added to the collection tube to neutralize the low pH of the Elution Buffer.

3.2.5 Electroelution

Thirty 150 mm cell culture dishes of Caco-2 cell monolayers (~10^7 cells) were each treated with 2.5 μg/ml nCPE in 15 ml of complete HBSS (with Ca^{2+}, cHBSS) for 45 min. Two plates were treated with 2.5μg/ml of Alexa-CPE for 45 min. Cells were harvested by gentle scraping and washed twice with cHBSS. Combined cell pellets were resuspended in 2 ml of cHBSS and incubated for 10 min with the addition of 20 μl of benzonase (Novagene, EMD). Cells were lysed by the addition of 2 ml of 2X Laemmli buffer. Lysates were loaded onto a single-well 4% SDS-PAGE preparative gel and electrophoresed at 40 mA for 4 h in the dark. Bands were visualized by fluorescence imaging using Typhoon scanning and the location of the bands was marked by a fluorescent ruler. CH-1 and CH-2 bands were excised from the gel and cut into 6 smaller gel pieces each. Two gel pieces were placed into dialysis tubing (MWCO 6-8000) containing 2 ml of Electroelution (EE) Buffer (25 mM Tris, 0.192 M glycine, 0.1% (w/v) SDS, pH 8.3). These dialysis sacks were sealed and electrophoresed at 50 mA for 5 h at 4°C in the dark. After EE, fluid was collected and combined for each CH-1 and CH-2 and concentrated using Amicon centrifuge concentrators to a final volume of ~500 μl. To eliminate SDS in samples which was found to prohibit successful immunoprecipitation, concentrated samples were washed with 5 ml of PBS and reconcentrated to 500 μl. This wash step was repeated for a total of 2 washes.

3.2.6 Immunoprecipitation

Concentrated EE samples were immunoprecipitated by the addition of 25 μl of affinity-purified rabbit anti-CPE antibody (see above). This solution was incubated overnight at 4°C with gentle rotation. The next day, 20 μl of Protein A-acrylic beads (Sigma) were incubated with the IP

reaction with gentle rotation for 1 h at 4°C. Immunoprecipitated material was pulled down by centrifugation. Pellets were washed 3 times with 0.1% TX-100/PBS buffer. To dissociate antibody and IPed material from the beads, 50 µl of 2X Laemmli was added to resuspend the beads and boiled for 5 min. Samples were centrifuged and supernatants were collected. One-tenth of the sample was run on 4% SDS-PAGE along with a samples of purified nCPE to act as a standard curve. The gel was transferred and Western blotted with a monoclonal mouse anti-CPE antibody (Mab3). Densitometry (using Quantity One Software, Biorad) was used to construct a standard curve to extrapolate the amount of CPE present in the EE/IP sample.

3.2.7 In-gel Digestions

After determining the amount of CPE present in the sample, the remaining sample was run on SDS-PAGE and the CH-1 and CH-2 bands were visualized by Typhoon scanning. Corresponding bands were excised from the gel and cut into 1.5 mm pieces. Gel pieces were rinsed 3X in 500 µL 50% Acetonitrile in 25 mM Ammonium bicarbonate with vigorous shaking for 15 min at RT. Gel slices were dehydrated by the addition of 500 µL of 100% Acetonitrile with 15 min shaking at RT. Fluid was evaporated by spinning samples in a Speed Vac for 15 min with low heat.

For trypsin digestions, 40 µl of trypsin (Sigma, proteomics grade) (20 µg/ml in 25 mM ammonium bicarbonate/0.9% acetonitrile) was added and let absorbed into gel slices. An additional 40 µl of trypsin was added and was allowed to absorb until gel pieces turned clear. Gel slices were overlayed with 100 µl of 25 mM ammonium bicarbonate and incubated at 37°C overnight. Liquid was transferred to a new tube. Peptides were extracted by adding 100 µl of 50% acetonitrile/2.5% Trifluoroacetic Acid (TFA) and shaken vigorously at RT for 15 min.

Extraction liquid was added to collection tube. The extraction was repeated twice. Peptides were dried by spinning in a Speed Vac (~1.5 h) with low heat.

For chymotrysin digestions, the same procedure was followed as for trypsin digestions, however, 1 μg/ml of chymotrypsin (Pierce, proteomics grade) was used.

3.2.8 LC-ESI MS/MS

After enzymatic digestion, the mixture of peptides were separated by capillary C18 HPLC (ThermoElectron Surveyor liquid chromatograph with a Micro AS autosampler) and direct analysis of the effluent on a ThermoElectron LCQ Deca XP Plus quadrupolar ion trap mass spectrometer utilizing a nanospray ionization source. The mass spectrometer was set up to perform both MS and MS/MS experiments. The computer algorithm controlling these experiments selected the three largest ions from a MS spectrum, then instructed the mass spectrometer to perform three separate MS/MS experiments on those three ions. This process was repeated every few seconds throughout the LC separation. The data was analyzed and searched against human and/or *C. perfringens* databases using the SEQUEST search engine in the BioWorks Browser (Thermo Fisher Scientific). MS analysis was performed by the Proteomics Core Facility at the University of Pittsburgh.

Liquid Chromatography

Instrument: Surveyor Dual Pump LC (Thermo Fisher Scientific Corp., San Jose, CA)

Column: BioBasic C18 , 75μm ID x 100mm, PicoFrit Column (New Objective, Inc., Woburn, MA)

Trap: Peptide Cap Trap, (Michrom BioResources, Inc., Auburn CA)

Trapping Conditions: Flow rate: 10μl/min. @ 100% H_2O/0.1% formic acid

LC Conditions:

Flow rate: 160nl/min.

Ramp from 5% ACN up to 50% ACN in 25 min.

Ramp from 50% ACN up to 98% ACN in 5 min.

Hold for 5 min. @ 98% ACN/2% H2O/0.1% formic acid

Ramp from 98% ACN down to 5% ACN in 5 min.

Hold for 10 min. @ 95% H2O/5% ACN/0.1% formic acid

Mass Spectrometry

Instrument: LCQ DECA XP Plus (Thermo Fisher Scientific Corp., San Jose, CA)

Spray Source: Nanospray (Thermo Fisher Scientific Corp., San Jose, CA)

Source Conditions: Spray voltage: 1800 volts; Capillary Tube Temperature: 180^{o}C

Mass Spectrometer Method: MS scan followed by three MS/MS scans of the three most intense ions from the MS scan with dynamic exclusion.

MS Scan Acquisition: Scan type: Positive mode; Masses: 300 - 2000 Da

Data Dependent Acquisition:

Top three most intense peaks

Exclusion mass width (amu): 1.50

Dynamic exclusion enabled

Repeat Count: 2

Repeat Duration (min.): 0.50

Exclusion Duration (min.): 1.50

Exclusion Mass width (amu): 1.50

3.3 RESULTS

3.3.1 Purification of CPE Complexes

The first step in identifying the protein composition of CPE complexes is to purify each complex (CH-1 and CH-2) to homogeneity prior to analysis by mass spectrometry. Multiple strategies of purification were employed to determine the best method for this purpose. These methods include affinity purification, 2D-PAGE, and a combination of electroelution and immunoprecipitation. The results of each method will be discussed individually in this Section.

3.3.1.1 Affinity Purification

The first strategy used to purify the CH-1 and CH-2 complex was to affinity purify the complexes from Caco-2 cells that had been treated with a recombinant, his_{6X}-tagged CPE (rCPE). It was necessary then to first purify rCPE to homogeneity for treatment of Caco-2 cells. After induction of toxin expression in *E. coli* by addition of IPTG, a Ni^{2+}-affinity column was used to purify rCPE from bacterial lysates. Fig. 3.2A is a Coomassie stained gel which shows the collected fractions from the affinity column. Elutions 2 and 3 (lanes 6 and 7) shows the presence of highly purified rCPE which was used for treatment of Caco-2 cells.

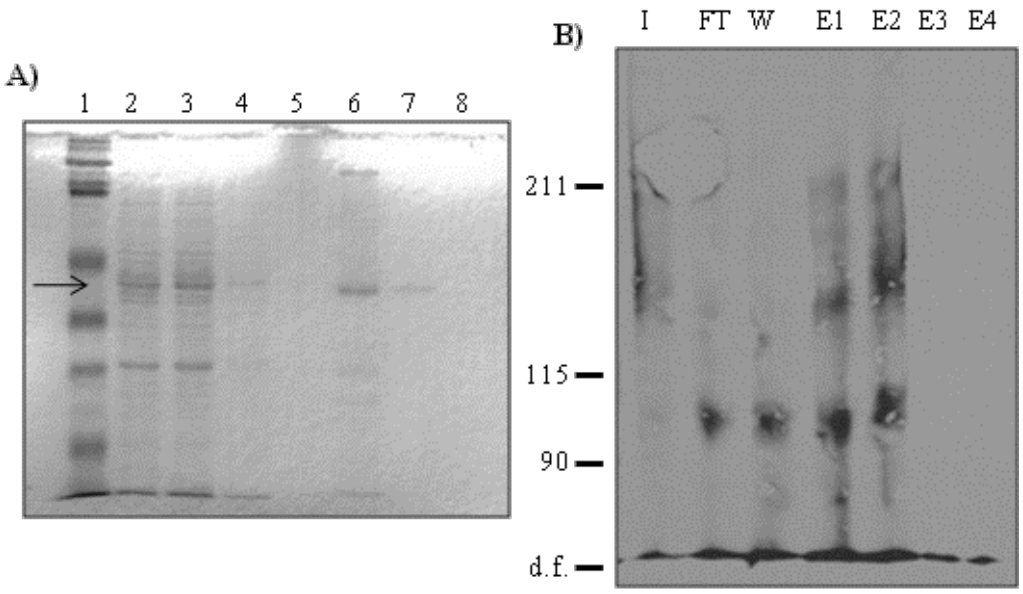

Figure 3.2 Affinity Purification of rCPE and rCPE-associated Complexes.
A) rCPE-expression *E. coli* lysates were added to a Ni^{2+}-affinity column and the flow through was collected (*lane 2*). *Lanes 3 and 4*: two washes with binding buffer. *Lanes 5-8*: Elution fractions 1-4. 10 µl of each fraction was loaded on a 12% SDS-PAGE gel followed by staining with Coomassie blue. Molecular weight marker was run in *Lane 1*. Arrow indicates migration of purified rCPE. B) anti-CPE Western blot of fractions from Ni^{2+}-affinity column in which TX-100 lysates of Caco-2 cells treated with rCPE were purified. "I" is the Input (Caco-2 treated cells) prior to addition to column. "FT" is the flow through from the column after addition of the Caco-2 cell lysate. "W" is a collected wash fraction. E1-4 are elutions from the column. Numbers on the left are molecular weight markers in kDa. d.f. is the migration of the dye front.

After successfully purifying his-tagged CPE, Caco-2 cells were treated with rCPE. CPE-treated Caco-2 cell lysates were then run through the Ni^{2+}-affinity column with the goal of binding his-tagged rCPE and any associated protein complexes that may be interacting with CPE on the membrane of cells. Western blot analysis (Fig. 3.2B) of fractions eluted from the affinity column shows the presence of CPE-immunoreactive high molecular weight complexes (E1 and E2). However, the sizes of these complexes are somewhat different than the sizes usually observed for the CH-1 and CH-2 complexes (Fig. 2.7). Additionally, there is a third complex of ~100 kDa that is not normally seen with nCPE treatment. When rCPE-treated Caco-2 TX-100 lysates are probed for CPE, the distinct CH-1 and CH-2 complexes are not observed (Fig. 3.2B,

"I"). A probable explanation for this is the inability of TX-100 to sufficiently extract the complexes from the membrane.

3.3.1.2 Electroelution and Immunoprecipiation

A common theme deduced from above is the poor extraction of CPE complexes using TX-100. Therefore, using SDS-PAGE as a first step of solubilization and separation was decided upon. Electroelution (EE) was used to accomplish this first step of this purification strategy. After CPE treatment of Caco-2 cells, lysates were run on SDS-PAGE and a small vertical slice of gel was then transferred and Western blotted to determine the migration of the CH-1 and CH-2. After lining up the Western blot with the preparative gel, the corresponding areas of the gel were excised and electroeluted. Electroeluted samples were concentrated and rerun on SDS-PAGE and Western blotted with an anti-CPE antibody (Fig. 3.3). The distinct separation of the CH-1 and CH-2 complexes is clearly seen after EE. It is also apparent that concentration of the samples is necessary.

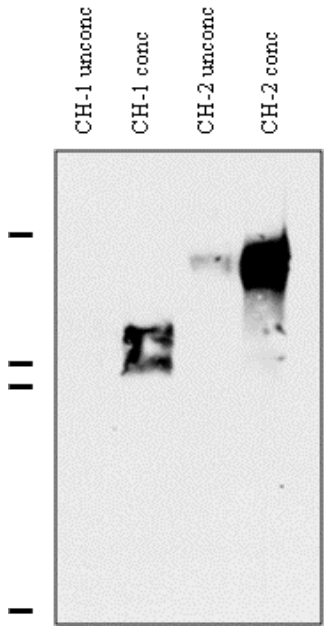

Figure 3.3 Electroelution of CH-1 and CH-2.
Ten 100 mm cell culture plates of Caco-2 cell monolayers were treated with 2.5 µg/ml of CPE for 45 min. After harvesting cells, lysates were run on a single-lane preparative 4% SDS-PAGE gel. After Western blotting to determine location of CH-1 and CH-2 bands, gel slices were electroeluted for 5 h. 25 µl of each CH-1 and CH-2 EE samples were collected (CH-1 unconc and CH-2 unconc). Samples were then concentrated using Amicon spin filters (~100X). 25µl of each sample (CH-1 conc and CH-2 conc) was run, along with unconcentrated samples, on 4% SDS-PAGE and Western blotted with a rabbit anti-CPE antibody.

To eliminate the need to perform Western blotting to determine the locations of the CH-1 and CH-2 bands, which can add significant time to the procedure, a fluorescently-labeled CPE was prepared to directly visualize the CH-1 and CH-2 bands on the preparative gel. CPE was labeled with the AlexaFluor488 dye (referred from now on as Alexa-CPE), which labels free amines. Gel filtration chromatography was performed to separate labeled protein from free label (Fig. 3.4A). Labeled CPE clearly elutes from the column in fraction #3, with nearly a 100% yield. This is distinct from free label which is only starting to come off the column at fractions 7 and 8. To test whether the toxin retains activity with the added label, Alexa-CPE was added to Caco-2 cells, and upon morphological analysis, labeled toxin was similarly cytotoxic as

compared to unlabeled CPE (data not shown). Caco-2 cells treated with Alexa-CPE were then lysed and run on SDS-PAGE to determine if CH-1 and CH-2 complexes are formed. Fig. 3.4B clearly shows the formation of both the CH-1 and CH-2 complexes (arrows). This was confirmed by performing Western blot analysis on the same Alexa-CPE-treated Caco-2 lysates with an anti-CPE antibody (Fig. 3.4C).

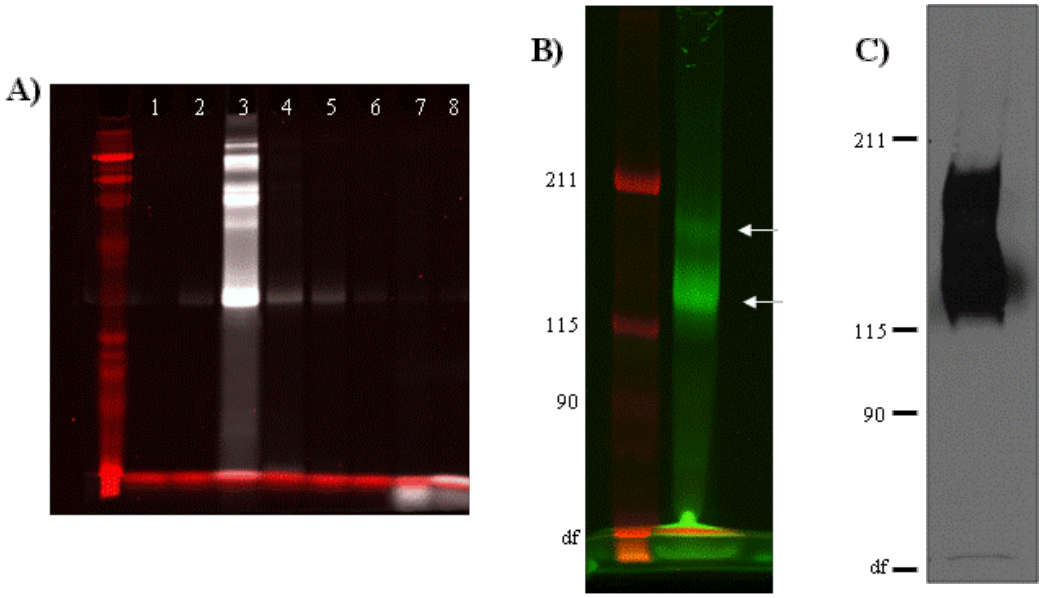

Figure 3.4 Purification and Complex Formation of AlexaFluor488-CPE.
A) Equal volumes of each fraction (#1-8) were loaded on a 12% SDS-PAGE gel. Gel was scanned using a Typhoon 9400 scanner. B) Caco-2 monolayers were treated with 2.5 μg/ml of Alexa-CPE for 45 min. The lysate was run on a 4% SDS-PAGE gel and scanned with a Typhoon 9400 scanner. Arrows indicate migration of the CH-1 and CH-2 complexes. C) Duplicate Alexa-CPE-treated Caco-2 cell lysates were run on 4% SDS-PAGE and Western blotted using a rabbit anti-CPE antibody. Numbers indicate molecular weight markers in kDa. d.f. is the migration of the dye front.

After establishing that the fluorescently-labeled CPE retains full cytotoxicity and the ability to form complexes, we proceeded with a full scale EE in which 30 150 mm plates of Caco-2 cells were treated with CPE and "spiked" with Alexa-CPE (the amount of unlabeled to labeled CPE was ~100:1). Caco-2 lysates were loaded onto a single-lane preparative gel and electrophoresed (Fig. 3.5) followed by Typhoon scanning. Corresponding bands for the CH-1 and CH-2 complexes were excised and were electroeluted and concentrated (data not shown).

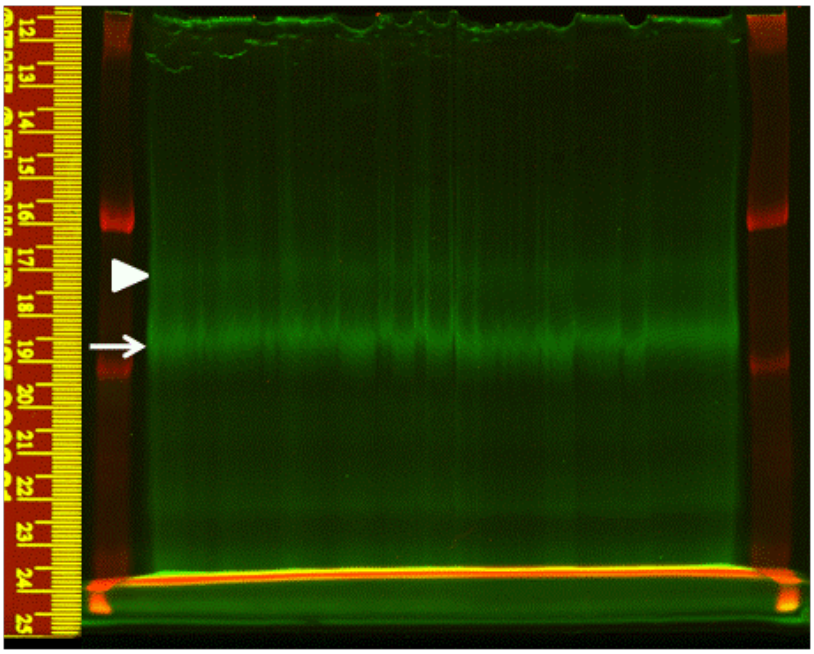

Figure 3.5 Large Scale Preparative Gel for Electroelution.
Lysates Caco-2 cells treated with 2.5 μg/ml of Alexa-CPE for 45 min were run on a single-lane 4% SDS-PAGE gel. The gel was then scanned using a Typhoon 9400 scanner. Arrow specifies migration of CH-1. Arrowhead indicates migration of the CH-2 complex.

Concentrated EE samples for each CH-1 and CH-2 were immunoprecipitated with an affinity-purified rabbit anti-CPE antibody (see Materials and Methods) and Protein A-agarose beads. Immunoprecipitated material was then run on SDS-PAGE and visualized by Typhoon scanning (Fig. 3.6A). Fluorescent complexes are visualized for both the CH-1 and CH-2 electroeluted samples. Peculiarly, the material immunoprecipitated from the CH-1 EE was at the same size as the material immunoprecipitated from the CH-2 EE. A possible explanation for this increase in size was due to the boiling of the samples that was necessary to dissociated immunoprecipitated material from the Protein A beads. Boiling has been known for some time to induce aggregation of purified CPE. Therefore, boiling might be inducing aggregation of the CPE-containing complexes as well. This was tested by simply taking CPE-treated Caco-2 cell lysates and boiling them, followed by SDS-PAGE and Western blot analysis. Fig. 3.6B shows that by simply boiling CPE complexes, only one band is present at a size that is similar to the

CH-2 band. In an IP experiment where only the CH-1 complex is present was used as the starting material (Fig. 3.6C, Input), after boiling there is an increase in its molecular weight (Fig. 3.6C, α-CPE IP). Boiling with DTT had no effect on the aggregated material. This suggests that boiling is causing aggregation of the CH-1 complex.

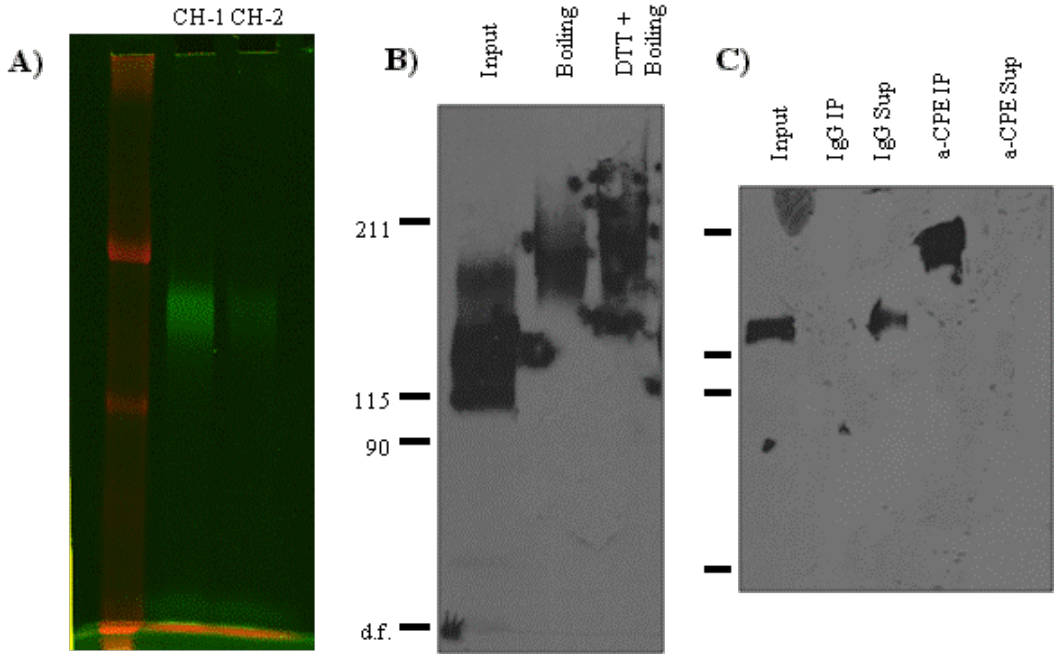

Figure 3.6 Immunoprecipitation of EE Samples.
A) Electroeluted CH-1 and CH-2 samples were immunoprecipitated with an affinity purified anti-CPE antibody. CPE-antibody complexes were pulled down with Protein A-agarose beads followed by boiling to dissociate CPE and associated proteins. Immunoprecipitated material was then loaded on a 4% SDS-PAGE gel and visualized by Typhoon scanning. B) Caco-2 cells were treated with nCPE and lysates were either boiled or not (Input). 4% SDS-PAGE and Western blotting was performed using a rabbit anti-CPE antibody. C) CPE-treated Caco-2 cells were lysed with RIPA buffer and either immunoprecipitated with rabbit IgG or affinity purified anti-CPE. IPs and supernatants were run on SDS-PAGE and Western blotted with a monoclonal anti-CPE antibody.

The two-step strategy of EE and IP established here appears to be a successful method of isolation and separation of the CH-1 and CH-2 complexes. Before analysis by mass spectrometry, we wished to quantify the amount of protein that was recovered by this method. To this end, a semi-quantitative Western blot was performed where a standard curve of known

CPE concentrations was generated to extrapolate and quantify the amount of CPE-immunoreactive protein in the recovered samples after EE and IP. From this analysis, it was calculated that we recovered ~700 ng of CPE protein, which equates to ~20 pmol of CPE.

3.3.2 Proteomic Analysis

The two-step strategy of EE/IP appears to be a useful method for the purification of the CH-1 and CH-2 complexes for analysis by MS. After running the CH-1 immunoprecipitated material on SDS-PAGE and determining its migration by fluorescence scanning, the CH-1 band was excised and in-gel trypsin digestion was performed as described in Materials and Methods. Tryptic peptides were then analyzed by LC-ESI MS/MS. Only one host protein was identified in the analysis (Appendix I, Table 1), and that was ribosome-binding protein 1 (RRBP1). As this protein in an ER-membrane bound protein (147), it is unlikely to associate with the CH-1 complex. Therefore, RRBP1 was not pursued further. Also of note is that when sequences were run through a *C. perfringens* database, CPE was identified in the analysis but with a low probability score of 1.0 (Appendix I, Table 2). As a control for the trypsin digestion procedure, 1 μg of each BSA and purified nCPE were digested by trypsin after SDS-PAGE and analyzed by MS. Results show protein good coverage and identification of both BSA and CPE (Appendix I, Table 3 and 4).

One of the possible explanations for the lack of meaningful data obtained from MS analysis was inefficient enzymatic digestion. Tryspin was initially used to produce peptides for analysis. A simple experiment was performed to determine how well trypsin dissociates the CPE complexes (Fig. 3.7A). CPE-treated Caco-2 lysates were digested with trypsin in a similar manner as performed prior to MS analysis. After trypsin treatment, lysates were run on SDS-

PAGE and Western blotted for CPE. The results in Fig. 3.7A show that the CH-1, and to some extent, the CH-2, are extremely resistant to trypsin digestion. There is some digestion as evidenced by significant smearing of the complexes. However, the majority of the complex formation remains intact. This could be a possible explanation, then, for the inability to obtain MS data from our EE/IP samples.

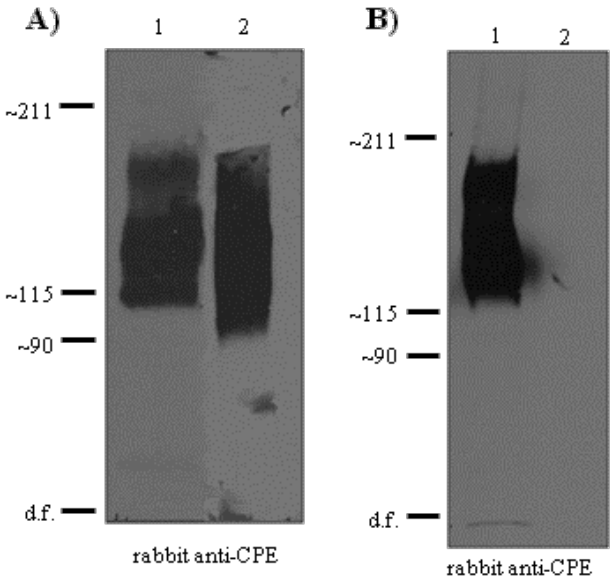

Figure 3.7 Sensitivity of CPE Complexes to Enzymatic Digestion.
A) Caco-2 monolayers were treated with 2.5 μg/ml of CPE for 45 min, harvested, and either mock treated (*Lane 1*) or treated (*Lane 2*) overnight with 1 μg/ml of trypsin at 37°C. SDS-PAGE and Western blotting was performed on treated samples. B) Caco-2 cells were treated with CPE as in *A*, and were either mock treated (*Lane 1)* or treated (*Lane 2*) overnight with 25 μg/ml of chymotrypsin at 37°C.

From the data in Fig. 3.7A it was apparent that trypsin digestion was not going to be useful for our MS studies. Therefore, we wanted to determine if another commonly used enzyme, chymotrypsin, is able to successfully digest the CPE complexes. In a similar experiment as performed in Fig. 3.7A, CPE-treated Caco-2 cells were treated with chymotrypsin, and the degree of complex digestion was measured by SDS-PAGE and Western blotting (Fig. 3.7B). The results from this experiment clearly indicate that complete digestion of the CH-1 and

CH-2 complexes is accomplished by chymotrypsin treatment (Fig. 3.7B, lane 2). This is in stark contrast to the ability of trypsin to digest the CPE complexes. After learning of the potential for chymotrypsin, the EE/IP procedure was repeated, however, in-gel digestion was performed with chymotrypsin as opposed to trypsin. Peptides were subsequently analyzed by LC-ESI MS/MS. Results from this analysis showed a number of potential proteins, however, all had very poor probability scores.

3.3.3 Tight Junction Protein Analysis

The hope in using MS analysis to identify proteins that associate with the CPE complexes was to avoid going on an "antibody fishing expedition" where antibody studies were performed for whichever proteins we decided to look for. However, with the minimal success we had with the MS studies, we decided to look specifically for a select few proteins in the tight junction that may be interacting with CPE and/or the CPE complexes. The first protein we investigated was JAM-A. Junctional Adhesion Molecule-A, or JAM-A, is a tight junction protein which serves to modulate many cellular functions including migration, polarity, paracellular permeability, and proliferation (171). These functions are mediated by the structural elements of JAM-A, such as the Ig-like folds and PDZ-binding domains, which serve to mediate intracellular signaling events. Immunoprecipitation and electroelution experiments were performed to determine whether JAM-A interacts with CPE and associates with the CH-1 and CH-2 complexes. Lysates of CPE-treated Caco-2 cells were immunoprecipitated with an affinity-purified anti-CPE antibody. Immunoprecipitated material was then probed for the presence of JAM-A which would indicate an association between CPE and JAM-A. Unfortunately, IP with CPE antibody did not pull-down JAM-A protein (data not shown). This was further shown and confirmed by

electroelution (Fig. 3.8). Caco-2 cells that were treated with CPE were lysed and run on SDS-PAGE, and after Western blotting to locate the migration of the CH-1 and CH-2 bands, corresponding gel slices were excised for the CH-1, CH-2, and dye front. These gel slices were then elecroeluted and concentrated. The concentrated EE samples were then treated with urea and boiled to dissociate protein complexes and run on 12% SDS-PAGE followed by Western blotting for CPE (Fig. 3.8A) or JAM-A (Fig. 3.8B). Fig. 3.8A shows the presence of CPE in all three EE samples (dye front, CH-1, and CH-2) as evidenced by the signal at ~35 kDa. Conversely, Western blot analysis of the EE samples for the presence of JAM-A reveals that there is no JAM-A present in either the CH-1 or CH-2 complexes (Fig. 3.8B). Caco-2 cells do express JAM-A as is evidenced by the presence of JAM-A in the dye front of EE samples (Fig. 3.8B). These experiments suggest that JAM-A does not interact with CPE or associate with the CPE complexes. Furthermore, similar IP and EE experiments were performed for another tight junction protein, MUPP1. The results from these experiments were similar to that of JAM-A and also suggested that CPE does not interact with or incorporate this protein into the CH-1 or CH-2 complexes (data not shown).

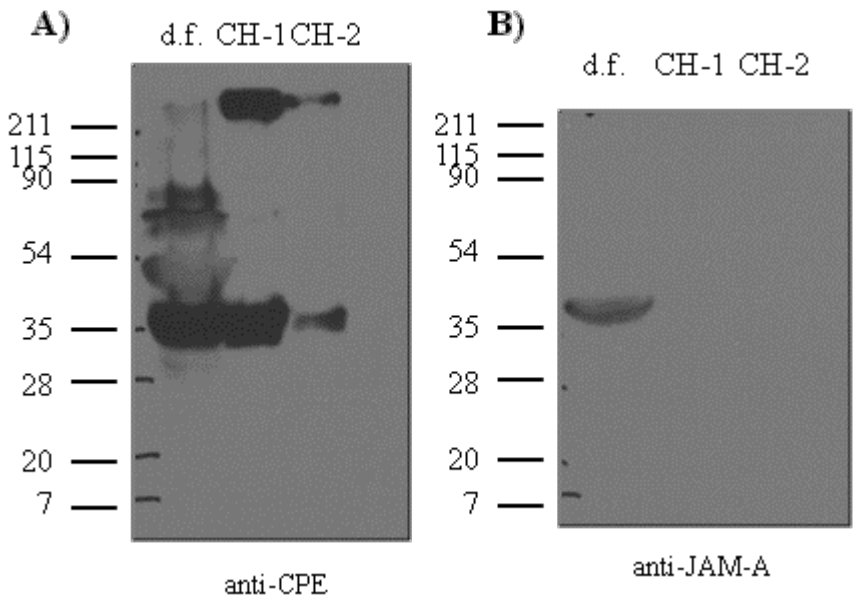

Figure 3.8 Electroelution of JAM-A.
Dye front (d.f.), CH-1, and CH-2 bands were electroeluted from gel slices of lysates of Caco-2 monolayers treated with 2.5 µg/ml of CPE for 45 min. After EE and concentration, each sample was treated with 10% SDS and 6 M urea, and boiled for 5 min to dissociate the complexes. Samples were run on a 12% SDS-PAGE gel in duplicate and transferred for Western blotting for CPE (A) or JAM-A (B).

The basis for this study partly stems from previous experiments that identified that both receptor and non-receptor claudins can be present in the CPE complexes (158). From this study by Robertson et al., it was determined that both claudin-3 and -4 (CPE receptors) and claudin-1 (a non-receptor) can be associated with the SC, CH-1 and CH-2. Because we were unable to detect the presence of other tight junction proteins (JAM-A or MUPP1) in these complexes, we wished to further the previous study by examining the association of other claudins with the CH-1 and CH-2. Electroelution was performed, as described above, for CPE-treated Caco-2 cells to determine if claudin-8 (a CPE binding capable claudin) is associated with CH-1 and/or CH-2. The results from Fig. 3.9 show that claudin-8 is expressed by Caco-2 cells as shown by immunoreactivity in the EE of dye front. Because of the intrinsic property of claudins to aggregate (133), immunoreactive bands are seen higher than the predicted molecular weight of

cldn-8 (~25 kDa). Furthermore, it is clear that cldn-8 is associated with the CH-1 complex. Additionally, there is a very small amount of cldn-8 that is present in the CH-2 complex (the band is very faint, but is present). The data presented in Fig. 3.9 show that, in addition to cldn-1, -3, and -4, cldn-8 can also be associated with the CPE complexes.

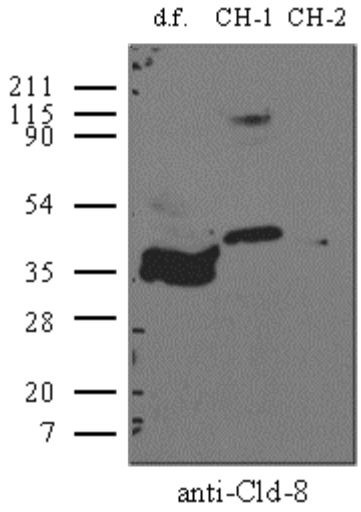

Figure 3.9 Electroelution of Claudin-8.
CPE treated Caco-2 lysates were electrophoresed on 4% SDS-PAGE and corresponding dye front (d.f.), CH-1, and CH-2 bands were excised and electroeluted and concentrated. Concentrated samples were run on 12% SDS-PAGE and Western blotted with a rabbit anti-Cldn-8 antibody. Numbers on the left are molecular weight markers in kDa.

3.4 DISCUSSION

Pore formation by CPE is mediated through large toxin-containing protein complexes on the membrane of target cells. These complexes represent the functional pore and induce ion permeability alterations in host cells. Much effort has been devoted to characterizing the biochemical interactions between CPE and host proteins and how the resultant complexes function on the membrane surface. Two large CPE-containing complexes were originally

identified, the ~155 kDa complex and the ~200 kDa complex, names based on the apparent size assessed by migration on SDS-PAGE (179). Under native conditions, however, the sizes of these complexes were reassessed to be ~450 kDa and ~600 kDa, respectively (158). Additionally, six copies of CPE were discovered to be present in each of these two large complexes, and therefore, the ~450 kDa complex was renamed as the CPE Hexamer-1 (CH-1), and the ~600 kDa complex was renamed CH-2. In addition to the six CPE molecules in each complex, both receptor and non-receptor claudins were found to be associated with the CH-1 and CH-2 (158), as well as the Small Complex. The observation that claudins can be present in all three CPE complexes suggests other TJ proteins may be associating with CPE. When one considers the complexity of the TJ (62), this is not an improbable presumption. Moreover, the TJ is increasingly being recognized as a target for pathogens and their products, such as bacterial toxins (63). We wished to develop a method for purification of CPE complexes for analysis by mass spectrometry to identify additional proteins that may compose the CPE complexes.

Multiple strategies were attempted to develop a useful method for CPE complex purification, and two of them have been discussed here (other methods included 2D-PAGE using Rotofor or IPG strips for isoelectric focusing). The first strategy employed was affinity purification using rCPE with a his-tag. A similar strategy has recently been used, except a GST tag was utilized (110). However, this study was not examining the composition of the CPE *complexes*, but rather was simply attempting to pull down claudins that were interacting with CPE and identify them by MS. This was partly the problem with the his-tagged rCPE method. We were unable to sufficiently extract CPE complexes from Caco-2 membranes that would allow for binding to the Ni^{2+} column. Another possible explanation for the inefficient

purification is that the his-tag is not sufficiently exposed to bind to the column after oligomerization into the large CPE complexes.

Our next purification method involved a two-step approach where CPE complexes were first isolated from treated Caco-2 cells by electroelution. The second step involved immunoprecipitation of CPE and associated complex proteins. With the addition of a fluorescently labeled CPE molecule, this procedure proved to be a very successful method for purification of the CH-1 and CH-2 complexes. Of particular importance, this method not only allows for purification of the complexes, but allows for purification of the complexes *individually*. This allows us to analyze the composition of each complex as opposed to simply determining what proteins are interacting with CPE. Although not attempted here, this procedure could also be utilized for the purification of the SC with the only major change being CPE treatment at 4°C. One possible drawback with this method is the amount of starting material required to get a yield that is compatible with the downstream MS analysis. The number of Caco-2 cells that was started with was ~10^7. This may be low for MS analysis, however, ~75 μg of CPE was used to treat these cells. The problem arises in that only ~1% of CPE binds to cells, which would be less than 1 μg of CPE to begin with. Perhaps increasing the input (number of cells) by at least 10-fold may increase level of material needed for MS.

Another hindrance that we encountered was the apparent resistance of the CH-1 and CH-2 complexes to digestion by trypsin. Although unfortunate, this finding was not totally surprising because we have found that to break apart these complexes it requires the addition of 10% SDS, 6M urea, and boiling (data not shown). It was shown, however, that CH-1 and CH-2 complexes are quite sensitive to chymotrypsin digestion. It may be that these complexes are too sensitive to chymotrypsin and overdigestion was accomplished. Limited chymotrypsin digestion

could be attempted to avoid this, as well as use of other digestion conditions such as using cyanogen bromide.

In lieu of MS, we performed some TJ protein antibody studies to examine the presence of these proteins in the CPE complexes. We found that neither JAM-A nor MUPP1 were present in the CH-1 or CH-2 complexes. Claudin-8, however, was found to be associated with CPE and the complexes. Cldn-8 was previously shown to be a somewhat weak CPE binder (100 times less binding affinity than cldn-3 or -4) (52). Although we were able to pull down cldn-8 with CPE by IP, it is not clear if this claudin is directly binding to CPE or is just loosely associated, as is the case with non-receptor claudins such as cldn-1 (158). Transfection of rat fibroblasts, which do not produce any claudins and are therefore CPE-insenstive, with just one claudin receptor become fully sensitive to CPE treatment (82, 157). Similar experiments are required, and are underway, for cldn-8 to determine if it is a functional receptor in the sense that it can mediate cytotoxicity when transfected into a naturally insensitive cell line. Up to this point, the claudin expression profile in Caco-2 cells has not been extensively studied. Currently, we know that cldn-1, -2, -3, -4, -6, -7, -8, and -14 are expressed in Caco-2 cells ((110, 158), Fig. 3.9, and unpublished results). Western blot and RT-PCR analyses are now being performed for all claudin family members to determine the full expression profile in Caco-2 cells. This is pertinent because from this study it now appears that claudins might be the only proteins associated with the CPE complexes. Any of the many claudins that may be expressed by Caco-2 cells may be associated with CPE.

CPE treatment by both non-toxic fragments and fully functional derivatives can result in the removal of proteins from the TJ (179, 187), an observation that has been exploited by researchers examining the use of CPE in drug delivery (42, 93). Another interesting question

regarding the claudin composition of CPE complexes is whether CPE treatment causes the incorporation of claudins from apposing cells as there is close interaction between neighboring claudin strands (Fig. 1.2). A co-culture experiment involving CPE treatment of transfectants expressing two different claudins would help to determine if CPE can pull claudins from neighboring cells. Rat fibroblasts do not express occludin, and therefore, do not form the CH-2 complexes upon CPE treatment, even when transfected to express receptor claudins. A similar co-culture experiment where one cell is expressing claudin and the other is expressing occludin would also be interesting to assess whether CPE also pulls occludin from adjacent cells.

4.0 DEVELOPMENT AND CHARACTERIZATION OF A MOUSE MODEL OF CPE-INDUCED INFLAMMATION AND DISEASE

4.1 INTRODUCTION AND RATIONALE

4.1.1 Cell Death Pathways Activated by CPE

As described above, in an *in vitro* Caco-2 cell model, CPE treatment can result in either apoptosis or oncosis depending on the toxin dose administered (32). A low CPE dose (1 μg/ml) results in the activation of the apoptotic pathway, while a high CPE dose (10 μg/ml) activates oncosis. Cell death at low doses, but not the high dose, could be inhibited by pre-treatment with caspase 3/7 inhibitors, confirming the activation of the classical apopotic pathway. However, the oncosis inhibitor, glycine, had the ability to inhibit cell death associated with the high CPE dose. This relationship is attributed to the levels of Ca^{2+} influx as a result of pore-formation, such that low toxin doses lead to a mild Ca^{2+} influx, whereas strong Ca^{2+} influx is a result of high toxin doses (31). An important distinction between apoptosis and oncosis is that inflammation is associated with oncosis while apoptosis is viewed as a non-inflammatory event (46). Epidemiological studies of human type A food poisoning outbreaks indicate that CPE can be present at concentrations ranging from <10 ng/ml to >100 μg/ml in the feces of patients (12, 15). This range of CPE concentration indicates that both apoptosis (non-inflammatory) and oncosis

(inflammatory) may be occurring during CPE-induced food poisoning. When histopathological damage is assessed in rabbit ileal loop models of CPE challenge, inflammatory infiltrates such as polymorphonuclear leukocytes are observed (125, 165).

4.1.2 Rationale

Despite the histological evidence for inflammation, the contribution of inflammatory cytokines to the local (intestinal) pathology in CPE-induced disease has not yet been examined. Generally speaking, inflammatory cytokines, such as TNFα, IL-1, IL-6, etc., have major effects on tight junction permeability by modulating expression patterns of various tight junction proteins and associated signaling molecules (5, 27). *C. difficile*, a close relative of *C. perfringens*, produces potent exotoxins in the gut (TcdA and TcdB) which are extremely pro-inflammatory. Therefore, it is plausible that CPE treatment results in the induction of inflammatory cytokines within the intestine. And it is the aim of this study to determine if cytokines are produced in response to CPE treatment in a novel mouse ileal loop model. Additionally, recent reports have indicated CPE in lethal cases of type A food poisoning (19, 155). Therefore, we wished to establish a mouse model of CPE action that mimics the lethality associated with CPE-associated disease. Finally, despite significant evidence for the role of CPE complex formation *in vitro* for CPE-induced cytotoxicity, this has not been demonstrated *in vivo*. The establishment of this mouse model also enables us to assess the ability of CPE to form toxin-containing complexes *in vivo*.

4.2 MATERIALS AND METHODS

4.2.1 Purification of CPE

Native enterotoxin was purified from *C. perfringens* strain NCTC 8239 as previously described (127). Briefly, strain NCTC 8239 is grown overnight in 20 L of Duncan-Strong Media to induce sporulation and production of CPE. Prior to the completion of sporulation, sporulating cultures are spun down to harvest CPE-producing bacteria. Pellets are resuspended in S200 Buffer (75 mM potassium phosphate, pH 6.8) and sonicated to release CPE. Precipitation of CPE is accomplished by addition of ammonium sulfate, and precipitated protein is run on a S200 gel filtration column. After chromatography, fractions are analyzed for the presence of CPE and CPE-containing fractions are combined and dialyzed against ddH_2O (pH 7.0). Following dialysis, purified toxin is lyophilized and stored.

4.2.2 Purification of Neutralizing Monoclonal Antibody

The monoclonal antibody (Mab2) used for loop neutralization and passive immunization experiments was purified from mouse ascites fluid, previously produced and characterized (218). Purification was performed using a pre-poured 1 ml Protein G chromatography column crosslinked to 6% agarose beads (Pierce) according to the manufacturer's instructions. Five milliliters of acites fluid was diluted 1:1 with Binding Buffer (50 mM sodium acetate, pH 5.0). To avoid clogging of the purification column, diluted fluid was filtered using 0.45 μm syringe filters. Using the Luer-Lok adapter system, a syringe filled with 10 column volumes (10 ml) of Binding Buffer was attached to the column, and to equilibrate the column Binding Buffer was

flowed through the column at a rate of ~1 ml/min. After equilibration, diluted ascites fluid was added through the column at a rate of ~1 ml/min. The column was then washed with 10 ml of Binding Buffer. Bound antibody was eluted from the column using 5 ml of Elution Buffer (0.1M Glycine, pH 2.0). Prior to elution, 500 µl of 1M Tris, pH 8.0 was added to the collection tube to neutralize the low pH of the Elution Buffer.

4.2.3 Animals and Ileal Loop Challenge

Male or female, 20 to 25 g Balb C mice were used. Mice were fasted 24 h before inoculation, but allowed access to water up to 1 h before the start of the experiments. Their abdomens were disinfected with iodine solution (Betadine, Purdue Pharma LP, Connecticut) immediately before surgery. The animals were anesthetized by intraperitoneal administration of Avertine (Winthrop Laboratories, New York). A midline laparotomy was performed and A ~ 5 cm long intestinal loop was prepared in the jejunum of each animal by double ligation of the intestine. Care was taken to avoid interfering with the blood supply. CPE or buffer was injected into each loop. Controls included in this assay consisted of replacement of CPE by buffer. The injections were performed by insertion of a 0.5-in., 27-gauge needle oblique to the intestinal lumen in a direction away from the stomach. After inoculation, the incision in the peritoneum, abdominal muscles and skin was sutured in one plane using super glue (Henkel Corporation, Avon, Ohio). The surgical procedure lasted approximately 3 min per animal.

The animals were kept anesthetized until they were euthanized at 2, 3 or 4 hrs after surgery, or until they died spontaneously. In those mice that survived until the end of the experiment, a blood sample was collected by cardiac punction. The serum was separated by

centrifugation and used for a trace element screen including potassium, sodium, as described below.

Euthanasia was performed by neck dislocation. The intestinal loops were removed; the length was measured and the content weighed. A weight/length ratio was calculated. The content of the loops plus specimens of intestinal loop tissue, liver and kidney were collected and frozen at -80 C until processing for analysis for ELISA and Complex formation.

Also, the gastrointestinal tract, brain, kidneys, lungs, heart, spleen and liver were collected and fixed by immersion in 10% formalin at pH 7.2 for a minimum of 24 h, before being processed routinely to obtain 4 μm thick sections which were stained with hematoxylin and eosin.

All procedures involving animals were reviewed and approved by the University of California, Davis Committee for Animal Care and Use (permit 04-11593). All animal surgeries were performed by Dr. Francisco Uzal and Juliann Saputo at the California Animal Health and Food Safety Laboratory.

4.2.4 Measurement of Cytokine Production

Cytokine production was measured from homogenized intestinal tissue supernatants. Intestinal tissue (0.07 g) from control mice, 50 μg, 100 μg, and 200 μg dose groups was homogenized by sonication (Misonix Sonicator 3000, output 2.5) with 3 10 second pulses in 0.5 ml Homogenization Buffer (Phosphate Buffered Saline containing: 0.4 M NaCl, 0.05% Tween-20, 0.5% BSA, 10 mM EDTA, and Protease Inhibitor Cocktail (GE)). Insoluble material was spun down by centrifugation at 1000 x g for 3 min. Supernatants were then used for detection of mouse IL-1β and IL-6 by ELISA using commercially available kits (CytoSet, Invitrogen)

according to manufacturer's instructions with some modifications. Immulon 1B plates (VWR) were coated overnight at 4°C with 100 µl of coating antibody at a final concentration of 1.25 µg/ml in Coating Buffer (50 mM sodium carbonate/bicarbonate, pH 9.4). After coating, wells were washed 4X with Wash Buffer (150 mM NaCl, 0.1% Tween-20, pH 7.4). Plate was then blocked with 100 µl Assay Buffer (PBS, 0.5% BSA, 0.1% Tween-20, pH 7.4) for 1 h at room temperature (RT) followed by 4 washes. Supernatants from homogenized tissue were diluted 1:4 in Assay buffer, and 100 µl of each sample, and cytokine standards, was added to plate and incubated for 2 h at RT. After 2 h incubation and washing, 100 µl of detection antibody was added at a final concentration of 0.125 µg/ml (anti-IL-1β biotin) or 0.05 µg/ml (anti-IL-6 biotin) in Assay Buffer and incubated for 2 h at RT. After 4 wash steps, 100 µl of streptavidin-HRP at a final concentration of 0.15 µg/ml (IL-1β) or 0.05 (IL-6) in Assay buffer and incubated for 30 min at RT. Wells were washed 4X, and 100 µl of 1-Step Ultra-TMB substrate (Pierce) was incubated in each well for 15 min at RT. The reaction was stopped by the addition of 100 µl 2M sulfuric acid. The plate was read in a microplate reader at 450 nm. The absorbances of cytokine standards were plotted against known concentrations to obtain a standard curve and the equation of the line of best fit to calculate the concentration of experimental samples.

4.2.5 Assessment of CPE Complex Formation in Tissues

To assess CPE binding and complex formation in intestinal, liver, and kidney tissue from mice that had been loop challenged with CPE, equal amounts of tissue (0.05 g) were homogenized in 0.5 ml RIPA Buffer (50 mM Tris, 1% NP-40, 0.25% sodium deoxycholate, 150 mM NaCl, 1 mM EDTA, Protease Inhibitor Cocktail, pH 7.4) + 5 µl benzonase (EMD Novagen) by sonication (as above). 25 µl of homogenates were added to 25 µl of 2X Laemmli Buffer, and

samples were loaded on 4% SDS-PAGE gels, followed by transfer to nitrocellulose membrane and Western blotting with a rabbit polyclonal anti-CPE antibody.

To assess the ability of CPE to form complexes in cell suspensions of intestinal, liver, and kidney tissues, equal amounts of tissue (0.05 g) from untreated mice were homogenized in 0.5 ml of Homogenization Buffer. Protein concentration was measured using BCA Kit (Pierce), and it was determined that equal amounts of total protein (400-500 μg) was present in each tissue. 100 μl of each homogenate was transferred to an eppendorf tube, and 2.5 μg/ml of CPE was added to each CPE-treated sample, or left untreated for control samples. Cell suspensions were incubated for 30 min with gentle rotation at 37°C. Samples were spun down in a microcentrigute at full speed for 5 min to pellet material. Pellets were washed 2X with PBS, and after final wash pellets were resuspended in 25 μl of PBS + 1 μl benzonase and then 25 μl of 2X Laemmli Buffer was added to each sample. 25 μl of each sample was analyzed by SDS-PAGE and Western blotting as above.

4.2.6 Measuring CPE in Serum

Mouse serum was analyzed for the presence of CPE by a sandwich ELISA which was developed for the first time in this current study. Wells of an Immulon 1B plate were coated overnight with 50 μl of a mouse anti-CPE antibody (Mab2, see above) diluted in PBS (pH 7.4) to a final concentration of 2 μg/ml. After coating, the plate was washed 4X with Wash Buffer and blocked with 50 μl of Assay Buffer for 1 h at RT. Following the blocking step and 4 washes, 50 μl of the serum samples and CPE standards were added to the plate and incubated for 2 h at RT. After 4 washes, an affinity purified rabbit anti-CPE antibody (purified from CPE rabbit anti-sera using Protein A columns (Pierce)) at a final concentration of 1 μg/ml and incubated for 2 h at RT.

After washing, an anti-rabbit-HRP conjugate (Sigma) secondary antibody was added at 1:30,000 in Assay Buffer and incubated for 1 h at RT. Following washing, TMB substrate was added for 15 min and 2M sulfuric acid was added to stop the reaction. Absorbance was read at 450 nm on a microplate reader. The absorbances of CPE standards were plotted against known concentrations to obtain a standard curve and the equation of the line of best fit to calculate the concentration of unknown serum samples.

4.2.7 CPE Treatment of HUVEC and MDCK Cells

HUVEC cells were maintained in M200 media (Invitrogen) supplemented with Low Serum Growth Supplement Kit (Invitrogen, containing 2% FBS, 1 μg/ml hydrocortisone, 10 ng/ml human epidermal growth factor, 3 ng/ml basic fibroblast growth factor, 10 μg/ml heparin, and gentamicin) at 37°C with 5% CO_2. MDCK cells were cultured in DMEM with glutamine (Invitrogen) supplemented with 10% FBS and grown at 37°C with 5% CO_2. For CPE treatment, cells were seeded at a density of 1 x 10^5 cells/ml in 60 mm cell culture dishes. When reaching confluency (4-5 days), monolayers were washed 2X with HBSS with Ca^{2+} (cHBSS) and CPE (2.5 μg/ml for MDCK; 0.5 μg/ml, 1.0 μg/ml, or 2.5 μg/ml for HUVEC) was added to the cells and incubated for 45 minutes (MDCK) or 6 h (HUVEC) at 37°C. For MDCK cells, images of the plates were captured at 10, 30, and 45 min. For HUVEC cells, pictures were taken every 15 minutes for the first hour of treatment, and then once every hour after that. After CPE treatment, cells were harvested by gentle scraping, pelleted by centrifugation, and washed 2X with cHBSS. Pellets were resuspended in 50 μl cHBSS + benzonase, and 50 μl of 2X Laemmli Buffer was added. 25 μl of samples were analyzed by 4% SDS-PAGE and Western blot as above.

4.2.8 Trace Element Screen

The Trace Element Screen was performed by Dr. Birgit Puschner in the Veterinary Toxicology Lab at the CA Animal Health and Food Safety Laboratory System. Serum was collected from mice at indicated times after intestinal loop treatment and was analyzed by ICP-AES. Zinc, copper, iron, magnesium, sodium, phosphorus, calcium and potassium levels were measured in serum samples utilizing inductively coupled argon plasma emission spectrometer (FISONS, Accuris Model, Thermo Optek Corporation, Franklin, MA) (129). After precipitation of proteins, the protein-free supernatant of each sample were analyzed simultaneously for the listed trace elements. Accuracy of ICP results for these elements was measured by analyzing quality assurance sera obtained from the Veterinary Laboratory Association Quality Assurance Program (Genzyme Diagnostics, Blaine, MD, USA). Data were accepted if analyzed quality assurance serum values were within 2 standard deviations of the reference values.

4.3 RESULTS

4.3.1 Assessment of CPE-induced Cytokine Release

To assess the ability of CPE to induce a localized inflammatory event, we wished to measure the ability of CPE to elicit the release of inflammatory cytokines in an *in vivo* intestinal challenge animal model. To study the various aspects of CPE pathogenesis *in vivo*, rabbit ileal loops have been and are currently the most commonly employed animal model (125, 165, 173, 183). Unfortunately, reagents (i.e. antibodies) against proteins of rabbit origin are not readily available

to analyze the presence of cytokines. We, therefore, wished to assess cytokine production in a more suitable animal model by using a mouse intestinal loop model. The only published report using mouse ileal loops to assess CPE pathogenesis was from a Japanese group in 1979 (220), so we first needed to develop a mouse model of our own (see Materials and Methods).

Ligated intestinal loops were challenged with buffer control (HBSS), 50 μg, 100 μg, or 200 μg of CPE for 2 h, and intestinal fluid, intestinal tissue, and serum was collected from the animals. Intestinal fluid and serum was analyzed by ELISA for the presence of the proinflammatory cytokines, IL-1β and IL-6. No appreciable levels of either cytokine were detected in our ELISA assays (data not shown). Additionally, intestinal fluid and serum were further analyzed for cytokine production by a Luminex multiplex assay for the presence of 10 different cytokines (GM-CSF, IL-1β, IL-2, IL-4, IL-5, IL-6, IL-10, IL-12 (p40/p70), IFN-γ and TNF-α). Again, no significant production of cytokines was detected in these samples (data not shown, most analytes were out of the range of detection). We next analyzed homogenized intestinal tissue from control and CPE-treated loops and assayed for IL-1β and IL-6 production by ELISA. Fig. 4.1A shows a dose-dependent increase in IL-1β production after CPE treatment. At this 2 h time point, the 50 μg dose did not induce production of IL-1β in animals as compared to buffer control animals. The 100 μg dose induced a 2-fold increase in IL-1β production, however, it did not reach statistical significance. However, the 200 μg dose did induced a statistically significant increase of ~10-fold in IL-1β production ($p<0.02$), at a value of ~130 pg/ml. A similar result is observed for IL-6 production; CPE elicited an increase in IL-6 production in a dose-dependent manner (Fig. 4.1B). For this cytokine, the increase is more pronounced for the 100 μg dose as compared with IL-1β with both the 100 μg and 200 μg doses producing ~4-fold more IL-6 than animals challenged with 50 μg of CPE.

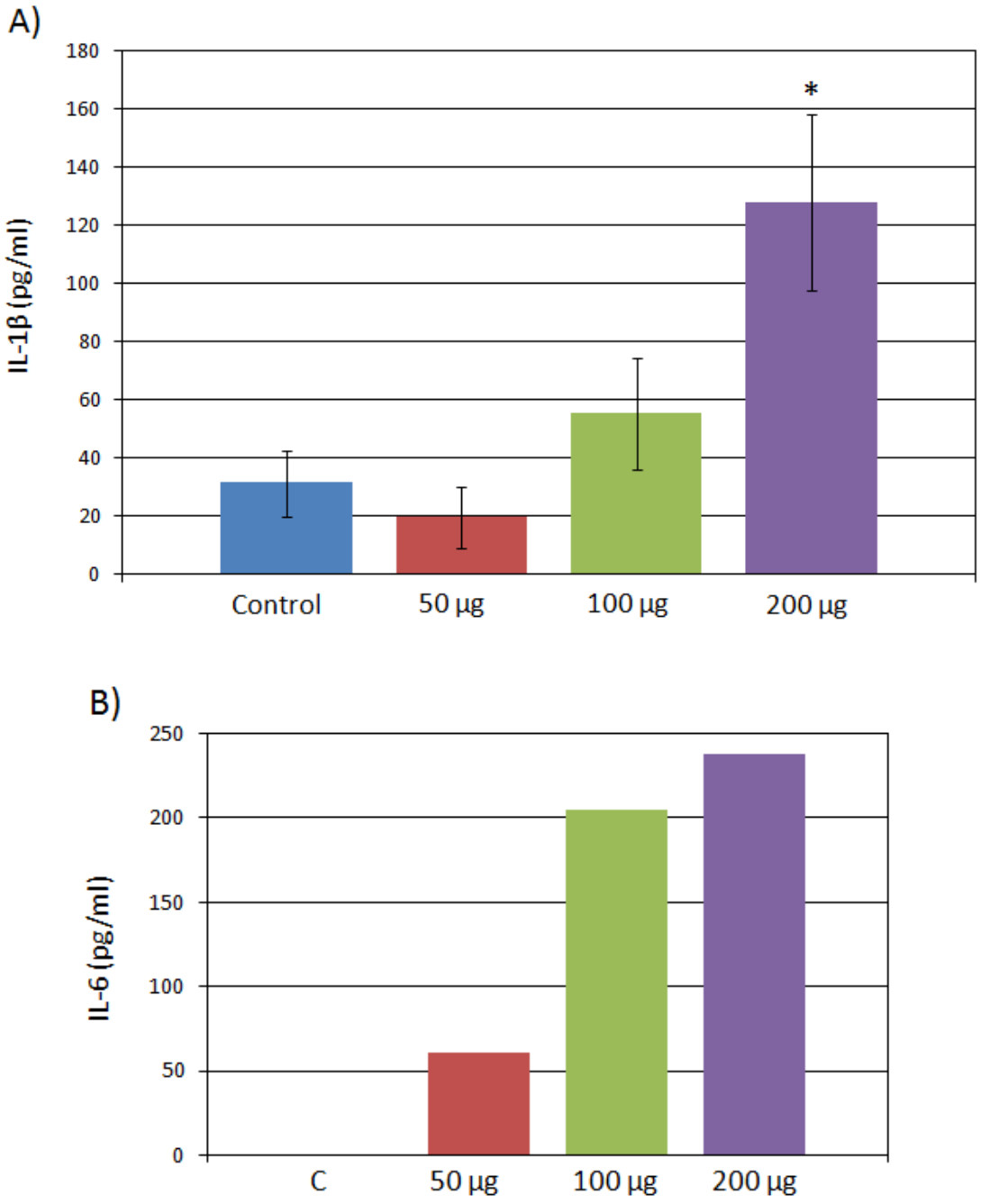

Figure 4.1 Induction of Proinflammatory Cytokines by CPE.
Homogenates of intestinal loops treated for 2 h with buffer control, 50 µg, 100 µg, and 200 µg of CPE were analyzed for the presence of IL-1β (A) and IL-6 (B) by ELISA as described in Materials and Methods. *p=0.02.

4.3.2 Formation of CPE Complexes in vivo

Using cell culture models, such as Vero and Caco-2 cells, it has long been established that CPE forms large molecular weight complexes on the membrane surface of target cells (88, 158, 178). Additionally, the formation of these complexes is necessary for the pore-forming activity of the toxin (122), allowing permeability alterations to occur. As evidenced by fluid accumulation seen in rabbit ileal loop models, these same permeability alterations observed in cell culture are also seen *in vivo* (125, 165). Additionally, direct binding of CPE to intestinal tissue has been observed *in vivo* in rabbit ileal loops as well as *ex vivo* to human ileum (45, 183). Despite this, formation of CPE complexes has never been observed *in vivo*. Therefore, we sought to analyze CPE-treated mouse intestinal loops for the presence of CPE complex formation. Intestinal tissue from CPE-treated mice was homogenized in detergent and lysates were analyzed by SDS-PAGE and Western blotting. Results from Fig. 4.2A demonstrate the ability of CPE to form large complexes *in vivo*. There is formation of a large CPE-containing complex of a molecular weight very similar to the CH-1 complex observed in Caco-2 cells. A second complex of higher molecular weight is also observed reminiscent of the CH-2 complex. However, this second complex is smaller than the CH-2 complex that is observed to form in Caco-2 cells. Despite the discrepancies in sizes of the complexes observed as compared to those seen in cell culture models, this is a novel finding in that it is the first time larger molecular weight CPE complexes have been observed *in vivo*. Furthermore, intestinal tissue from untreated mice was homogenized and subsequently treated in a cell suspension with 2.5 μg/ml of CPE for 30 min (Fig. 4.2B). After treatment, we are able to see the formation of the CH-1 complex. However, no CH-2 complex was observed in this experiment.

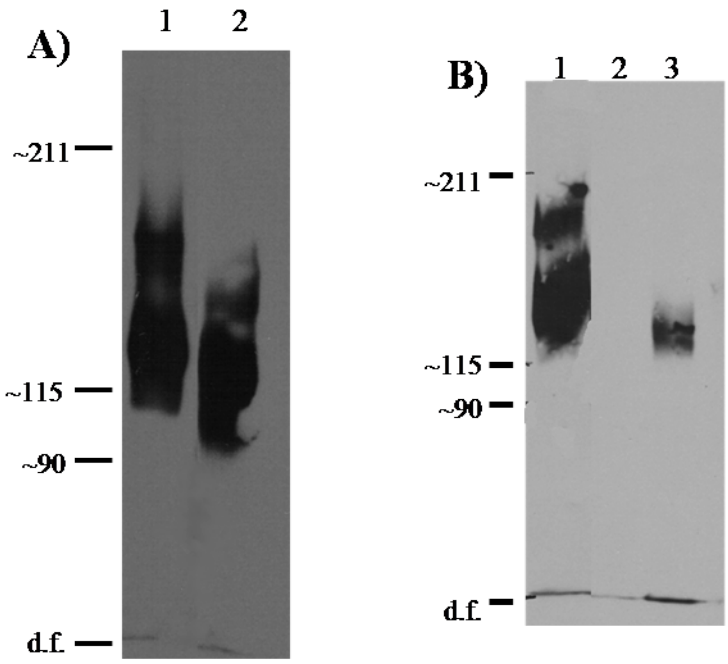

Figure 4.2 Formation of CPE Complexes in the Mouse Intestine.
A) *Lane 1*: SDS Lysates of Caco-2 cell monolayers treated with 2.5 μg/ml of CPE for 45 min, and *Lane 2*: RIPA homogenate lysates of mouse intestinal loops treated with 200 μg of CPE for 2 h were analyzed by SDS-PAGE and Western blotted using a polyclonal rabbit anti-CPE antibody. B) *Lane 1*: Lysates of Caco-2 cell monolayers treated with 2.5 μg/ml of CPE for 45 min, *Lanes 2 & 3*: Cell suspensions of homogenized control mouse intestines were either left untreated (*Lane 2*) or treated with 2.5 μg/ml of CPE for 30 min (*Lane 3*). Lysates were analyzed by SDS-PAGE and Western blot as in A). Numbers on the left represent molecular weight markers in kDa. d.f. indicates the migration of the dye front of the gel.

4.3.3 Mouse Survival in the Intestinal Loop Model

This study has provided some novel findings up to this point. We have established that CPE induces the expression of inflammatory cytokines and that CPE can form high molecular weight complexes *in vivo*. An intriguing observation was made when we examined the survival of the mice used in our intestinal loop model (Table 4.1). When mice were challenged with CPE for 2 h there was complete survival at all doses (control, 50 μg, 100 μg, and 200 μg). Interestingly, we observed a high mortality rate in mice at the 4 h time point with the administration of higher

doses of CPE (100 μg and 200 μg). Full survival was seen for mice treated with buffer alone or the lower 50 μg CPE dose.

Table 4.1 Survival of Intestinal Loop-Challenged Mice

	2 h				4 h			
Treatment	**Control**	**50 μg**	**100 μg**	**200 μg**	**Control**	**50 μg**	**100 μg**	**200 μg**
No. Survival	4/4	3/3	3/3	3/3	7/7	8/8	2/8	1/8
Percent Survival	100	100	100	100	100	100	25	12.5

This low survival effect in mice at the 4 h time point with the CPE high doses was reversed when CPE was pre-incubated with a neutralizing monoclonal antibody before administration into the intestinal loop (Table 4.2). All mice (4/4) survived with this CPE neutralization experiment when challenged with 200 μg of CPE for 4 h. This suggested that the death we were observing required the intestinal activity of CPE, and presumably the pathological effects due to CPE action, i.e. villous blunting and epithelial desquamation. What was particularly striking was the effect we observed when mice were administered the neutralizing monoclonal antibody by the IV route prior to CPE challenge via the intestinal loop model (Table 4.2). Similar to the neutralizing experiment, survival of mice was fully restored with this systemic immunoprotection treatment. The results from this immunoprotection experiment suggested that there may be a systemic component behind the high lethality observed, possibly due to CPE gaining access to the blood.

Table 4.2 Neutralization and Immunoprotection of Mice

Treatment	Survival
mAb Neutralization*	4/4
mAb Protection**	4/4

*Pre-incubation of mAb prior with 200 μg of CPE to 4 h loop challenge
**IV administration of mAb prior to 4 h loop challenge with 200 μg of CPE

4.3.4 Histopathological Effects of Mouse Lethality Model

As suggested above, the lethality observed appears to be dose-dependent. Furthermore, the neutralization of CPE prior to intestinal challenge seems to prevent the observed lethality in our mouse model. This suggests that intestinal damage may be contributing to lethality in some manner. We, therefore, wished to analyze histological damage in our model at the various doses. Histology of control loops (Fig. 4.3A) show healthy villi and crypts with no significant damage. A small amount of shortening of the villi was observed with 50 μg of CPE at the 2 h time point (Fig. 4.3B), but ~75% of the villi remained intact. In contrast, severe histological damage was observed by 2 h for the 100 μg and 200 μg doses (Fig 4.3C and D). Desquamation and necrosis of the epithelium, necrosis of the lamina propria, and severe blunting of the villi was observed for these higher doses. No evidence of edema was observed. A summary of the histological observations is shown in Table 4.3. Figure 4.4 graphically represents the overall severity of the lesions observed, taking into consideration all of the criteria outlined in Table 4.3. All three doses (50 μg, 100 μg, and 200 μg) are statistically more severe as compared to buffer control treatment ($p<0.01$ for 50 μg, $p<0.001$ for 100 μg and 200 μg). Additionally, both the 100 μg and 200 μg histology scores are statistically more severe than the 50 μg dose ($p<0.02$). However, there is no statistical difference between the 100 μg and 200 μg dose. In general, there is an obvious dose-dependent relationship between overall histological damage and dose of CPE administered into the intestinal loops.

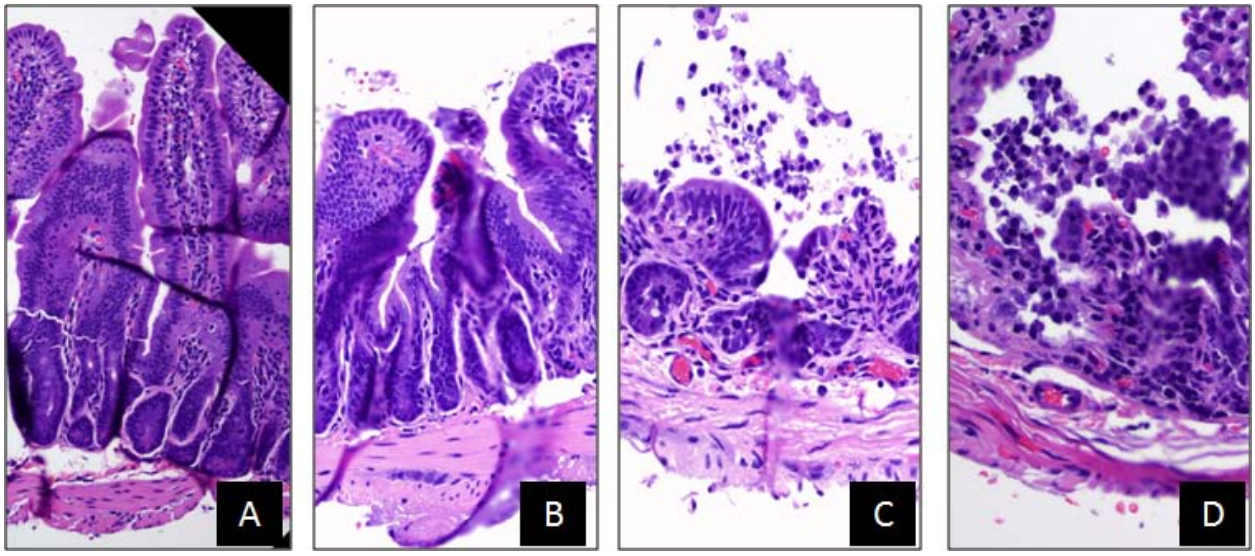

Figure 4.3 Histolopathogy Induced by CPE Doses.
After 2 h of treatment, loop tissues were formalin fixed and embedded in paraffin. Hematoxylin and eosin was used to stain 4 mm-thick sections of intestinal tissue treated with buffer control (A), 50 µg (B), 100 µg (C), or 200 µg (D). In each panel, L represents the intestinal lumen, while LP identifies the lamina propria. Final magnification of each photomicrograph, 400X. Histology was performed by Dr. Francisco Uzal.

Table 4.3 Scoring of Individual Histological Criteria for CPE Doses

Inoculum	Desquamation epithelium	Necrosis epithelium	Necrosis lamina propria	Inflammation	Dilated lymphatics	Edema	Villous blunting	Overall severity of lesions
Control	-	-	-	-	-	-	-	-
15 µg	-	-	-	-	-	-	-	-
50 µg	+	+	+	-	-	-	+	+
100 µg	+++	+++	+++	-	-	-	++	+++
200 µg	++++	++++	++++	+	-	-	+++	++++

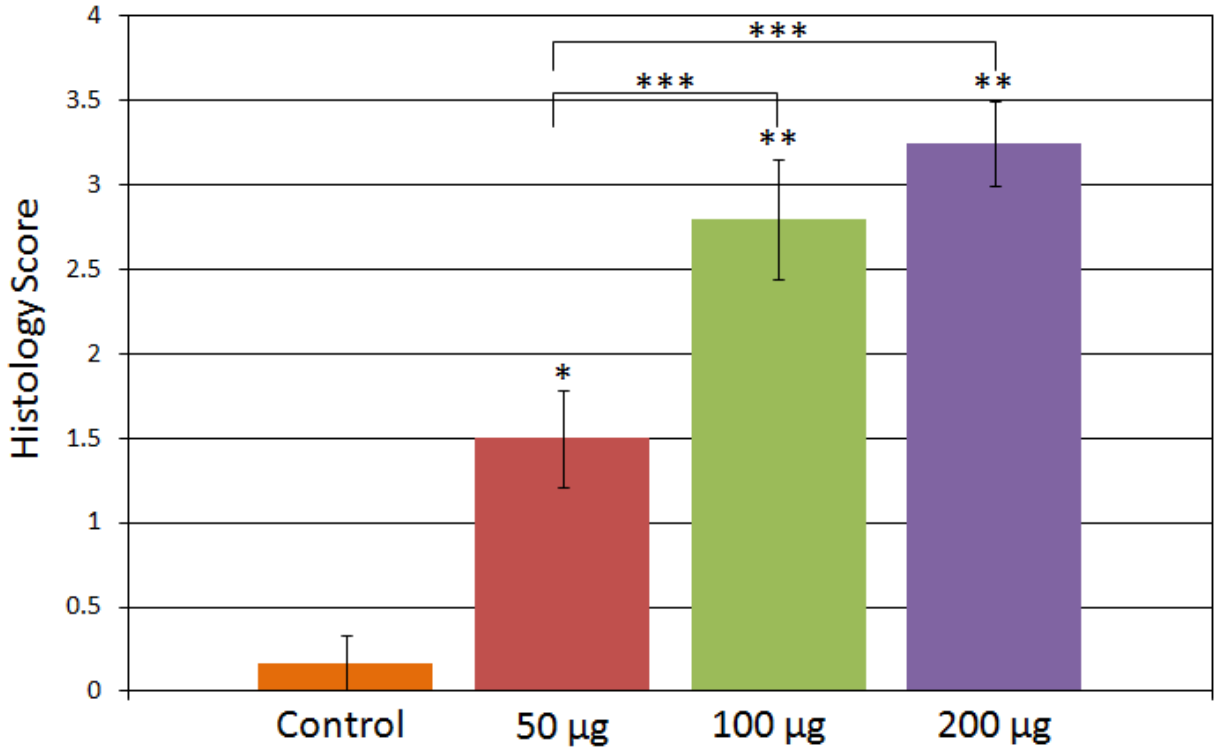

Figure 4.4 Overall Histology Score.
Taking into consideration the criteria from Table 4.3, an overall score of severity of histopathological damage was determined. Histology scoring was performed blind by a veterinary pathologist and was based on a scale of 0 to 4, with 4 being the most severe. Data is the mean of 4 mice per group (Control, 50 µg, 100 µg, 200 µg) after 2 h of loop challenge. Error bars represent the standard error of the mean. *p<0.01, **p<0.001, ***p<0.02. Histology was performed by Dr. Francisco Uzal.

4.3.5 CPE Gains Access to the Circulation

A recent epidemiology survey (19) of a food poisoning outbreak in Oklahoma at a residential care facility for mentally ill patients in 2001 was performed in 2 deaths were described and attributed to contamination by *cpe*$^{+}$ type A *C. perfringens*. Upon histological analysis, severe necrosis of the colons of those patients that died was observed (Fig. 4.5A). The intestines of our mice had a similar phenotype in which punctuate areas of hemorrhaging can be seen (Fig. 4.5B), possibly a precursor to the severe necrosis seen in the Oklahoma patients. The authors

concluded that the outstanding risk factor for these deaths was due to the constipation and fecal impaction as a result of the psychiatric medications the patients were taking. It is thought that this constipation and fecal impaction impeded the ability of these individuals to flush out the released CPE in the intestine as usually accomplished through diarrhea. As a result, CPE accumulated within the intestine, causing severe damage. Ultimately, the authors conclude, this possibly led to the ability of CPE to cross the intestinal barrier and gain access to the blood stream, which caused the death of these individuals. We, therefore, wished to explore this as a possible mechanism of lethality that we are observing in our mouse model.

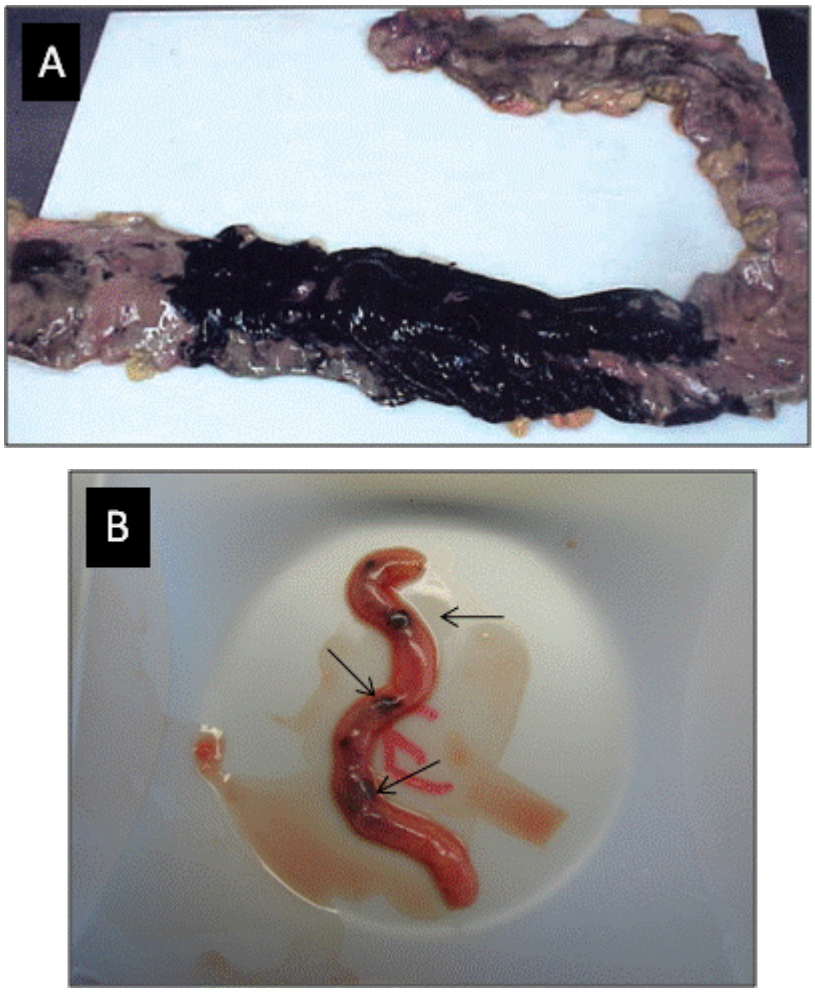

Figure 4.5 Intestinal Gross Pathology.
A) Gross pathology of the colon of a patient that died from the Oklahoma outbreak reveals a large region of black, necrotic lesions. Unaffected areas do exist. Reproduced from (19). B) A representative

intestinal loop (from a mouse treated with 100 μg of CPE for 2 h) reveals punctuate areas of hemorrhaging (arrows).

To this end, we analyzed the ability of CPE to gain access to the bloodstream. For this, we analyzed serum collected from mice treated with varying doses of CPE for 2 h in the intestinal loop challenge model. Serum was analyzed by an in-house developed sandwich ELISA for the presence of CPE after intestinal loop challenge with varying doses. Figure 4.6 shows that there is a significant amount of CPE within the serum after only 2 h treatment with the 200 μg dose (~800 ng/ml). The lower 50 μg dose has far less CPE within the serum (~300 ng/ml), and a lower 15 μg dose had undetectable levels of CPE. These results demonstrate that CPE has the ability to gain access to the bloodstream, and this may be a mechanism by which mice in the model are dying.

A possible mechanism to explain the ability of CPE to access the bloodstream is that CPE is cytotoxic to endothelial cells lining the microvasculature within the intestinal tissue. To test the ability of CPE to be cytotoxic to endothelial cells, we assessed morphological damage to human umbilical vein endothelial cells (HUVEC) after CPE treatment. Three doses of CPE (0.5 μg/ml, 1.0 μg/ml, and 2.5 μg/ml) were used to treat HUVEC cells. Morphological damage was assessed after 1 h of treatment. No damage to the cells was observed after 1 h of treatment for any of the doses used (Fig. 4.7). The morphology of the cells did not change as compared to untreated HUVEC cells (Fig. 4.7A). There was no rounding or detachment of the cells which is typically observed when other cell types, such as Caco-2 or Vero cells, are treated with CPE (178). HUVEC cytotoxicity was followed out to 6 h of CPE treatment, and still no morphological damage or CPE complex formation was seen (data not shown). This suggests that endothelial cells, at least HUVEC cells, are insensitive to the cytotoxic effects of CPE treatment. Endothelial cells, like epithelial cells, form tight junctions between adjacent cells. However,

claudin expression Western blots (data not shown) indicated no detectable levels of claudin in HUVEC cells. Further cytotoxicity studies using other types of endothelial cells is necessary to determine if this is a plausible mechanism by which CPE is gaining access to the bloodstream in our mouse model.

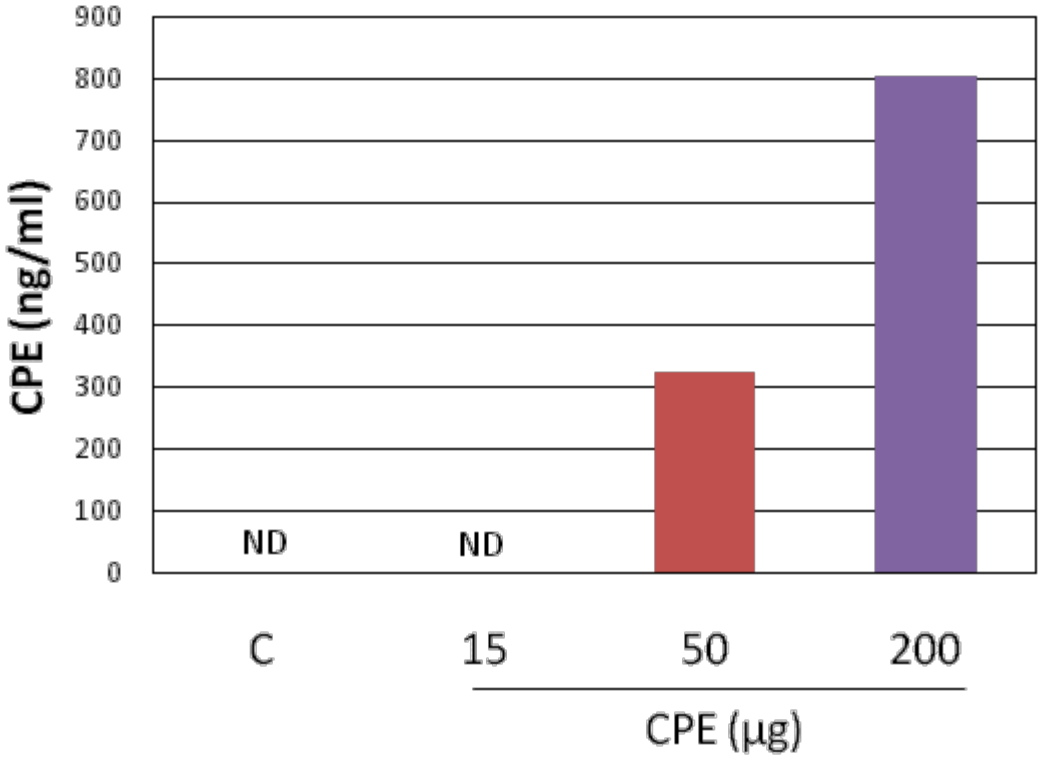

Figure 4.6 Analysis of Serum for the Presence of CPE within the Bloodstream.
After 2 h of CPE treatment at indicated doses, serum was collected from mice. Serum was analyzed by a sandwich ELISA specific for the presence of CPE. ND = not dectected.

4.3.6 Binding of CPE to Other Organs

The results of Fig. 4.6 provides evidence for the presence of CPE within the circulation after CPE challenge in the intestinal loop model. Previous studies examining the effects of IV administration of CPE revealed that the greatest quantities of CPE are distributed in the liver and,

to a lesser extent, the kidney, within 10-15 min after injection (180). With this in mind, we hypothesized that due to the presence of CPE within the blood, a large amount of CPE may be binding to the liver, as well as the kidney. We, therefore, wished to determine the ability of CPE to bind and form complexes within these systemic organs. Livers and kidneys from CPE-treated mice were harvested and homogenized. Homogenates were analyzed by SDS- PAGE and Western blotting with an anti-CPE antibody for the presence of CPE binding and complex formation.

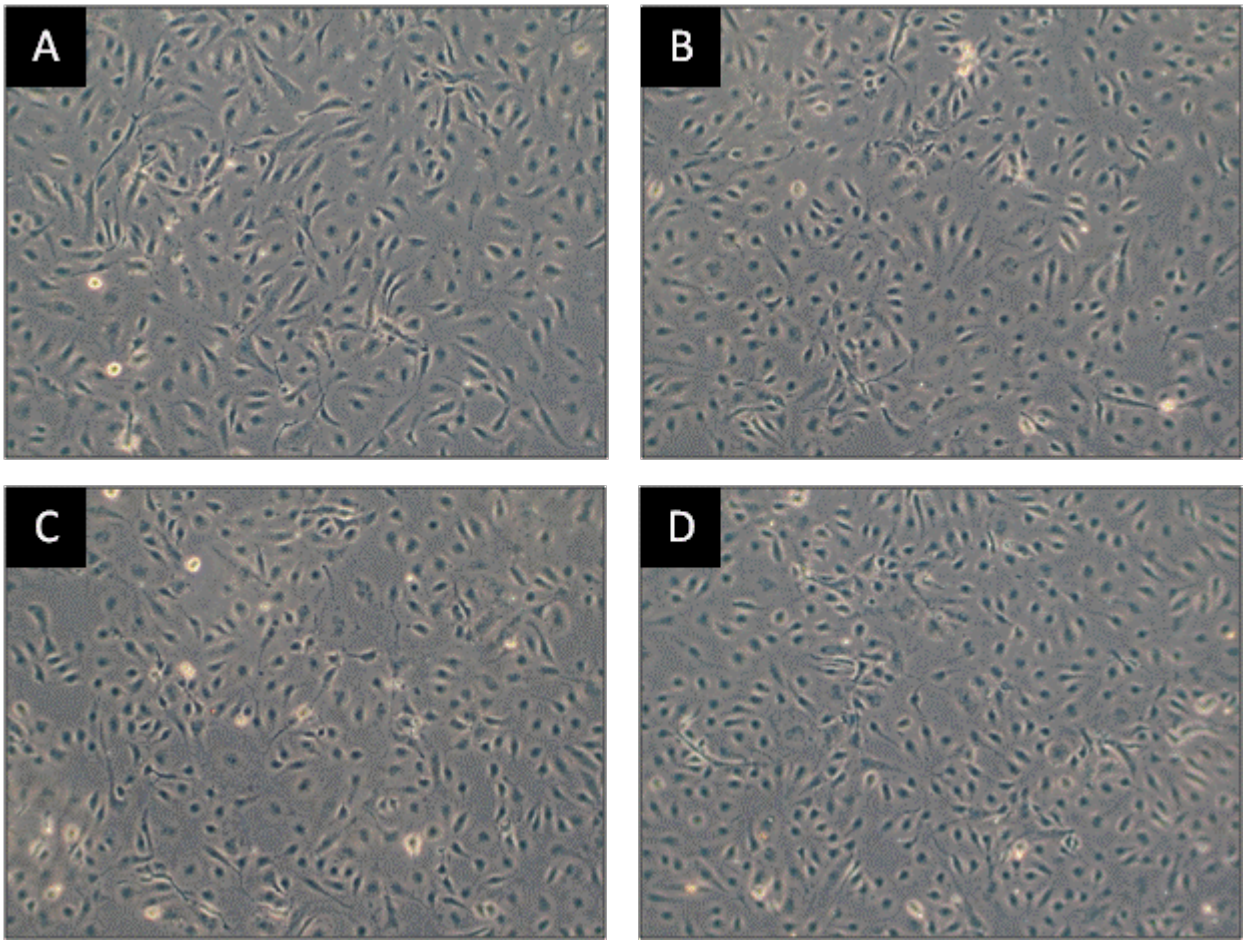

Figure 4.7 Assessment of Morphological Damage of HUVECs.
Monolayers of HUVEC cells were left untreated (A) or treated with 0.5 μg/ml (B), 1.0 μg/ml (C), or 2.5 μg/ml (D) of CPE for 1 h. Morphological damage was assessed by light microscopy.

The data presented in Fig. 4.8A show significant immunoreactivity within the livers of mice treated with the 200 μg dose, however, much less immunoreactivity is observed for the lower 50 μg dose. This suggests that CPE has the ability to bind to the liver. Despite the lack of a distinct complex comparable to the CH-1 or CH-2 complexes that is observed in CPE-treated Caco-2 cells, higher molecular weight CPE-containing material is present within the homogenized liver tissue, suggesting CPE is interacting with additional host proteins. Liver tissue from untreated mice was homogenized in detergent-free buffer and treated with 2.5 μg/ml of CPE for 30 min in a cell suspension. Following toxin treatment, cell lysates were analyzed by Western blot and the results from this experiment (Fig. 4.8B) demonstrate that CPE has the ability to form, at least, the CH-1 complex. However, no CH-2 complex formation was observed. As evidenced by the formation of the CH-1 complex, it can be suggested that CPE can be cytotoxic to hepatocytes in the liver.

Similar studies as described for the liver were performed for the kidneys of CPE-challenged mice. SDS-PAGE and Western blot analysis of homogenized kidneys of CPE-treated mice shows some binding to these organs (Fig. 4.8A). The binding of CPE to the kidney appears to be less than that of CPE to the liver, despite similar amounts of total protein extracted (see Materials and Methods). Again, as was observed with the livers of mice intestinally challenged with CPE, there is a lack of formation of distinct CPE complexes that are comparable to the CH-1 or CH-2 that are observed in Caco-2 cells. Yet, higher molecular weight immunoreactivity is seen which indicates CPE is possibly associating with host proteins. As was done for liver tissues, kidneys from untreated mice were harvested and homogenized in detergent-free buffer. These kidney homogenates were treated for 30 min with 2.5 μg/ml of CPE in a cell suspension. Lysates of these CPE-treated kidney cell suspensions were then analyzed by SDS-PAGE and

Western blot. Results from this experiment (Fig. 4.8B) show the ability of CPE to form the CH-1 complex in isolated cells from the kidney. This is in agreement with CPE treatment of Madin Darby Canine Kidney (MDCK) cells, an established cell line of kidney origin, in which significant changes in cell morphology is observed and formations of CPE complexes occurs (Fig. 4.9). Similar to what was observed for isolated hepatocytes treated in suspension, no CH-2 formation in homogenized kidneys was detected in our Western blot analysis. In summary, the data presented in Fig. 4.8 illustrate the ability of CPE to bind to systemic organs (liver and kidney) after gaining access to the bloodstream after damage to the intestinal epithelium due to toxin treatment in our intestinal loop model. Additionally, the results shown in Fig.4.8 suggest that the necessary host proteins, presumably claudins, are present within both the liver and kidney which allow for the ability to form, at least the CH-1, the large CPE-containing complexes.

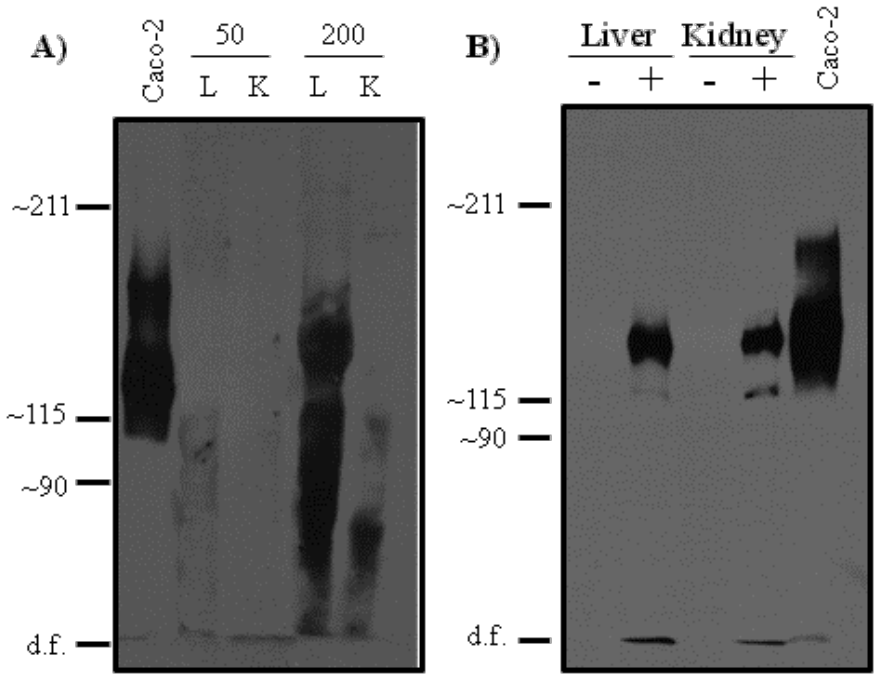

Figure 4.8 CPE Complex Formation in Systemic Organs.
A) Livers (L) and Kidneys (K) from mice treated with 50 μg or 200 μg of CPE for 2 h were harvested and homogenized in RIPA Buffer. Lysates were analyzed by SDS-PAGE and Western blotting with a rabbit anti-CPE antibody. SDS Lysates of Caco-2 cells treated with 2.5 μg/ml of CPE for 45 min were loaded

as controls for CH-1 and CH-2 complex formation. B) Livers and Kidneys from control mice were homogenized into cell suspensions and were left untreated (-) or treated (+) with 2.5 μg/ml of CPE for 30 min. Lysates were loaded on SDS-PAGE gels and analyzed by Western blotting as in A). Numbers on left identify molecular weight markers in kDa. d.f. marks the migration of the dye front.

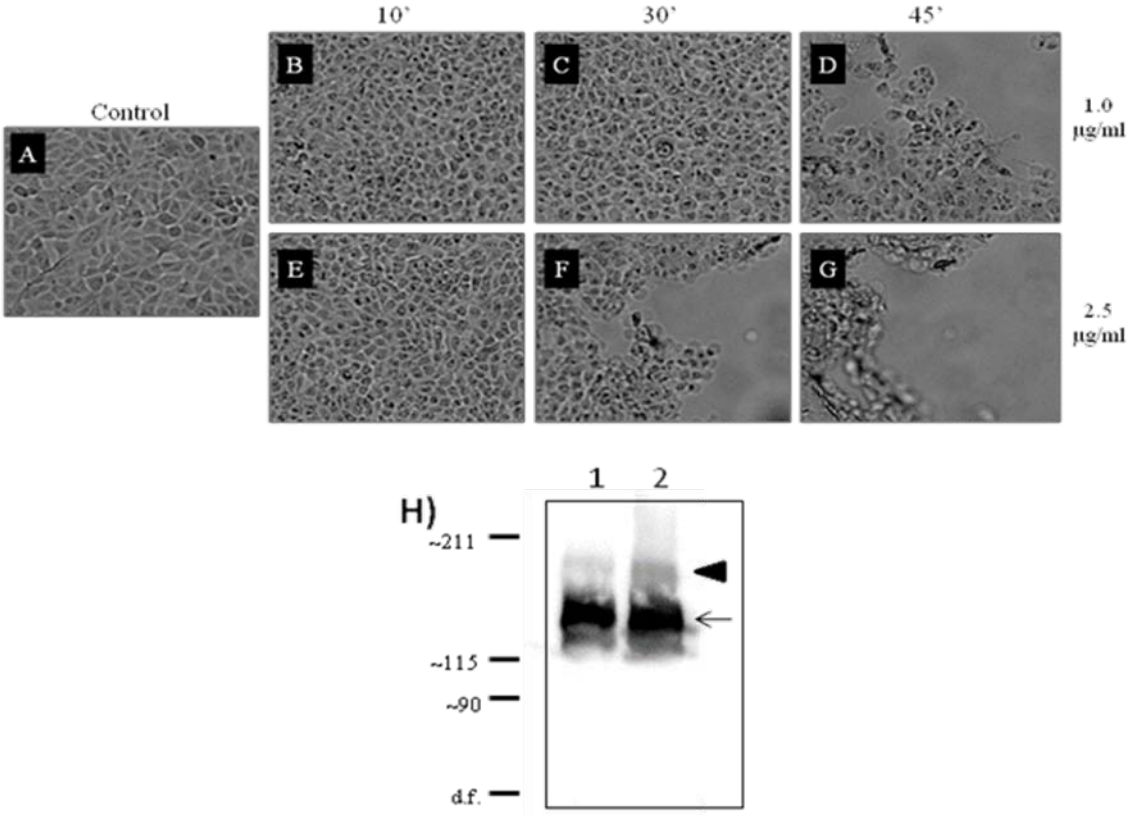

Figure 4.9 CPE-induced Cytotoxicity and Complex Formation in MDCK cells.
A-G) Assessment of morphological damage of MDCK cell monolayers treated with either 1 μg/ml (B-D) or 2.5 μg/ml (E-G) of CPE for 10 min (B, E), 30 min (C, F), or 45 min (D, G). Untreated MDCK cell morphology is shown in A. H) MDCK cells treated for 45 min with 1.0 μg/ml (Lane 1) or 2.5 μg/ml (Lane 2) of CPE were harvested and lysates were run on 4% SDS-PAGE gels followed by Western blotting with a rabbit anti-CPE antibody. Numbers on the left are molecular weight markers in kDA. d.f. is the migration of the dye front. Arrow shows the migration of the CH-1. Arrowhead illustrates the migration of the CH-2 complex.

4.3.7 CPE Challenge Results in Elevated Levels of Potassium in the Serum

In our mouse model of CPE lethality, the ability of CPE to damage the intestinal epithelium and gain access to the blood allows the toxin to preferentially bind to the liver and, to a lesser extent, the kidney. These results are in agreement with the previous study by Skjelkvale et al. (180) that assessed the accumulation of toxin in various organs following IV administration of CPE, as introduced above. Another study investigated the effects of IV administration of CPE in mice and rats in which animals died within 4-15 min (189). In this study by Sugimoto et al., rapid changes in ECG patterns and a fall in blood pressure, followed by respiratory depression was observed. The cardiac dysfunction associated with IV administration of CPE was found to be the result of increased levels of potassium within the blood of animals and not due to direct cytotoxicity of cardiac tissue by CPE. Additionally, the source of the excess potassium was attributed to release from the damaged liver, thus, linking this study with that of Skjelkvale et al., suggesting a model where CPE preferentially binds to the liver, resulting in damage and lysis of hepatocytes and causing the release of potassium into the circulation. These elevated levels of potassium in the blood, in turn, may cause cardiac dysfunction and eventual death.

Because we were observing significant binding of CPE to the liver after intestinal challenge, we hypothesized that CPE may be causing the release of potassium from damage liver cells into the blood and this is responsible for the lethality we were observing. Therefore, levels of potassium in the serum of mice challenged with different doses of CPE was assessed. After 2 or 3 h of incubation with 50 μg, 100 μg, or 200 μg of CPE, or buffer control, in intestinal loops, serum from treated mice was collected and analyzed for potassium levels by inductively coupled plasma atomic emission spectroscopy (ICP-AES). As shown in Fig. 4.10A, the basal level of potassium in the serum of control animals is within the normal range at ~6 mM. Intestinal loop

treatment with 50 μg of CPE for 2 h resulted in no statistically significant increase in levels of potassium. Similarly, treatment with the 100 μg CPE dose also did not result in an increase in potassium levels in the serum of mice challenged for 2 h. However, with the 200 μg dose of CPE, there was a statistically significant increase in potassium levels to ~14 mM in the serum after 2 h of treatment. The increase that was observed is at a level that would be lethal to animals. This 2 h data indicates that increased levels of potassium may potentially be playing a role in the lethality observed with the 200 μg dose.

Despite the increased levels of potassium at 2 h for mice treated with 200 μg of CPE, we did not observe death until the 4 h time point (Table 4.1). This suggests that there is a lag between increased potassium in the serum and actual death. Additionally, when mice were challenged with 100 μg of CPE for 2 h, we did not observe an increase in potassium levels despite seeing a high rate of lethality at 4 h (Fig 4.10A and Table 4.1). This discrepancy with the 100 μg and 200 μg doses, where we are seeing lethality in both but only potassium increases with the 200 μg dose, prompted us to examine the effects of intestinal loop challenge at 3 h.

When potassium levels in the serum of mice challenged for 3 h were analyzed by ICP-AES (Fig. 4.10B), we observed a statistically significant increase in potassium levels with the 100 μg dose to a lethal level (~16 mM). This level is similar to that of what we observed for the 200 μg dose at 2 h (Fig. 4.10A). Mice treated with 200 μg of CPE for 3 h showed a continued rise in potassium in the serum to an exceedingly high level (~26 mM). However, it must be noted that by this time point the majority of mice in these group were dead (Fig. 4.11), and autolysis may have occurred resulting in an inaccurate representation of the serum potassium profile of these mice. Potassium levels in mice that were treated with 50 μg of CPE for 3 h still did not show an increase over buffer control mice.

When the 3 h lethality data is combined with our existing data for 2 h and 3h (Fig. 4.11), one can observed that between 2 and 3 h there is a drastic increase in the rate of lethality for the 200 μg CPE dose (survival falling from 100% to 37.5%). This interval seems to correlate with the increase in potassium in the serum of mice as illustrated in Fig. 4.10A. Fig. 4.11 reveals only a modest increase in the rate of lethality between 2 and 3 h (survival falling only from 100% to 75%) for the 100 μg CPE dose group. However, severe lethality rates are observed for the 100 μg group at 4 h (37.5% survival), which correlates to the observed potassium increase at 3 h (Fig. 4.10B). For the 50 μg CPE dose, survival remains at 100 % for 3 h, and only falls to 93.75% at 4 h. This correlates with the stable levels of potassium that is observed for this dose (Fig.4.10A and B). Taken together, Figs. 4.10 and 4.11 demonstrate a dose and time-dependent relationship between CPE treatment in intestinal loops and lethality. Furthermore, Figs. 4.10 and 4.11 demonstrate that a rise in potassium levels within the blood precedes and is a likely cause of death in our mouse model.

The dose and time-dependent change in potassium levels in the serum appears to be fairly specific to that one ion. Analysis of the serum by ICP-AES allows for the simultaneous assaying of multiple ions in the same sample. Therefore, we measured the levels other trace elements such as Mg^{2+}, Ca^{2+}, PO_4^{3-}, Na^{+}, Fe^{3+}, Zn^{2+}, and Cu^{2+} in the serum of mice that were intestinally challenged with the different doses of CPE at 2 h. When comparing the serum levels of these elements between each dose, there are not statistically significant differences between the 3 doses over buffer controls. The only exception is for phosphorus, where the 200 μg group shows a statistically significant increase ($p<0.008$) in levels as compared to buffer control animals. However, the levels for this element between doses is somewhat variable. For instance, the 50 μg group has levels above control, whereas the 100 μg CPE dose group has similar levels as the

control group. The significance of a phosphorus levels in the 200 μg CPE treatment group is unknown at this time. Additionally, there is a trend towards a dose-dependent decrease in Cu^{2+} levels with increased dose, however, this observed decrease does not reach statistical significance for any data point ($p=0.135$).

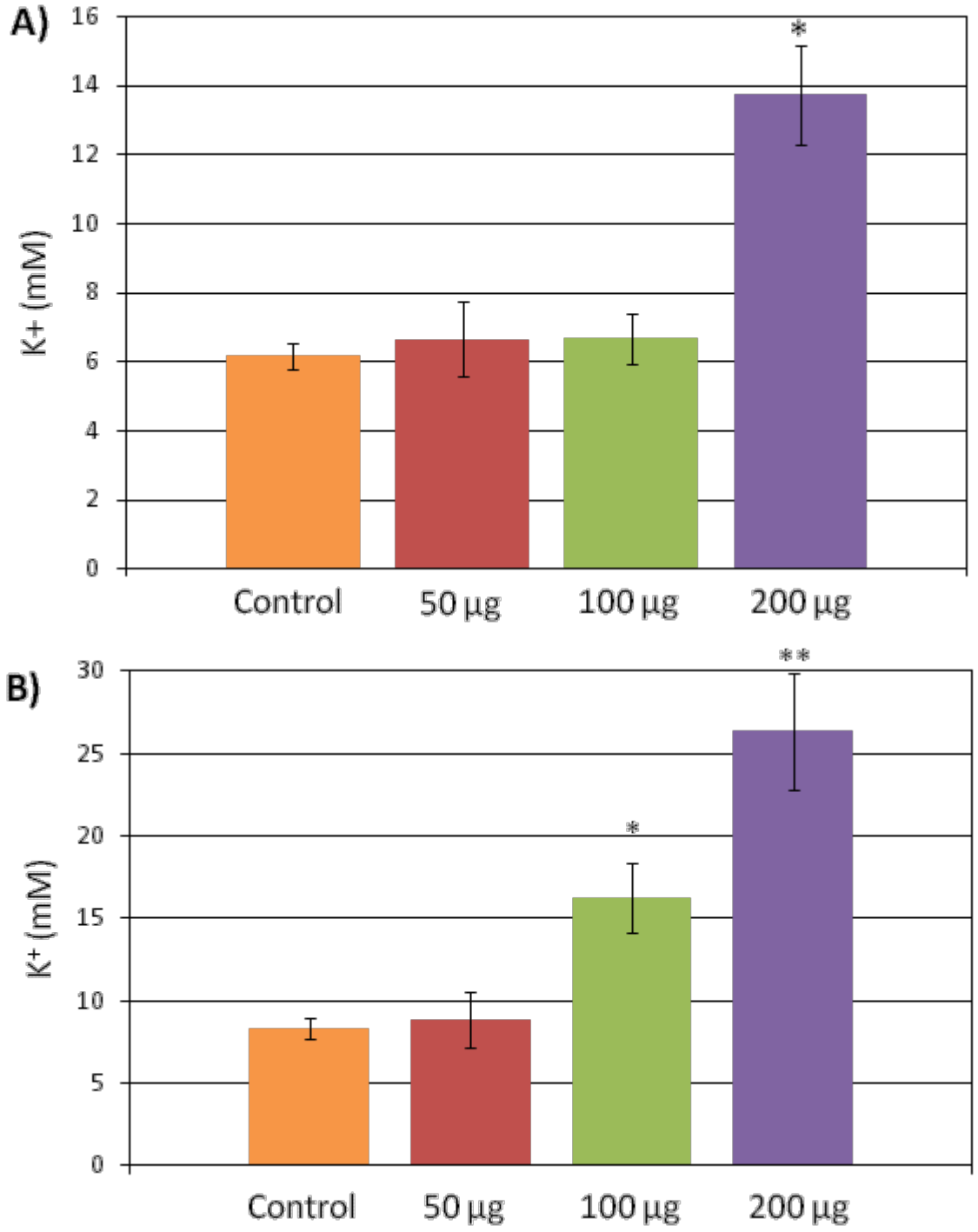

Figure 4.10 CPE Challenge Results in Hyperpotassemia.
After 2 h (A) or 3 h (B) of intestinal loop treatment with buffer control (orange bars), 50 µg (red bars), 100 µg (green bars), or 200 µg (purple bars) of CPE, serum was collected from mice. Serum was analyzed by utilizing inductively coupled argon plasma emission spectrometry. After precipitation of proteins, the protein-free supernatant of each sample was analyzed for potassium levels. Accuracy of results was measured by analyzing quality assurance sera obtained from the Veterinary Laboratory Association Quality Assurance Program. Data were accepted if analyzed quality assurance serum values

were within 2 standard deviations of the reference values. Data is from the mean of 8 mice. Error bars represent the standard error of the mean. A) *p<0.01; B) *p<0.02, **p<0.0002

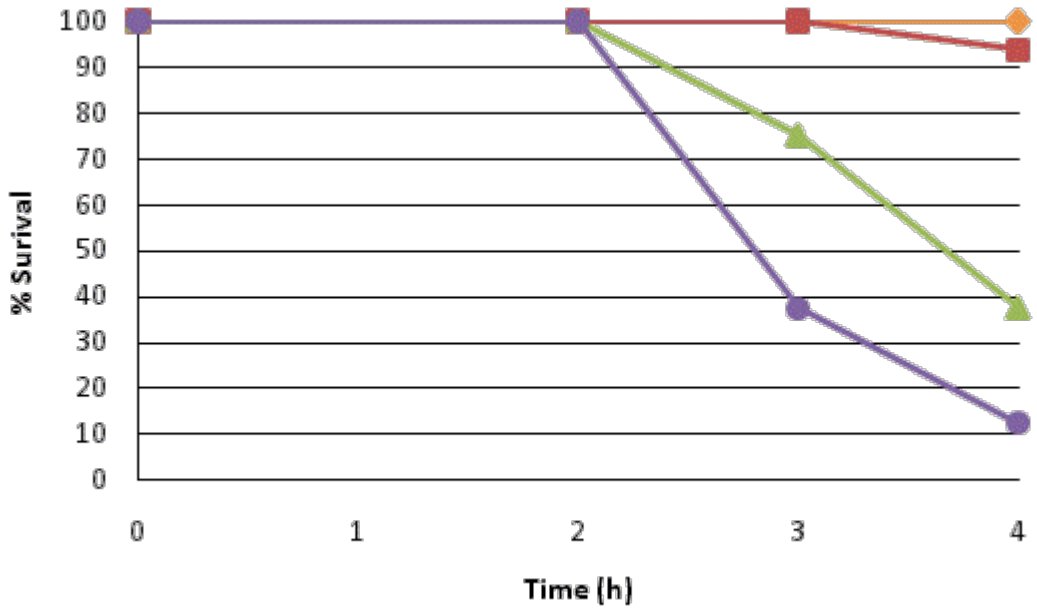

Figure 4.11 Time and Dose-Dependent Representation of Mouse Survival.
The percent survival of mice was calculated and plotted against the time of treatment (in hours, x-axis) for each dose of CPE at 2, 3, and 4 h. Buffer control animals (-♦-), 50 µg treatment (-■-), 100 µg treatment (-▲-), 200 µg treatment (-●-). Survival was calculated from 7 animals at 2 h, 8 animals for 3 h, and 15 animals at the 4 h time point for control, 50 µg, and 100 µg animals. Survival was calculated from 7 mice at 2 h, 8 mice at 3 h, and 8 animals at 4 h for the 200 µg CPE dose. Since the majority of mice die by 3 h with 200 µg of CPE, additional 4 h treatments with 200 µg doses were eliminated to cut down on mouse usage.

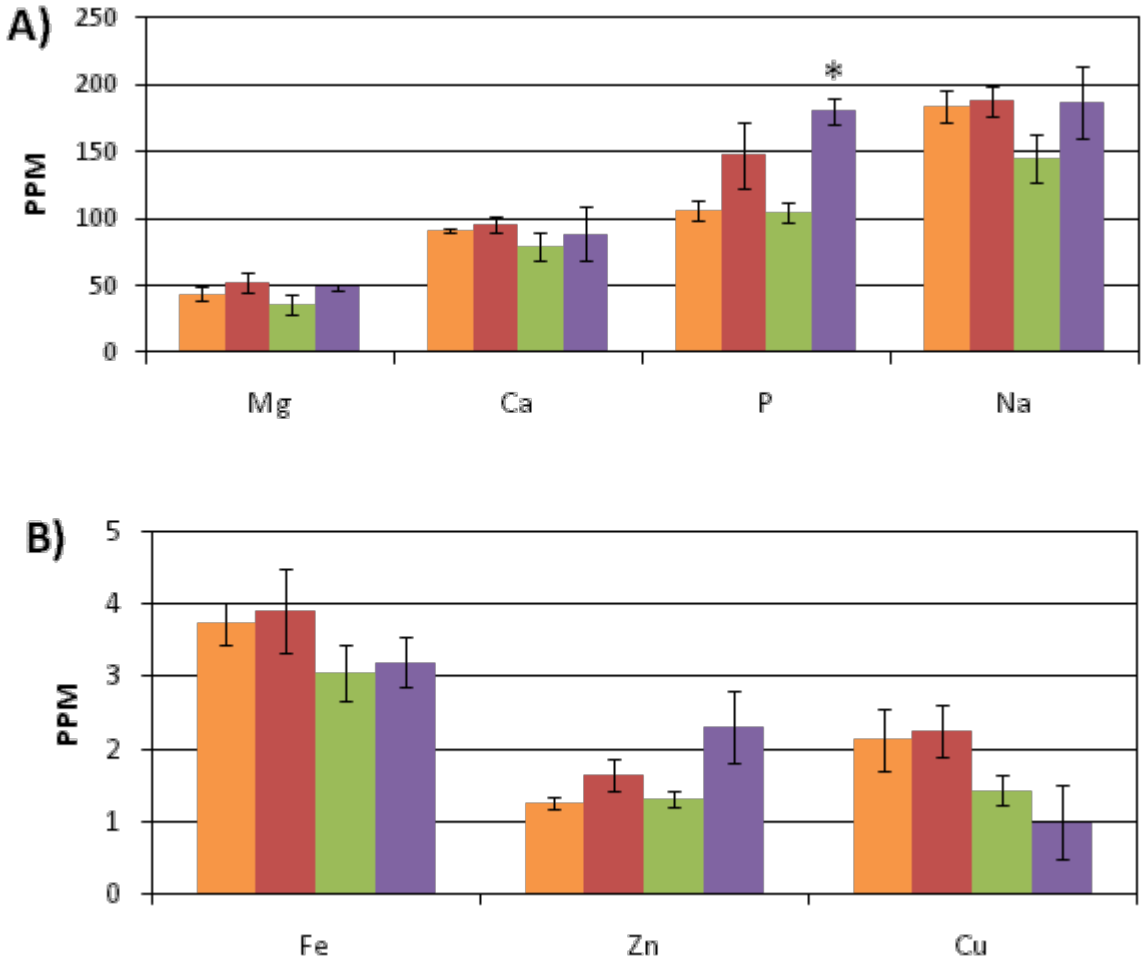

Figure 4.12 Trace Element Screen.
Serum was collected from control mice (orange bars) or mice treated for 2 h with 50 µg (red bars), 100 µg (green bars), or 200 µg (purple bars), and analyzed by ICP-AES for the levels of various elements. Mg (magnesium), Ca (calcium), P (phosphorus), Na (sodium), Fe (iron), Zn (zinc), Cu (copper). Data is the mean of 4 mice per group. Error bars represent the standard error of the mean. *$p<0.008$.

4.4 DISCUSSION

4.4.1 Induction of Inflammatory Cytokines by CPE in a Mouse Model

On a molecular level, a cell employs multiple mechanisms to undergo cell death depending on the stimuli exposed to the cell. The various cell death pathways that have been described include apoptosis, oncosis, autophagy, and pyroptosis, among others (46, 97). At a cellular level, the mechanism by which a cell undergoes cell death is important for controlling the inflammatory state of the environment. In comparing apoptosis versus oncosis, a distinguishing characteristic of these two mechanisms is that apoptosis is non-inflammatory while oncosis is inflammatory. Multiple pathogens, including their products such as toxins, have been experimentally shown to induce apoptosis (54, 211). However, more and more evidence is making it apparent that pathogens can also induce oncosis (4, 32, 55, 81, 149, 195, 227). As many pathogens are reported to cause the induction of inflammatory cytokines in both cell culture and in animal models, it would not be surprising that oncosis is a common mechanism of cell death in infectious disease.

Interestingly, CPE has been shown to induce both apoptosis and oncosis in a Caco-2 cell culture model (32). As this was shown to be dependent upon toxin dose, CPE may induce inflammatory events at higher doses. Prior studies demonstrated that treatment of human PBMCs *in vitro* with CPE elicited production of IL-6, however TNF-α, IFNγ, IL-1, and IL-2 production was not detected (94). We wished to determine the inflammatory cytokine profile in an *in vivo* mouse model. Particularly, we were interested in measuring the local production of cytokines within the intestine, where CPE directly acts upon target cells. A ligated ileal loop CPE challenge model was developed for this purpose. This is in contrast to a previous study

looking at systemic cytokine production in the serum of mice challenged by the intraperitoneal (IP) and intragastric (IG) routes (210). In our ileal loop model, we were able to detect significant levels of IL-1β and IL-6 production in homogenized intestinal tissue in response to CPE (Fig.4.1). This induction of cytokines by CPE appears to be dose-dependent. Further analysis of homogenized intestinal tissue at later time points is needed to determine the duration of this inflammatory response. When intestinal fluid and serum were analyzed by Luminex for various cytokines, we did not observe any detectable levels of cytokines in either case. Regarding the intestinal fluid, it may be that no significant amount of cytokines are secreted into the lumen as the only probable source would be epithelial cells. Despite being able to produce pro-inflammatory cytokines in response to various stimuli, we did not observe any detectable production of TNFα from supernatants of CPE-treated Caco-2 cells (data not shown). Likewise, RT-PCR analysis of RNA extracted from CPE-treated Caco-2 cells did not show the production of IL-1β, IL-6, or TNFα (data not shown).

CPE treatment of intestinal loops at high doses (100 μg and 200 μg) results in severe damage to the intestinal villi, leading to necrosis of the epithelial cells that compose the villi and the lamina propria that underlies the villi (Fig. 4.3, Table 4.3). This high degree of tissue destruction is possibly a signal to inflammatory cells such as neutrophils to migrate to this area. Macrophages and monocytes are the primary sources for IL-1β production, however, dying cells can also produce this cytokine (176). The IL-1β production we observe in the mouse intestine in response to CPE treatment may, therefore, be produced from neutrophils trafficking to the area or dying epithelial cells themselves. Further experiments are required to distinguish between these possible sources of this cytokine.

Alarmins are a recently identified class of molecules, equivalent to pathogen-associated molecular patterns (PAMPs), which mediate signals to alert the body of tissue and cell damage (14). HMBG1 is the best-characterized alarmin, and is produced by dying cells and by macrophages that have been exposed to factors such as LPS, TNFα, or IL-1. HMGB1 is normally found within the nucleus, but cells undergoing non-apoptotic death (necrosis, possibly oncosis) passively release HMBG1 into the extracellular milieu, whereas those undergoing apoptotic death do not release HMGB1 (170). HMGB1 mediates endothelial cell activation, angiogenesis, stem cell migration, and recruitment and activation of innate immune effectors (112). Interestingly, although apoptotic cells do not release HMGB1, macrophages that engulf them are induced to secrete HMGB1 (156). Therefore, it seems as though clearance of a small amount of apoptotic cells is not inflammatory, but clearance of a large number of apoptotic cells could be (14). It is plausible then to be able to detect both the apoptotic and oncotic forms of cell death observed in Caco-2 cells in our *in vivo* model. In our mouse model, HMGB1 may be mediating some of the inflammatory events that are being observed. HMGB1 may be involved in the secretion of IL-1 that we detected, as shown below (Fig. 4.13), where dying cells may be releasing either IL-1 or HMGB1, and in turn, either IL-1 or the dying cells themselves are activating macrophages to produce HMGB1. Analysis of intestinal loop tissue and fluid for the presence of HMGB1 would prove to be an interesting next step in characterizing the inflammatory response in our model. HMGB1 release from CPE-treated Caco-2 cells could also be investigated.

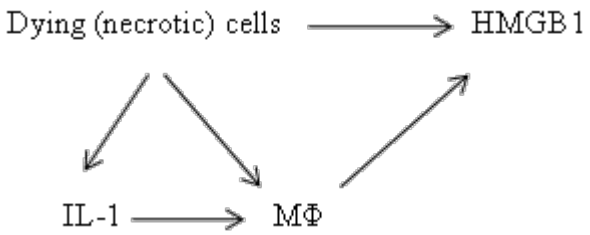

Figure 4.13 Possible Mechanism of HMBG1 Production

In human type A diseases, CPE is not the only *C. perfringens* toxin that may be contributing to disease, e.g. beta2 toxin may also be involved in AAD cases (47). Furthermore, CPE is probably not the only *C. perfringens* bacterial product encountered by the host. Many toxins and enzymes produced by *C. perfringens*, and particularly lipoteichoic acid (LTA) (38), could be immunostimulatory. Therefore, to obtain a comprehensive picture of the innate immune events occurring during type A food poisoning, it may be prudent to use bacterial lysates or sporulating cultures to supplement this current study.

4.4.2 In Vivo CPE Complex Formation

Previous studies have examined the ability of CPE to bind to the intestinal epithelium in association with histological damage in rabbit animal models (183) and the human colon (45). These studies have demonstrated direct CPE binding to the intestine, however, binding is not sufficient to cause cytotoxicity in cell culture models (122, 126), and presumably histological damage *in vivo*. Formation of the CPE-containing pore complexes (CH-1, and possibly CH-2) is necessary to induce the permeability alterations associated with the cytotoxicity of CPE action (122). The CH-1 and CH-2 complexes are large, SDS-resistant complexes formed on target membranes in various cell culture models ((178), Fig. 4.9) and migrate at ~155 kDa and ~200

kDa, respectively, on SDS-PAGE. Formation of the CH-1 and CH-2 complexes has never been demonstrated *in vivo* prior to this current study. When intestinal tissue from CPE-treated mouse ileal loops were homogenized and analyzed by SDS-PAGE and Western blotting (Fig. 4.2A), we were able to show, for the first time, the formation of high molecular weight CPE-containing complexes that were comparable in size to the CH-1 and CH-2 complexes that are observed in Caco-2 cells. There are small size difference between these instances and the difference of the complexes may be attributed to the access of CPE to various claudins *in vivo*. Additionally, claudin expression may be altered between normal intestinal tissue and that of Caco-2 cells, an immortalized cancer cell line. It is firmly established that claudins, particularly the CPE receptors, claudin-3 and -4, are overexpressed in cancers (89). Expression levels of claudin-1,-2,-3, and -4 and occludin are fairly consistent throughout the small intestine (75), whereas other claudins are quite variable in their expression along the intestine (51). Furthermore, the similarity between human claudins and mouse claudins is quite high (~90%), and importantly, they share the same important motif for binding of CPE (FYNP for binding-capable cldn-3 and -4, or FYDP for non-binding cldn-1 and -2 (157, 215)) (Fig. 4.14).

However, it is not as though CPE cannot form toxin complexes, such as CH-1 and CH-2 as observed in Caco-2 cells, when in contact with mouse intestinal cells. We were able to demonstrate that CPE treatment of cells isolated from homogenized intestinal tissue from untreated mice results in the formation of the CH-1 complex (Fig. 4.2B), although no observable CH-2 formation was seen. This suggests that mouse intestinal epithelia express the necessary proteins required for formation of the CH-1 complex. Interestingly, early studies examining the molecular interactions of CPE with target cells, utilized brush border membranes (BBMs) isolated from rabbit intestines (217). When treated with CPE, BBMs form the CH-1 complex

but do not form the CH-2 complex (182). It is interesting to note that the procedure for isolating BBMs is very similar to that which was utilized for obtaining intestinal cells from the mice in this study. Furthermore, when Caco-2 cells are grown as fully polarized monolayers in Transwell filters, formation of the CH-2 requires more extended CPE treatment times (Fig. 2.7, (178)). Therefore, one must consider whether the formation of the CH-2 complex actually occurs *in vivo* when cells are in a fully differentiated and polarized state within a three-dimensional tissue, or if the formation of this complex is merely an artefact of CPE treatment of cancerous Caco-2 cells in an unpolarized state.

CLAUDIN-1

```
90.5% identity in 211 residues overlap; Score: 1025.0; Gap frequency: 0.0%

CLD1_HUMAN      1 MANAGLQLLGFILAFLGWIGAIVSTALPQWRIYSYAGDNIVTAQAMYEGLWMSCVSQSTG
CLD1_MOUSE      1 MANAGLQLLGFILASLGWIGSIVSTALPQWKIYSYAGDNIVTAQAIYEGLWMSCVSQSTG
                  *************** ***** ********* *************** ***************

CLD1_HUMAN     61 QIQCKVFDSLLNLSSTLQATRALMVVGILLGVIAIFVATVGMKCMKCLEDDEVQKMRMAV
CLD1_MOUSE     61 QIQCKVFDSLLNLNSTLQATRALMVIGILLGLIAIFVSTIGMKCMRCLEDDEVQKMWMAV
                  ************** ************ ***** ***** * ***** ********** ***

CLD1_HUMAN    121 IGGAIFLLAGLAILVATAWYGNRIVQEFYDPMTPVNARYEFGQALFTGWAAASLCLLGGA
CLD1_MOUSE    121 IGGIIFLISGLATLVATAWYGNRIVQEFYDPLTPINARYEFGQALFTGWAAASLCLLGGV
                  *** ***  *** ******************** ** ************************

CLD1_HUMAN    181 LLCCSCPRKTTSYPTPRPYPKPAPSSGKDYV
CLD1_MOUSE    181 LLSCSCPRKTTSYPTPRPYPKPTPSSGKDYV
                  ** ******************** ********
```

CLAUDIN-2

```
91.3% identity in 230 residues overlap; Score: 1096.0; Gap frequency: 0.0%

CLD2_HUMAN      1 MASLGLQLVGYILGLLGLLGTLVAMLLPSWKTSSYVGASIVTAVGFSKGLWMECATHSTG
CLD2_MOUSE      1 MASLGVQLVGYILGLLGLLGTSIAMLLPNWRTSSYVGASIVTAVGFSKGLWMECATHSTG
                  ***** ***************  ***** * ******************************

CLD2_HUMAN     61 ITQCDIYSTLLGLPADIQAAQAMMVTSSAISSLACIISVVGMRCTVFCQESRAKDRVAVA
CLD2_MOUSE     61 ITQCDIYSTLLGLPADIQAAQAMMVTSSAMSSLACIISVVGMRCTVFCQDSRAKDRVAVV
                  ******************************** ******************** *********

CLD2_HUMAN    121 GGVFFILGGLLGFIPVAWNLHGILRDFYSPLVPDSMKFEIGEALYLGIISSLFSLIAGII
CLD2_MOUSE    121 GGVFFILGGILGFIPVAWNLHGILRDFYSPLVPDSMKFEIGEALYLGIISALFSLVAGVI
                  ********* ********************************************* **** ** *

CLD2_HUMAN    181 LCFSCSSQRNRSNYYDAYQAQPLATRSSPRPGQPPKVKSEFNSYSLTGYV
CLD2_MOUSE    181 LCFSCSPQGNRTNYYDGYQAQPLATRSSPRSAQQPKAKSEFNSYSLTGYV
                  ****** * ** **** **************  * ** **************
```

CLAUDIN-3

```
90.9% identity in 220 residues overlap; Score: 1033.0; Gap frequency: 0.5%

CLD3_HUMAN      1 MSMGLEITGTALAVLGWLGTIVCCALPMWRVSAFIGSNIITSQNIWEGLWMNCVVQSTGQ
CLD3_MOUSE      1 MSMGLEITGTSLAVLGWLCTIVCCALPMWRVSAFIGSSIITAQITWEGLWMNCVVQSTGQ
                  ********** ******* ******************* *** *  ***************

CLD3_HUMAN     61 MQCKVYDSLLALPQDLQAARALIVVAILLAAFGLLVALVGAQCTNCVQDDTAKAKITIVA
CLD3_MOUSE     61 MQCKMYDSLLALPQDLQAARALIVVSILLAAFGLLVALVGAQCTNCVQDETAKAKITIVA
                  **** ********************* ********************** **********

CLD3_HUMAN    121 GVLFLLAALLTLVPVSWSANTIIRDFYNPVVPEAQKREMGAGLYVGWAAAALQLLGGALL
CLD3_MOUSE    121 GVLFLLAALLTLVPVSWSANTIIRDFYNPLVPEAQKREMGAGLYVGWAAAALQLLGGALL
                  ***************************** ******************************

CLD3_HUMAN    181 CCSCPPREKKYTATKVVYSAPRSTGPGASLGTGYDRKDYV
CLD3_MOUSE    181 CCSCPPRDK-YAPTKILYSAPRSTGPGTGTGTAYDRKDYV
                  ******* * *  **  **********   ** *******
```

CLAUDIN-4

```
83.3% identity in 210 residues overlap; Score: 941.0; Gap frequency: 0.5%

CLD4_HUMAN      1 MASMGLQVMGIALAVLGWLAVMLCCALPMWRVTAFIGSNIVTSQTIWEGLWMNCVVQSTG
CLD4_MOUSE      1 MASMGLQVLGISLAVLGWLGIILSCALPMWRVTAFIGSNIVTAQTSWEGLWMNCVVQSTG
                  ******** ** *******   * ****************** ** ***************

CLD4_HUMAN     61 QMQCKVYDSLLALPQDLQAARALVIISIIVAALGVLLSVVGGKCTNCLEDESAKAKTMIV
CLD4_MOUSE     61 QMQCKMYDSMLALPQDLQAARALMVISIIVGALGMLLSVVGGKCTNCMEDETVKAKIMIT
                  ***** *** **************  ***** *** ************ ***  *** **

CLD4_HUMAN    121 AGVVFLLAGLMVIVPVSWTAHNIIQDFYNPLVASGQKREMGASLYVGWAASGLLLLGGGL
CLD4_MOUSE    121 AGAVFIVASMLIMVPVSWTAHNVIRDFYNPMVASGQKREMGASLYVGWAASGLLLLGGGL
                  ** **  *     ********* * ***** ******************************

CLD4_HUMAN    181 LCCNCPPRT-DKPYSAKYSAARSAAASNYV
CLD4_MOUSE    181 LCCSCPPRSNDKPYSAKYSAARSVPASNYV
                  *** ****  **************  *****
```

Figure 4.14 Sequence Alignment of Human and Mouse Claudins.
Protein sequence alignment of human and mouse claudins shows >90% identity exists between species for cldn-1, -2, and -3 and >80% for cldn-4. Yellow box highlights the motif shown to be important for CPE binding (FYxP, where x is an N for binding claudins or a D or S for non-binding claudins). Alignment performed with SIM Alignment Tool accessed from ExPASy.

4.4.3 Mouse Lethality Correlates with Histological Damage

The ileal loop model was established long ago as a model for investigating the effects of CPE action (39). The histopathological effects seen with CPE treatment include blunting of the villi tips and desquamation of the epithelial layer (125). Secondly, CPE-induced permeability alterations result in the loss of fluid absorption and cause secretion of fluid into the intestinal lumen. Fluid accumulation can be easily measured and is a common metric for the degree of CPE damage. Rabbit ileal loops are the most commonly used model for investigating CPE action, however, a mouse ileal loop model was needed to assess the inflammatory response as discussed above. Mouse ileal loops have only been used once to assess CPE action (220), and we needed to establish this model for ourselves. CPE-treatment of mouse ileal loops resulted in dose- and time-dependent histopathologic damage that mimics what is observed in the rabbit (Figs. 4.3 and 4.4, and Table 4.3). When employing rabbit ileal loops, death of the animals is rarely seen. However, we observed a high rate of lethality in mice treated with 100 μg and 200 μg of CPE (Table 4.1 and Fig. 4.11), particularly after 3-4 h of CPE treatment. The degree of histologic damage correlated with the rate of lethality that was observed. Interestingly, we did not observe detectable changes in fluid accumulation in the loops of treated mice as compared to control (data not shown). The reason behind this lack of fluid accumulation is not known. It may be that the damage to the intestinal epithelia is too rapid for passive fluid accumulation to

occur. It was shown, however, that histologic damage induced by CPE treatment is necessary for lethality because neutralization of CPE with a monoclonal antibody prior to injection into the ileal loop prevented death of mice at the highest 200 μg dose (Table 4.2).

4.4.4 Lethality is Associated with CPE in the Circulation

Not only does neutralization of CPE in the intestinal loop prevent lethality of mice, but so does passive immunization, i.e. IV administration of a neutralization monoclonal antibody prior to intestinal loop challenge with CPE (Table 4.2). The results from this experiment suggest that CPE is gaining access to the blood, and that neutralization of CPE within the circulation is sufficient to reverse the lethality that is observed. This was further proven by ELISA analysis of serum collected from control and CPE-treated mice (Fig. 4.6), where significant amounts of CPE was detected in the serum of mice with loops treated with 200 μg of CPE. Far less CPE was detected in mice that received the 50 μg dose, and an even lower dose of 15 μg did not produce any detectable levels of CPE within the serum (Fig. 4.6). Intriguingly, despite very little intestinal damage by the 50 μg dose (Fig. 4.3), some CPE was detected in the blood. In fact, it must be noted that the percentage of total CPE administered that was present in the blood for the lower 50 μg dose was greater than the 200 μg dose (0.6% vs. 0.4%). This suggests that severe damage might not be entirely required for CPE to gain access to the circulation. Many studies are investigating CPE as a tool for drug delivery, and have shown that non-toxic CPE fragments are capable of increasing intestinal permeability simply by interacting with claudins in the tight junctions (93, 201). Perhaps there is a threshold at lower concentrations of toxin where fully active CPE can initiate permeability alterations without causing severe damage.

The association between CPE within the circulation and mouse lethality is suggestive of an enterotoxemia. Enterotoxemias are common diseases in animals caused by *C. perfringens*. Type C strains of *C. perfringens* cause severe and often fatal diseases in humans and animals. Deaths attributed to type C infections are most often due to enterotoxemias where toxins are produced in the intestine and subsequently absorbed into the circulation (186). It has been demonstrated that CPB toxin is the major virulence determinant in type C disease (169, 207) and lethality (202). Interestingly, in the recently developed model for type C enterotoxemia, lethality is observed in the absence of any marked intestinal damage even though severe necrotizing enteritis is normally observed in animals that die from entertoxemias (202), which is in contrast to what we observe in this current CPE lethality model where we are able to mimic both the intestinal and systemic effects of CPE lethal disease (19).

4.4.5 Access to the Blood Allows for CPE Binding to Other Organs

One result of the ability of CPE to gain access to the blood after severe tissue destruction in the intestine is to allow CPE binding to other organs besides the intestine. We show that CPE can bind to the livers and kidneys of mice challenged with high toxin doses (Fig. 4.8). Additionally, homogenized control liver and kidney tissue was treated with CPE in cell suspensions and the formation of the CH-1 complex was detected in these cells (Fig. 4.8). The ability of CPE to bind to liver and kidney is not surprising since claudin expression is relatively high in these tissues (37). In addition, we demonstrated that MDCK cells are quite sensitive to CPE treatment, and can form both CH-1 and CH-2 complexes (Fig. 4.9). Also of note is that hepatitis C virus, a virus that targets the liver, uses claudin-1 as a receptor for entry into hepatocytes (43), and can utilize other claudins as co-receptors (128, 226), further supporting the expression of claudins

within the liver. Similar to isolated intestinal cells (Fig. 4.2), no formation of the CH-2 complex was detected in liver or kidney CPE-treated cells. This again brings up the issue of the CH-2 complex as discussed above. Immunohistochemistry and histological analyses of liver and kidney tissue are ongoing to determine where CPE binding is occurring in these organs, and to determine the extent of damage to these tissues due to CPE binding.

The mechanism by which CPE gains access to the bloodstream is not known at the present time. CPE treatment of endothelial HUVEC cells did not result is any observable cytotoxicity or binding (Fig. 4.7, data not shown), suggesting this is not a plausible mechanism. Previous studies have shown, however, that CPE has capillary permeability and vasodilatation activities (144, 188). Claudin expression in HUVEC cells is not well-characterized, and claudin-5, a non-receptor for CPE, seems to be the only claudin identified as being expressed in these cells (49, 159). Western blot analysis of HUVEC cell lysates showed no presence of claudin-1 or -4 (data not shown). Claudin expression may be quite different in the endothelial cells that line the intestinal microvasculature, so the binding capability and cytotoxicity of other types of endothelial cells should be investigated. More likely, CPE is gaining access to the blood simply due to the overwhelming tissue destruction in the intestine, where the underlying microvasculature is becoming exposed. Specifically, the portal vein system connects the GI tract directly to the liver, which would explain the abundance of CPE binding to this organ.

4.4.6 Hyperpotassemia Plays a Role in Lethality

As mentioned above, IV injection of CPE into animals results in binding to the liver and kidneys and elevated levels of potassium in the blood which results in cardiac dysfunction and eventually respiratory depression and death (180, 189). Because we were observing a high degree of toxin

binding to the liver of dying mice, we analyzed the levels of potassium in the serum of these mice. We found both a dose- and time-dependent increase in potassium with lethal levels (normal levels: 4-6 mM, lethal levels: >7 mM) being reached at 2 h for the 200 μg dose mice and 3 h for the 100 μg dose group (Fig. 4.10). Both of these time points just precede the drastic drop in survival of the mice in each group (Fig 4.11) which suggests a cause and effect relationship. Based on the previous study documenting CPE-induced hyperpotassemia (189), it is hypothesized that the source of the elevated levels of potassium in this study is from the liver. Liver function tests, such as measuring the serum levels of alanine transaminase and aspartate transaminase (25), are needed to confirm this suggestion.

4.4.7 A Model for CPE Lethality in Humans?

The current study has developed a novel mouse model of CPE lethality where intestinal challenge with CPE mimics some of the characteristics of IV CPE challenge, such as liver targeting and hyperpotassemia. More importantly, the model developed here mimics the case reports of deaths associated with type A food poisoning (19, 155) both experimentally (i.e. ligation of the intestine to model constipation) and histopathologically (i.e. necrosis of the intestine, Fig. 4.5). In this regard, intestinal challenge that results in lethality due to absorption of toxin from the GI tract to systemic circulation, more closely models a real-life scenario in humans, as opposed to IV injection. Although intestinal ligation can be considered as the extreme model of constipation, it would be interesting to administer to mice the drugs individuals were reported to be taking that resulted in the constipation and was attributed to their deaths. Since we are able to delineate between a lethal CPE dose (200 μg) and one that is not lethal (50 μg), in addition to study lethality as an endpoint, we are able to investigate why CPE

rarely results in death in humans. Moreover, this model lends itself to investigation of the involvement of innate immune responses in CPE action *in vivo*, as discussed above. Finally, this model can prove to be a valuable tool in modeling other toxins in which complications of enterotoxemias can occur.

5.0 FINAL SUMMATION

C. perfringens type A food poisoning is a significant contributor to bacterial foodborne-related illness in the US. Type A food poisoning is the result of contamination of food products by CPE-producing *C. perfringens* isolates. CPE has a complex and unique mechanism of action that involves close association with proteins in the membranes of target cells resulting in the formation of a series of toxin complexes on the surface of cells. These interactions ultimately results in the demise of the cell that encountered the CPE insult. Understanding the intimate associations between CPE and intestinal epithelial cells can help to provide better therapies for CPE-related diseases. With this in mind, three Specific Aims were stated at the start of this dissertation to investigate the mechanisms in which CPE interacts with target cells and elicits host responses. These proposed aims were i) to investigate the role of lipid rafts in the molecular mechanism of action of CPE, ii) to develop a method for CPE complex isolation and compositional analysis by mass spectrometry, and iii) to develop and characterize a mouse model of CPE-induced inflammation and lethality.

The research presented in this dissertation directly addresses the questions proposed in the Specific Aims. First, the data presented here clearly indicates that CPE is a novel pore-forming toxin which does NOT require lipid rafts for its action. To this date, there are no other reports of other bacterial toxins where lipid rafts do not play a role in toxin action. Binding, oligomerization, and cytotoxicity are all steps in the mechanism of CPE that do not appear to

rely on membrane rafts. This lipid raft study provides evidence for the non-raft-association of the CPE-receptor, claudin, as well. CPE treatment and complex formation results in the removal of occludin from raft domains.

Secondly, significant effort has been devoted to establishing a valuable method for purification of the CH-1 and CH-2 complexes. This was accomplished by the using a two-step method incorporating electroelution and immunoprecipitation in tandem. Despite the inability to obtain usable MS data in this current study, this method can prove to be useful in future endeavors where the purification of large protein complexes is necessary. Antibody experiments revealed that other tight junction proteins such as JAM-A and MUPP1 are not present in the CPE complexes. However, experiments did demonstrate that multiple claudins are most likely associated with CPE complexes.

Lastly, a mouse intestinal loop model has been developed which allows for the study of CPE-induced inflammation and lethality. Inflammatory cytokines were shown to be produced in response to CPE-induced intestinal damage. This mouse model lends itself to the design of future experiments investigating the *in vivo* innate immune responses of CPE. CPE complex formation was also shown to occur *in vivo*. This model helps to transition from *in vitro* work that has been done with CPE into an animal model. The hope is to demonstrate that the mechanisms of CPE action elucidated in cell culture can be reproduced *in vivo*. Additionally, the development of this model closely mimics the absorption of CPE from the intestine into the circulation that is seen in some instances of death associated with type A food poisoning.

A unifying theme of these 3 Aims is the ability of CPE to form toxin complexes on the membrane of target cells dictates cell death. The data presented in Aim 1 illustrates the unique toxin-host interactions at play in the mechanism of action of CPE. It appears that the formation

of the CH-1 and CH-2 complexes does not involve an elegant mechanism in which specialized microdomains (lipid rafts) are required. Importantly, the ability to form pore complexes is mediated by the ability of CPE to bind target cells via claudin. Because claudins are mainly localized to non-raft domains, the formation of CPE oligomers occurs independently of lipid rafts. An important distinction between CPE and many other pore-forming toxins that require lipid rafts for their action is that CPE binds to an identified proteinaceous receptor. For example, the CDC toxin family binds cholesterol and aerolysin binds to the GPI-anchor of proteins, both of which are enriched in raft domains. Furthermore, CPE is the only PFT that has been demonstrated to have its protein receptor associated with its toxin oligomer. This was further examined in Aim 2 where it was apparent that only claudins may be present in the CH-1 complex. These observations regarding claudin illustrate how claudin expression drives the complex formation and the action of CPE.

Despite demonstrating a correlation between cytotoxicity and enterotoxicity, where toxin mutants that are non-cytotoxic in cell culture also do not elicit damage *in vivo*, CPE complex formation has never been demonstrated to occur *in vivo* prior to the research presented here. Additionally, a rCPE mutant (TM1), in which the putative transmembrane stem domain has been deleted, is non-cytotoxic to Caco-2 cells, yet can still form CPE oligomers in a pre-pore state. To fully correlate *in vivo* complex formation with the ability to cause damage to the intestinal epithelium, it would be interesting to determine if the TM1 mutant also forms the pre-pore complex when administered in an animal model. In addition to demonstrating complex formation in the intestinal tissue of CPE-treated mice, we also showed the ability of CPE to bind and form high molecular weight complexes in livers and kidneys. In all three instances (intestine, liver, and kidney) the sizes of the CPE complexes were somewhat different that what

is observed in CPE-treated Caco-2 cells. Using the EE/IP procedure established in Aim 2, followed by MS analysis, would be an advantageous way to determine the compositional differences between the complexes that form in Caco-2 cells and those that form in tissues of mice.

APPENDIX

Table 1: MS Analysis of CH-1 (Trypsin)

Human

	Reference			P (pro)	Score	Coverage	MW
	Scan(s)	Peptide	MH+	P (pep)	XC	DeltaCn	Sp
1	Gene_Symbol=RRBP1 Isoform 3 of Ribosome-binding protein 1			5.92E-05	10.21		152470.8
	927 - 934	R.DALNQATSQVESK.Q	1391.46643	5.92E-05	4.25	0.61	1681.1

C. perfringens

	Reference			P (pro)	Score	Coverage	MW
	Scan(s)	Peptide	MH+	P (pep)	XC	DeltaCn	Sp
1	ELTB_CLOPE RecName: Full=Heat-labile enterotoxin B chain; Flags: Precursor			1.00E+00	20.20		35330.2
	662	K.TSADSLGNIDQGSLIETGE R.C	2064.15405	1.00E+00	4.09	0.51	1848.4
	1091 - 1442	K.EVFLISEDLK.T	1193.37109	1.00E+00	2.79	0.22	900.1
2	chromosome segregation protein SMC [Clostridium perfringens SM101]			1.00E+00	10.12		136081.2
	948 - 952	-.YKDKLTNM*K.-	1157.36548	1.00E+00	2.32	0.08	641.0
	chromosome segregation protein SMC [Clostridium perfringens str. 13]			1.00E+00	10.12		136009.2
3	948 - 952	-.YKDKLTNM*K.-	1157.36548	1.00E+00	2.32	0.08	641.0
	chromosome segregation protein SMC [Clostridium perfringens ATCC 13124]			1.00E+00	10.12		136141.4
	948 - 952	-.YKDKLTNM*K.-	1157.36548	1.00E+00	2.32	0.08	641.0
4	chromosome segregation protein SMC [Clostridium perfringens ATCC 13124]			1.00E+00	10.12		136141.4
	948 - 952	-.YKDKLTNM*K.-	1157.36548	1.00E+00	2.32	0.08	641.0
	chromosome segregation protein SMC [Clostridium perfringens D str. JGS1721]			1.00E+00	10.12		136056.2
5	948 - 952	-.YKDKLTNM*K.-	1157.36548	1.00E+00	2.32	0.08	641.0
	chromosome segregation protein SMC [Clostridium perfringens NCTC 8239]			1.00E+00	10.12		136018.2
	948 - 952	-.YKDKLTNM*K.-	1157.36548	1.00E+00	2.32	0.08	641.0
6	chromosome segregation protein SMC [Clostridium perfringens NCTC 8239]			1.00E+00	10.12		136018.2
	948 - 952	-.YKDKLTNM*K.-	1157.36548	1.00E+00	2.32	0.08	641.0
	chromosome segregation protein SMC [Clostridium perfringens D str. JGS1721]			1.00E+00	10.12		136056.2
7	948 - 952	-.YKDKLTNM*K.-	1157.36548	1.00E+00	2.32	0.08	641.0
	chromosome segregation protein SMC [Clostridium perfringens CPE str. F4969]			1.00E+00	10.12		136120.3
	948 - 952	-.YKDKLTNM*K.-	1157.36548	1.00E+00	2.32	0.08	641.0
8	chromosome segregation protein SMC [Clostridium perfringens B str. ATCC 3626]			1.00E+00	10.12		136124.4
	948 - 952	-.YKDKLTNM*K.-	1157.36548	1.00E+00	2.32	0.08	641.0
	chromosome segregation protein SMC [Clostridium perfringens CPE str. F4969]			1.00E+00	10.12		136120.3
9	948 - 952	-.YKDKLTNM*K.-	1157.36548	1.00E+00	2.32	0.08	641.0
	CLPB_CLOPE RecName: Full=Chaperone protein clpB			1.00E+00	10.10		97938.3
	1107	-.AELDEARGLAEK.-	1302.41602	1.00E+00	2.08	0.28	839.3
10	phosphoesterase [Clostridium perfringens str. 13]			9.98E-01	10.10		31171.1
	847 - 854	-.VKVNILGMFEKPK.-	1503.87756	9.98E-01	2.08	0.02	342.1
11	phage minor structural protein [Clostridium perfringens CPE str. F4969]			1.00E+00	10.10		111405.4
	944 - 947	-.IVYEKYIEFSNLKFK.-	1922.25513	1.00E+00	2.00	0.04	163.9
12	helicase [Clostridium perfringens D str. JGS1721]			1.00E+00	8.11		112032.2
	1091 - 1442	-.VKSFKNIDLK.-	1192.43274	1.00E+00	2.18	0.31	425.2
13	sensory box protein/histidinol phosphate phosphatase family protein [Clostridium perfringens SM101]			1.00E+00	8.11		73070.8
	948 - 952	K.YIKCIKEFL.-	1157.45020	1.00E+00	2.14	0.16	854.6
14	glycerophosphoryl diester phosphodiesterase family protein [Clostridium perfringens ATCC 13124]			9.98E-01	8.10		27579.5
	847 - 854	-.LNVDIKLGVLYEK.-	1504.79578	9.98E-01	2.04	0.07	581.3
15	beta-galactosidase [Clostridium perfringens SM101]			1.00E+00	8.10		92534.2
	662	-.SM*NKLEVTPDNLELSLDK.	2063.31579	1.00E+00	2.02	0.52	351.2

Table 2: BSA (Trypsin)

	Reference			P (pro)	Score	Coverage	MW
	Scan(s)	Peptide	MH+	P (pep)	XC	DeltaCn	Sp
1	Gene_Symbol=ALB Serum albumin			2.32E-06	160.30	26.60	69513.3
	383 - 391	K.LVTDLTK.V	789.94010	1.00E+00	1.80	0.27	561.5
	384 - 407	K.CCTESLVNR.R	1025.18585	5.27E-01	2.03	0.22	734.8
	434 - 438	K.AEFVEVTK.L	923.04499	3.22E-02	2.36	0.05	655.3
	439 - 442	R.FKDLGEEHFK.G	1250.38445	3.78E-03	4.30	0.30	2524.6
	440	K.AEFVEVTK.L	923.04499	1.82E-01	1.88	0.01	575.5
	443 - 644	K.AEFVEVTK.L	923.04499	2.96E-01	2.04	0.12	889.7
	447 - 450	R.FKDLGEEHFK.G	1250.38445	7.03E-03	3.25	0.29	1172.5
	555 - 562	K.YLYEIAR.R	928.06646	6.33E-02	2.00	0.00	238.1
	563 - 566	K.HLVDEPQNLIK.Q	1306.49269	2.32E-01	2.58	0.28	530.7
	570 - 582	K.YLYEIAR.R	928.06646	3.08E-01	2.62	0.00	542.1
	595 - 600	K.LVVSTQTALA.-	1003.17478	3.16E-02	2.41	0.41	677.9
	604 - 606	R.KVPQVSTPTLVEVSR.S	1640.90605	1.46E-04	4.25	0.42	1695.0
	607 - 610	R.KVPQVSTPTLVEVSR.S	1640.90605	9.74E-03	3.99	0.54	970.0
	622 - 626	R.RHPEYAVSVLLR.L	1440.67507	4.46E-05	4.99	0.48	2743.2
	623 - 627	R.RHPEYAVSVLLR.L	1440.67507	2.32E-06	3.91	0.50	1339.3
	651 - 654	K.VPQVSTPTLVEVSR.S	1512.73313	2.85E-06	3.27	0.52	1352.4
	672 - 1683	K.LVNELTEFAK.T	1164.33301	2.84E-02	3.11	0.32	731.3
	676 - 980	K.LVNELTEFAK.T	1164.33301	1.00E+00	2.17	0.20	546.1
	750 - 763	K.LGEYGFQNALIVR.Y	1480.69283	3.33E-04	4.69	0.53	1596.9
	755 - 831	R.RHPYFYAPELLYYANK.Y	2046.31490	3.19E-06	5.92	0.59	2345.1
	756 - 759	R.RHPYFYAPELLYYANK.Y	2046.31490	4.69E-04	5.57	0.62	1577.8
	811 - 814	R.HPYFYAPELLYYANK.Y	1890.12854	2.60E-03	3.79	0.59	653.5
	874 - 1594	K.DAFLGSFLYEYSR.R	1568.71057	1.92E-04	4.63	0.48	1681.4
	880 - 883	K.DAFLGSFLYEYSR.R	1568.71057	1.00E+00	2.36	0.31	158.9
	958 - 964	K.GLVLIAFSQYLQQCPFDEHVK.L	2436.81362	1.76E-02	3.52	0.51	750.1
	1680 - 1815	K.YLYEIAR.R	928.06646	6.78E-01	2.32	0.00	425.5

Table 3: CPE (Trypsin)

	Reference			P (pro)	Score	Coverage	MW
	Scan(s)	Peptide	MH+	P (pep)	XC	DeltaCn	Sp
1	enterotoxin [Clostridium perfringens]			2.41E-09	196.40		35330.2
	243 - 398	K.LEQSLGDGVK.D	1046.15649	9.95E-01	2.46	0.37	718.8
	283 - 287	K.LEQSLGDGVK.D	1046.15649	1.00E+00	2.15	0.25	499.2
	426 - 490	R.ISHGNISDDGSIYK.L	1506.59912	1.44E-08	4.06	0.54	1778.0
	530 - 626	R.SSNSYPWTQK.L	1198.26636	2.30E-03	2.50	0.36	660.9
	543 - 546	R.SSNSYPWTQK.L	1198.26636	9.20E-02	1.52	0.18	261.9
	575 - 1024	R.SVSTTAGPNEYVYYK.V	1679.80811	2.48E-05	5.04	0.49	1000.8
	592	R.SVSTTAGPNEYVYYK.V	1679.80811	3.00E-02	2.49	0.49	453.5
	595 - 600	R.SVSTTAGPNEYVYYK.V	1679.80811	3.54E-02	2.20	0.41	311.2
	639 - 644	R.C#VLTVPSTDIEK.E	1362.57458	9.21E-01	2.10	0.12	462.9
	662 - 1092	-.M*LSNNLNPM*VFENAK.E	1755.00973	1.17E-03	5.94	0.48	1482.0
	671 - 1200	K.TSADSLGNIDQGSLIETGER.C	2064.15405	8.95E-08	5.46	0.61	1249.8
	675 - 988	K.TSADSLGNIDQGSLIETGER.C	2064.15405	4.98E-09	5.60	0.57	1513.1
	680	K.LNLHLTITATGQK.Y	1410.64404	3.49E-05	3.58	0.44	1007.0
	698 - 706	K.EILDLAAATER.L	1202.33960	1.50E-01	3.44	0.54	1829.7
	699 - 735	-.MLSNNLNPM*VFENAK.E	1739.01033	3.92E-05	5.04	0.26	1008.5
	699 - 735	-.M*LSNNLNPMVFENAK.-	1739.01033	6.31E-01	2.95	0.51	438.4
	703 - 707	K.EILDLAAATER.L	1202.33960	8.76E-01	1.51	0.22	157.7
	710 - 1224	K.LTGIWLSK.T	918.11469	1.37E-01	2.75	0.37	439.0
	711 - 715	K.LTGIWLSK.T	918.11469	1.00E+00	1.99	0.30	467.5
	752 - 1055	K.TPINITNSNSNLSDGLYVIDK.G	2279.48950	5.93E-09	5.31	0.65	1758.6
	780 - 1339	K.EVFLISEDLK.T	1193.37109	2.02E-01	2.70	0.25	829.0
	783 - 1004	K.EVFLISEDLK.T	1193.37109	1.01E-01	2.99	0.15	734.4
	822 - 1320	K.ANSSYSGNYPYSILFQK.-	1940.10107	1.43E-03	4.28	0.59	707.6
	823 - 827	K.ANSSYSGNYPYSILFQK.-	1940.10107	2.89E-02	5.27	0.53	1646.0
	831 - 1084	K.IVDFNIYSNNFNNLVK.L	1915.13794	4.01E-02	4.63	0.38	960.0
	847 - 852	K.IVDFNIYSNNFNNLVK.L	1915.13794	9.73E-01	5.26	0.36	1458.3
	858 - 1208	R.LNLTDALNSNPAGNLYDWR.S	2148.32080	2.41E-09	6.30	0.65	2276.4
	859 - 1062	R.LNLTDALNSNPAGNLYDWR.S	2148.32080	6.40E-02	5.44	0.46	1756.6
	915	K.IVDFNIYSNNFNNLVK.L	1915.13794	1.51E-02	3.01	0.49	603.4
	922 - 926	K.GDGWILGEPSVVSSQILNPNETGTFSQSLTK.S	3263.55713	1.40E-07	8.06	0.55	3590.7
	932	K.TSADSLGNIDQGSLIETGER.C	2064.15405	1.74E-02	2.93	0.53	648.3
	942 - 946	K.ANSSYSGNYPYSILFQKF.-	2087.27588	3.31E-05	4.28	0.58	726.2
	944 - 948	K.ANSSYSGNYPYSILFQKF.-	2087.27588	4.33E-02	4.22	0.43	954.2
	958	K.ANSSYSGNYPYSILFQK.-	1940.10107	4.42E-01	2.85	0.55	526.1
	1010 - 1014	R.C#VLTVPSTDIEKEILDLAAATER.L	2545.89162	4.95E-02	3.36	0.46	517.9
	1030 - 1052	K.ANSSYSGNYPYSILFQK.-	1940.10107	1.27E-02	3.23	0.59	667.3
	1095	K.TSADSLGNIDQGSLIETGER.C	2064.15405	2.59E-02	3.03	0.47	744.6
	1188 - 1190	K.TPINITNSNSNLSDGLYVIDK.G	2279.48950	2.79E-06	5.42	0.62	1858.3

1258	K.ANSSYSGNYPYSILFQK.-	1940.10107	1.58E-04	2.88	0.56	615.9
1467	R.LNLTDALNSNPAGNLYDWR.S	2148.32080	1.62E-01	2.98	0.57	458.0
1475	K.IVDFNIYSNNFNNLVK.L	1915.13794	1.73E-01	2.70	0.46	800.4
1516 - 1519	K.EVFLISEDLK.T	1193.37109	4.74E-01	2.96	0.11	878.6
1556 - 1560	K.LTGIWLSK.T	918.11469	2.23E-02	2.19	0.45	446.9

BIBLIOGRAPHY

1. **Abrami, L., S. H. Leppla, and F. G. van der Goot.** 2006. Receptor palmitoylation and ubiquitination regulate anthrax toxin endocytosis. J Cell Biol **172:**309-320.
2. **Adak, G. K., S. M. Long, and S. J. O'Brien.** 2002. Trends in indigenous foodborne disease and deaths, England and Wales: 1992 to 2000. Gut **51:**832-841.
3. **Agarwal, R., T. D'Souza, and P. J. Morin.** 2005. Claudin-3 and claudin-4 expression in ovarian epithelial cells enhances invasion and is associated with increased matrix metalloproteinase-2 activity. Cancer Res **65:**7378-7385.
4. **Agu, C. A., R. Klein, J. Lengler, F. Schilcher, W. Gregor, T. Peterbauer, U. Blasi, B. Salmons, W. H. Gunzburg, and C. Hohenadl.** 2007. Bacteriophage-encoded toxins: the lambda-holin protein causes caspase-independent non-apoptotic cell death of eukaryotic cells. Cell Microbiol **9:**1753-1765.
5. **Al-Sadi, R., M. Boivin, and T. Ma.** 2009. Mechanism of cytokine modulation of epithelial tight junction barrier. Front Biosci **14:**2765-2778.
6. **Anderson, J. M., and C. M. Van Itallie.** 2009. Physiology and function of the tight junction. Cold Spring Harb Perspect Biol **1:**a002584.
7. **Asha, N. J., D. Tompkins, and M. H. Wilcox.** 2006. Comparative analysis of prevalence, risk factors, and molecular epidemiology of antibiotic-associated diarrhea due to Clostridium difficile, *Clostridium perfringens*, and Staphylococcus aureus. J Clin Microbiol **44:**2785-2791.
8. **Asha, N. J., and M. H. Wilcox.** 2002. Laboratory diagnosis of *Clostridium perfringens* antibiotic-associated diarrhoea. J Med Microbiol **51:**891-894.
9. **Awad, M. M., A. E. Bryant, D. L. Stevens, and J. I. Rood.** 1995. Virulence studies on chromosomal alpha-toxin and theta-toxin mutants constructed by allelic exchange provide genetic evidence for the essential role of alpha-toxin in *Clostridium perfringens*-mediated gas gangrene. Mol Microbiol **15:**191-202.
10. **Awad, M. M., D. M. Ellemor, R. L. Boyd, J. J. Emmins, and J. I. Rood.** 2001. Synergistic effects of alpha-toxin and perfringolysin O in *Clostridium perfringens*-mediated gas gangrene. Infect Immun **69:**7904-7910.
11. **Balda, M. S., and K. Matter.** 2008. Tight junctions at a glance. J Cell Sci **121:**3677-3682.
12. **Bartholomew, B. A., M. F. Stringer, G. N. Watson, and R. J. Gilbert.** 1985. Development and application of an enzyme linked immunosorbent assay for *Clostridium perfringens* type A enterotoxin. J Clin Pathol **38:**222-228.

13. **Beeman, N. E., H. K. Baumgartner, P. G. Webb, J. B. Schaack, and M. C. Neville.** 2009. Disruption of occludin function in polarized epithelial cells activates the extrinsic pathway of apoptosis leading to cell extrusion without loss of transepithelial resistance. BMC Cell Biol **10:**85.
14. **Bianchi, M. E.** 2007. DAMPs, PAMPs and alarmins: all we need to know about danger. J Leukoc Biol **81:**1-5.
15. **Birkhead, G., R. L. Vogt, E. M. Heun, J. T. Snyder, and B. A. McClane.** 1988. Characterization of an outbreak of *Clostridium perfringens* food poisoning by quantitative fecal culture and fecal enterotoxin measurement. J Clin Microbiol **26:**471-474.
16. **Borriello, S. P., F. E. Barclay, A. R. Welch, M. F. Stringer, G. N. Watson, R. K. Williams, D. V. Seal, and K. Sullens.** 1985. Epidemiology of diarrhoea caused by enterotoxigenic *Clostridium perfringens*. J Med Microbiol **20:**363-372.
17. **Borriello, S. P., H. E. Larson, A. R. Welch, F. Barclay, M. F. Stringer, and B. A. Bartholomew.** 1984. Enterotoxigenic *Clostridium perfringens*: a possible cause of antibiotic-associated diarrhoea. Lancet **1:**305-307.
18. **Borriello, S. P., and R. K. Williams.** 1985. Treatment of *Clostridium perfringens* enterotoxin-associated diarrhoea with metronidazole. J Infect **10:**65-67.
19. **Bos, J., L. Smithee, B. McClane, R. F. Distefano, F. Uzal, J. G. Songer, S. Mallonee, and J. M. Crutcher.** 2005. Fatal necrotizing colitis following a foodborne outbreak of enterotoxigenic *Clostridium perfringens* type A infection. Clin Infect Dis **40:**e78-83.
20. **Brett, M. M., J. C. Rodhouse, T. J. Donovan, G. M. Tebbutt, and D. N. Hutchinson.** 1992. Detection of *Clostridium perfringens* and its enterotoxin in cases of sporadic diarrhoea. J Clin Pathol **45:**609-611.
21. **Briehl, M. M., and R. L. Miesfeld.** 1991. Isolation and characterization of transcripts induced by androgen withdrawal and apoptotic cell death in the rat ventral prostate. Mol Endocrinol **5:**1381-1388.
22. **Brown, D. A.** 2006. Lipid rafts, detergent-resistant membranes, and raft targeting signals. Physiology (Bethesda) **21:**430-439.
23. **Brown, D. A., and E. London.** 1998. Functions of lipid rafts in biological membranes. Annu Rev Cell Dev Biol **14:**111-136.
24. **Brown, D. A., and J. K. Rose.** 1992. Sorting of GPI-anchored proteins to glycolipid-enriched membrane subdomains during transport to the apical cell surface. Cell **68:**533-544.
25. **Calvaruso, V., and A. Craxi.** 2009. Implication of normal liver enzymes in liver disease. J Viral Hepat **16:**529-536.
26. **Camacho, N., C. Espinoza, C. Rodriguez, and E. Rodriguez.** 2008. Isolates of *Clostridium perfringens* recovered from Costa Rican patients with antibiotic-associated diarrhoea are mostly enterotoxin-negative and susceptible to first-choice antimicrobials. J Med Microbiol **57:**343-347.
27. **Capaldo, C. T., and A. Nusrat.** 2009. Cytokine regulation of tight junctions. Biochim Biophys Acta **1788:**864-871.
28. **Carman, R. J., S. Sayeed, J. Li, C. W. Genheimer, M. F. Hiltonsmith, T. D. Wilkins, and B. A. McClane.** 2008. *Clostridium perfringens* toxin genotypes in the feces of healthy North Americans. Anaerobe **14:**102-108.

29. **Cascales, E., S. K. Buchanan, D. Duche, C. Kleanthous, R. Lloubes, K. Postle, M. Riley, S. Slatin, and D. Cavard.** 2007. Colicin biology. Microbiol Mol Biol Rev **71:**158-229.
30. **Cato, E. P., W. L. George, and S. M. Finegold.** 1984. Clostridium, p. 1141-1200. *In* P. H. A. Sneath, N. S. Mair, M. E. Sharpe, and J. G. Holt (ed.), Bergey's Manual of Systematic Bacteriology, vol. 2. Williams and Wilkins, Baltimore.
31. **Chakrabarti, G., and B. A. McClane.** 2005. The importance of calcium influx, calpain and calmodulin for the activation of CaCo-2 cell death pathways by *Clostridium perfringens* enterotoxin. Cell Microbiol **7:**129-146.
32. **Chakrabarti, G., X. Zhou, and B. A. McClane.** 2003. Death pathways activated in CaCo-2 cells by *Clostridium perfringens* enterotoxin. Infect Immun **71:**4260-4270.
33. **Collie, R. E., J. F. Kokai-Kun, and B. A. McClane.** 1998. Phenotypic characterization of enterotoxigenic *Clostridium perfringens* isolates from non-foodborne human gastrointestinal diseases. Anaerobe **4:**69-79.
34. **Collie, R. E., and B. A. McClane.** 1998. Evidence that the enterotoxin gene can be episomal in *Clostridium perfringens* isolates associated with non-food-borne human gastrointestinal diseases. J Clin Microbiol **36:**30-36.
35. **Cornillot, E., B. Saint-Joanis, G. Daube, S. Katayama, P. E. Granum, B. Canard, and S. T. Cole.** 1995. The enterotoxin gene (cpe) of *Clostridium perfringens* can be chromosomal or plasmid-borne. Mol Microbiol **15:**639-647.
36. **Czeczulin, J. R., P. C. Hanna, and B. A. McClane.** 1993. Cloning, nucleotide sequencing, and expression of the *Clostridium perfringens* enterotoxin gene in Escherichia coli. Infect Immun **61:**3429-3439.
37. **D'Souza, T., C. A. Sherman-Baust, S. Poosala, J. M. Mullin, and P. J. Morin.** 2009. Age-related changes of claudin expression in mouse liver, kidney, and pancreas. J Gerontol A Biol Sci Med Sci **64:**1146-1153.
38. **Draing, C., S. Sigel, S. Deininger, S. Traub, R. Munke, C. Mayer, L. Hareng, T. Hartung, S. von Aulock, and C. Hermann.** 2008. Cytokine induction by Gram-positive bacteria. Immunobiology **213:**285-296.
39. **Duncan, C. L., and D. H. Strong.** 1969. Ileal loop fluid accumulation and production of diarrhea in rabbits by cell-free products of *Clostridium perfringens*. J Bacteriol **100:**86-94.
40. **Duraisamy, Y., D. Lambert, A. O'Neill C, and P. J. Padfield.** 2007. Differential incorporation of docosahexaenoic acid into distinct cholesterol-rich membrane raft domains. Biochem Biophys Res Commun **360:**885-890.
41. **Ebihara, C., M. Kondoh, M. Harada, M. Fujii, H. Mizuguchi, S. Tsunoda, Y. Horiguchi, K. Yagi, and Y. Watanabe.** 2007. Role of Tyr306 in the C-terminal fragment of *Clostridium perfringens* enterotoxin for modulation of tight junction. Biochem Pharmacol **73:**824-830.
42. **Ebihara, C., M. Kondoh, N. Hasuike, M. Harada, H. Mizuguchi, Y. Horiguchi, M. Fujii, and Y. Watanabe.** 2006. Preparation of a claudin-targeting molecule using a C-terminal fragment of *Clostridium perfringens* enterotoxin. J Pharmacol Exp Ther **316:**255-260.
43. **Evans, M. J., T. von Hahn, D. M. Tscherne, A. J. Syder, M. Panis, B. Wolk, T. Hatziioannou, J. A. McKeating, P. D. Bieniasz, and C. M. Rice.** 2007. Claudin-1 is a hepatitis C virus co-receptor required for a late step in entry. Nature **446:**801-805.

44. **Fernandez-Miyakawa, M. E., B. H. Jost, S. J. Billington, and F. A. Uzal.** 2008. Lethal effects of *Clostridium perfringens* epsilon toxin are potentiated by alpha and perfringolysin-O toxins in a mouse model. Vet Microbiol **127:**379-385.
45. **Fernandez Miyakawa, M. E., V. Pistone Creydt, F. A. Uzal, B. A. McClane, and C. Ibarra.** 2005. *Clostridium perfringens* enterotoxin damages the human intestine in vitro. Infect Immun **73:**8407-8410.
46. **Fink, S. L., and B. T. Cookson.** 2005. Apoptosis, pyroptosis, and necrosis: mechanistic description of dead and dying eukaryotic cells. Infect Immun **73:**1907-1916.
47. **Fisher, D. J., K. Miyamoto, B. Harrison, S. Akimoto, M. R. Sarker, and B. A. McClane.** 2005. Association of beta2 toxin production with *Clostridium perfringens* type A human gastrointestinal disease isolates carrying a plasmid enterotoxin gene. Mol Microbiol **56:**747-762.
48. **Fivaz, M., L. Abrami, Y. Tsitrin, and F. G. van der Goot.** 2001. Aerolysin from *Aeromonas hydrophila* and related toxins. Curr Top Microbiol Immunol **257:**35-52.
49. **Fontijn, R. D., J. Rohlena, J. van Marle, H. Pannekoek, and A. J. Horrevoets.** 2006. Limited contribution of claudin-5-dependent tight junction strands to endothelial barrier function. Eur J Cell Biol **85:**1131-1144.
50. **Francis, S. A., J. M. Kelly, J. McCormack, R. A. Rogers, J. Lai, E. E. Schneeberger, and R. D. Lynch.** 1999. Rapid reduction of MDCK cell cholesterol by methyl-beta-cyclodextrin alters steady state transepithelial electrical resistance. Eur J Cell Biol **78:**473-484.
51. **Fujita, H., H. Chiba, H. Yokozaki, N. Sakai, K. Sugimoto, T. Wada, T. Kojima, T. Yamashita, and N. Sawada.** 2006. Differential expression and subcellular localization of claudin-7, -8, -12, -13, and -15 along the mouse intestine. J Histochem Cytochem **54:**933-944.
52. **Fujita, K., J. Katahira, Y. Horiguchi, N. Sonoda, M. Furuse, and S. Tsukita.** 2000. *Clostridium perfringens* enterotoxin binds to the second extracellular loop of claudin-3, a tight junction integral membrane protein. FEBS Lett **476:**258-261.
53. **Furuse, M., H. Sasaki, and S. Tsukita.** 1999. Manner of interaction of heterogeneous claudin species within and between tight junction strands. J Cell Biol **147:**891-903.
54. **Gao, L., and Y. Abu Kwaik.** 2000. Hijacking of apoptotic pathwaysby bacterial pathogens. Microbes Infect **2:**1705-1719.
55. **Goldmann, O., I. Sastalla, M. Wos-Oxley, M. Rohde, and E. Medina.** 2009. *Streptococcus pyogenes* induces oncosis in macrophages through the activation of an inflammatory programmed cell death pathway. Cell Microbiol **11:**138-155.
56. **Gouaux, J. E., O. Braha, M. R. Hobaugh, L. Song, S. Cheley, C. Shustak, and H. Bayley.** 1994. Subunit stoichiometry of staphylococcal alpha-hemolysin in crystals and on membranes: a heptameric transmembrane pore. Proc Natl Acad Sci U S A **91:**12828-12831.
57. **Granum, P. E.** 1985. The effect of Ca++ and Mg++ on the action of *Clostridium perfringens* enterotoxin on Vero cells. Acta Pathol Microbiol Immunol Scand B **93:**41-48.
58. **Granum, P. E., and M. Richardson.** 1991. Chymotrypsin treatment increases the activity of *Clostridium perfringens* enterotoxin. Toxicon **29:**898-900.

59. **Granum, P. E., J. R. Whitaker, and R. Skjelkvale.** 1981. Trypsin activation of enterotoxin from *Clostridium perfringens* type A: fragmentation and some physicochemical properties. Biochim Biophys Acta **668:**325-332.
60. **Greber, U. F., and M. Gastaldelli.** 2007. Junctional gating: the achilles' heel of epithelial cells in pathogen infection. Cell Host Microbe **2:**143-146.
61. **Gu, J. M., S. O. Lim, Y. M. Park, and G. Jung.** 2008. A novel splice variant of occludin deleted in exon 9 and its role in cell apoptosis and invasion. FEBS J **275:**3145-3156.
62. **Guillemot, L., S. Paschoud, P. Pulimeno, A. Foglia, and S. Citi.** 2008. The cytoplasmic plaque of tight junctions: a scaffolding and signalling center. Biochim Biophys Acta **1778:**601-613.
63. **Guttman, J. A., and B. B. Finlay.** 2009. Tight junctions as targets of infectious agents. Biochim Biophys Acta **1788:**832-841.
64. **Hale, M. L., J. C. Marvaud, M. R. Popoff, and B. G. Stiles.** 2004. Detergent-resistant membrane microdomains facilitate Ib oligomer formation and biological activity of *Clostridium perfringens* iota-toxin. Infect Immun **72:**2186-2193.
65. **Han, X., M. P. Fink, and R. L. Delude.** 2003. Proinflammatory cytokines cause NO*-dependent and -independent changes in expression and localization of tight junction proteins in intestinal epithelial cells. Shock **19:**229-237.
66. **Hanna, P. C., T. A. Mietzner, G. K. Schoolnik, and B. A. McClane.** 1991. Localization of the receptor-binding region of *Clostridium perfringens* enterotoxin utilizing cloned toxin fragments and synthetic peptides. The 30 C-terminal amino acids define a functional binding region. J Biol Chem **266:**11037-11043.
67. **Hanna, P. C., E. U. Wieckowski, T. A. Mietzner, and B. A. McClane.** 1992. Mapping of functional regions of *Clostridium perfringens* type A enterotoxin. Infect Immun **60:**2110-2114.
68. **Harada, M., M. Kondoh, C. Ebihara, A. Takahashi, E. Komiya, M. Fujii, H. Mizuguchi, S. Tsunoda, Y. Horiguchi, K. Yagi, and Y. Watanabe.** 2007. Role of tyrosine residues in modulation of claudin-4 by the C-terminal fragment of *Clostridium perfringens* enterotoxin. Biochem Pharmacol **73:**206-214.
69. **Harrison, B., D. Raju, H. S. Garmory, M. M. Brett, R. W. Titball, and M. R. Sarker.** 2005. Molecular characterization of *Clostridium perfringens* isolates from humans with sporadic diarrhea: evidence for transcriptional regulation of the beta2-toxin-encoding gene. Appl Environ Microbiol **71:**8362-8370.
70. **Hartlova, A., L. Cerveny, M. Hubalek, Z. Krocova, and J. Stulik.** 2010. Membrane rafts: a potential gateway for bacterial entry into host cells. Microbiol Immunol **54:**237-245.
71. **Hauschild, A. H., L. Niilo, and W. J. Dorward.** 1970. Enteropathogenic factors of food-poisoning *Clostridium perfringens* type A. Can J Microbiol **16:**331-338.
72. **Hauschild, A. H., L. Niilo, and W. J. Dorward.** 1971. The role of enterotoxin in *Clostridium perfringens* type A enteritis. Can J Microbiol **17:**987-991.
73. **Hauser, D., M. W. Eklund, P. Boquet, and M. R. Popoff.** 1994. Organization of the botulinum neurotoxin C1 gene and its associated non-toxic protein genes in *Clostridium botulinum* C 468. Mol Gen Genet **243:**631-640.

74. **Heikinheimo, A., M. Lindstrom, P. E. Granum, and H. Korkeala.** 2006. Humans as reservoir for enterotoxin gene--carrying *Clostridium perfringens* type A. Emerg Infect Dis **12:**1724-1729.
75. **Holmes, J. L., C. M. Van Itallie, J. E. Rasmussen, and J. M. Anderson.** 2006. Claudin profiling in the mouse during postnatal intestinal development and along the gastrointestinal tract reveals complex expression patterns. Gene Expr Patterns **6:**581-588.
76. **Horiguchi, Y., T. Uemura, S. Kozaki, and G. Sakaguchi.** 1986. Effects of Ca2+ and other cations on the action of *Clostridium perfringens* enterotoxin. Biochim Biophys Acta **889:**65-71.
77. **Hulkower, K. I., A. P. Wnek, and B. A. McClane.** 1989. Evidence that alterations in small molecule permeability are involved in the *Clostridium perfringens* type A enterotoxin-induced inhibition of macromolecular synthesis in Vero cells. J Cell Physiol **140:**498-504.
78. **Iacovache, I., F. G. van der Goot, and L. Pernot.** 2008. Pore formation: an ancient yet complex form of attack. Biochim Biophys Acta **1778:**1611-1623.
79. **Itoh, M., M. Furuse, K. Morita, K. Kubota, M. Saitou, and S. Tsukita.** 1999. Direct binding of three tight junction-associated MAGUKs, ZO-1, ZO-2, and ZO-3, with the COOH termini of claudins. J Cell Biol **147:**1351-1363.
80. **Joshy, L., R. Chaudhry, B. Dhawan, L. Kumar, and B. K. Das.** 2006. Incidence and characterization of *Clostridium perfringens* isolated from antibiotic-associated diarrhoeal patients: a prospective study in an Indian hospital. J Hosp Infect **63:**323-329.
81. **Kalischuk, L. D., G. D. Inglis, and A. G. Buret.** 2007. Strain-dependent induction of epithelial cell oncosis by *Campylobacter jejuni* is correlated with invasion ability and is independent of cytolethal distending toxin. Microbiology **153:**2952-2963.
82. **Katahira, J., N. Inoue, Y. Horiguchi, M. Matsuda, and N. Sugimoto.** 1997. Molecular cloning and functional characterization of the receptor for *Clostridium perfringens* enterotoxin. J Cell Biol **136:**1239-1247.
83. **Kinugasa, T., T. Sakaguchi, X. Gu, and H. C. Reinecker.** 2000. Claudins regulate the intestinal barrier in response to immune mediators. Gastroenterology **118:**1001-1011.
84. **Knox, R., and E. K. MacDonald.** 1943. Outbreaks of food poisoning in certain Leicester institutions. Medical Officer **69:**21-22.
85. **Kohler, H., T. Sakaguchi, B. P. Hurley, B. J. Kase, H. C. Reinecker, and B. A. McCormick.** 2007. *Salmonella enterica* serovar Typhimurium regulates intercellular junction proteins and facilitates transepithelial neutrophil and bacterial passage. Am J Physiol Gastrointest Liver Physiol **293:**G178-187.
86. **Kokai-Kun, J. F., K. Benton, E. U. Wieckowski, and B. A. McClane.** 1999. Identification of a *Clostridium perfringens* enterotoxin region required for large complex formation and cytotoxicity by random mutagenesis. Infect Immun **67:**5634-5641.
87. **Kokai-Kun, J. F., and B. A. McClane.** 1997. Deletion analysis of the *Clostridium perfringens* enterotoxin. Infect Immun **65:**1014-1022.
88. **Kokai-Kun, J. F., and B. A. McClane.** 1996. Evidence that a region(s) of the *Clostridium perfringens* enterotoxin molecule remains exposed on the external surface of the mammalian plasma membrane when the toxin is sequestered in small or large complexes. Infect Immun **64:**1020-1025.
89. **Kominsky, S. L.** 2006. Claudins: emerging targets for cancer therapy. Expert Rev Mol Med **8:**1-11.

90. **Kominsky, S. L., P. Argani, D. Korz, E. Evron, V. Raman, E. Garrett, A. Rein, G. Sauter, O. P. Kallioniemi, and S. Sukumar.** 2003. Loss of the tight junction protein claudin-7 correlates with histological grade in both ductal carcinoma in situ and invasive ductal carcinoma of the breast. Oncogene **22:**2021-2033.
91. **Kominsky, S. L., B. Tyler, J. Sosnowski, K. Brady, M. Doucet, D. Nell, J. G. Smedley, 3rd, B. McClane, H. Brem, and S. Sukumar.** 2007. *Clostridium perfringens* Enterotoxin as a Novel-Targeted Therapeutic for Brain Metastasis. Cancer Res **67:**7977-7982.
92. **Kominsky, S. L., M. Vali, D. Korz, T. G. Gabig, S. A. Weitzman, P. Argani, and S. Sukumar.** 2004. *Clostridium perfringens* enterotoxin elicits rapid and specific cytolysis of breast carcinoma cells mediated through tight junction proteins claudin 3 and 4. Am J Pathol **164:**1627-1633.
93. **Kondoh, M., A. Masuyama, A. Takahashi, N. Asano, H. Mizuguchi, N. Koizumi, M. Fujii, T. Hayakawa, Y. Horiguchi, and Y. Watanbe.** 2005. A novel strategy for the enhancement of drug absorption using a claudin modulator. Mol Pharmacol **67:**749-756.
94. **Krakauer, T., B. Fleischer, D. L. Stevens, B. A. McClane, and B. G. Stiles.** 1997. *Clostridium perfringens* enterotoxin lacks superantigenic activity but induces an interleukin-6 response from human peripheral blood mononuclear cells. Infect Immun **65:**3485-3488.
95. **Kristan, K. C., G. Viero, M. Dalla Serra, P. Macek, and G. Anderluh.** 2009. Molecular mechanism of pore formation by actinoporins. Toxicon **54:**1125-1134.
96. **Kuske, C. R., S. M. Barns, C. C. Grow, L. Merrill, and J. Dunbar.** 2006. Environmental survey for four pathogenic bacteria and closely related species using phylogenetic and functional genes. J Forensic Sci **51:**548-558.
97. **Labbe, K., and M. Saleh.** 2008. Cell death in the host response to infection. Cell Death Differ **15:**1339-1349.
98. **Lafont, F., L. Abrami, and F. G. van der Goot.** 2004. Bacterial subversion of lipid rafts. Curr Opin Microbiol **7:**4-10.
99. **Lambert, D., C. A. O'Neill, and P. J. Padfield.** 2005. Depletion of Caco-2 cell cholesterol disrupts barrier function by altering the detergent solubility and distribution of specific tight-junction proteins. Biochem J **387:**553-560.
100. **Lambert, D., P. J. Padfield, J. McLaughlin, S. Cannell, and C. A. O'Neill.** 2007. Ochratoxin A displaces claudins from detergent resistant membrane microdomains. Biochem Biophys Res Commun **358:**632-636.
101. **Li, J., and B. A. McClane.** 2006. Comparative effects of osmotic, sodium nitrite-induced, and pH-induced stress on growth and survival of *Clostridium perfringens* type A isolates carrying chromosomal or plasmid-borne enterotoxin genes. Appl Environ Microbiol **72:**7620-7625.
102. **Li, J., and B. A. McClane.** 2006. Further comparison of temperature effects on growth and survival of *Clostridium perfringens* type A isolates carrying a chromosomal or plasmid-borne enterotoxin gene. Appl Environ Microbiol **72:**4561-4568.
103. **Li, J., and B. A. McClane.** 2008. A novel small acid soluble protein variant is important for spore resistance of most *Clostridium perfringens* food poisoning isolates. PLoS Pathog **4:**e1000056.
104. **Li, J., K. Miyamoto, and B. A. McClane.** 2007. Comparison of virulence plasmids among *Clostridium perfringens* type E isolates. Infect Immun **75:**1811-1819.

105. **Li, J., S. Sayeed, and B. A. McClane.** 2007. Prevalence of enterotoxigenic *Clostridium perfringens* Isolates in Pittsburgh (Pennsylvania) area soils and home kitchens. Appl Environ Microbiol **73:**7218-7224.
106. **Lindsay, J. A.** 1988. The effect of a *Clostridium perfringens* 8-6 enterotoxin on viability and macromolecular synthesis in Vero cells. Biochem Biophys Res Commun **151:**1371-1377.
107. **Lingwood, D., J. Ries, P. Schwille, and K. Simons.** 2008. Plasma membranes are poised for activation of raft phase coalescence at physiological temperature. Proc Natl Acad Sci U S A **105:**10005-10010.
108. **Litkouhi, B., J. Kwong, C. M. Lo, J. G. Smedley, B. A. McClane, M. Aponte, Z. Gao, J. L. Sarno, J. Hinners, W. R. Welch, R. S. Berkowitz, S. C. Mok, E. I. Garner.** 2007. Claudin-4 overexpression in epithelial ovarian cancer is associated with hypomethylation and is a potential target for modulation of tight junction barrier function using a C-terminal fragment of *Clostridium perfringens* enterotoxin. Neoplasia **9:**304-314.
109. **Loffler, A., and R. Labbe.** 1986. Characterization of a parasporal inclusion body from sporulating, enterotoxin-positive *Clostridium perfringens* type A. J Bacteriol **165:**542-548.
110. **Lohrberg, D., E. Krause, M. Schumann, J. Piontek, L. Winkler, I. E. Blasig, and R. F. Haseloff.** 2009. A strategy for enrichment of claudins based on their affinity to *Clostridium perfringens* enterotoxin. BMC Mol Biol **10:**61.
111. **Long, H., C. D. Crean, W. H. Lee, O. W. Cummings, and T. G. Gabig.** 2001. Expression of *Clostridium perfringens* enterotoxin receptors claudin-3 and claudin-4 in prostate cancer epithelium. Cancer Res **61:**7878-7881.
112. **Lotze, M. T., H. J. Zeh, A. Rubartelli, L. J. Sparvero, A. A. Amoscato, N. R. Washburn, M. E. Devera, X. Liang, M. Tor, and T. Billiar.** 2007. The grateful dead: damage-associated molecular pattern molecules and reduction/oxidation regulate immunity. Immunol Rev **220:**60-81.
113. **Lynch, M., J. Painter, R. Woodruff, and C. Braden.** 2006. Surveillance for Foodborne-Disease Outbreaks --- United States, 1998--2002. Morb. Mortal. Wkly. Rep. Surveill. Summ. **55:**1-34.
114. **Lynch, R. D., S. A. Francis, K. M. McCarthy, E. Casas, C. Thiele, and E. E. Schneeberger.** 2007. Cholesterol depletion alters detergent-specific solubility profiles of selected tight junction proteins and the phosphorylation of occludin. Experimental Cell Research **313:**2597-2610.
115. **Manes, S., G. del Real, and A. C. Martinez.** 2003. Pathogens: raft hijackers. Nat Rev Immunol **3:**557-568.
116. **Masuyama, A., M. Kondoh, H. Seguchi, A. Takahashi, M. Harada, M. Fujii, H. Mizuguchi, Y. Horiguchi, and Y. Watanabe.** 2005. Role of N-terminal amino acids in the absorption-enhancing effects of the c-terminal fragment of *Clostridium perfringens* enterotoxin. J Pharmacol Exp Ther **314:**789-795.
117. **Matsuda, M., K. Ozutsumi, H. Iwahashi, and N. Sugimoto.** 1986. Primary action of *Clostridium perfringens* type A enterotoxin on HeLa and Vero cells in the absence of extracellular calcium: rapid and characteristic changes in membrane permeability. Biochem Biophys Res Commun **141:**704-710.

118. **McClane, B. A.** 1994. *Clostridium perfringens* enterotoxin acts by producing small molecule permeability alterations in plasma membranes. Toxicology **87:**43-67.
119. **McClane, B. A., and J. L. McDonel.** 1980. Characterization of membrane permeability alterations induced in Vero cells by *Clostridium perfringens* enterotoxin. Biochim Biophys Acta **600:**974-985.
120. **McClane, B. A., and J. L. McDonel.** 1979. The effects of *Clostridium perfringens* enterotoxin on morphology, viability, and macromolecular synthesis in Vero cells. J Cell Physiol **99:**191-200.
121. **McClane, B. A., and J. L. McDonel.** 1981. Protective effects of osmotic stabilizers on morphological and permeability alterations induced in Vero cells by *Clostridium perfringens* enterotoxin. Biochim Biophys Acta **641:**401-409.
122. **McClane, B. A., and A. P. Wnek.** 1990. Studies of *Clostridium perfringens* enterotoxin action at different temperatures demonstrate a correlation between complex formation and cytotoxicity. Infect Immun **58:**3109-3115.
123. **McDonel J.L., D. F.** 1986. The role of toxins in bacterial pathogenesis. *In* D. J. Dorner F. (ed.), Pharmacology of Bacterial Toxins. Pergamon Press, New York.
124. **McDonel, J. L.** 1980. Binding of *Clostridium perfringens* [125I]enterotoxin to rabbit intestinal cells. Biochemistry **19:**4801-4807.
125. **McDonel, J. L., and C. L. Duncan.** 1975. Histopathological effect of *Clostridium perfringens* enterotoxin in the rabbit ileum. Infect Immun **12:**1214-1218.
126. **McDonel, J. L., and B. A. McClane.** 1979. Binding versus biological activity of *Clostridium perfringens* enterotoxin in Vero cells. Biochem Biophys Res Commun **87:**497-504.
127. **McDonel, J. L., and B. A. McClane.** 1988. Production, purification, and assay of *Clostridium perfringens* enterotoxin. Methods Enzymol **165:**94-103.
128. **Meertens, L., C. Bertaux, L. Cukierman, E. Cormier, D. Lavillette, F. L. Cosset, and T. Dragic.** 2008. The tight junction proteins claudin-1, -6, and -9 are entry cofactors for hepatitis C virus. J Virol **82:**3555-3560.
129. **Melton, L. A., M. L. Tracy, and G. Moller.** 1990. Screening trace elements and electrolytes in serum by inductively-coupled plasma emission spectrometry. Clin Chem **36:**247-250.
130. **Melville, S. B., R. Labbe, and A. L. Sonenshein.** 1994. Expression from the *Clostridium perfringens* cpe promoter in *C. perfringens* and *Bacillus subtilis*. Infect Immun **62:**5550-5558.
131. **Michl, P., M. Buchholz, M. Rolke, S. Kunsch, M. Lohr, B. McClane, S. Tsukita, G. Leder, G. Adler, and T. M. Gress.** 2001. Claudin-4: a new target for pancreatic cancer treatment using *Clostridium perfringens* enterotoxin. Gastroenterology **121:**678-684.
132. **Mietzner, T. A., J. F. Kokai-Kun, P. C. Hanna, and B. A. McClane.** 1992. A conjugated synthetic peptide corresponding to the C-terminal region of *Clostridium perfringens* type A enterotoxin elicits an enterotoxin-neutralizing antibody response in mice. Infect Immun **60:**3947-3951.
133. **Mitic, L. L., V. M. Unger, and J. M. Anderson.** 2003. Expression, solubilization, and biochemical characterization of the tight junction transmembrane protein claudin-4. Protein Sci **12:**218-227.
134. **Miyamoto, K., D. J. Fisher, J. Li, S. Sayeed, S. Akimoto, and B. A. McClane.** 2006. Complete sequencing and diversity analysis of the enterotoxin-encoding plasmids in

Clostridium perfringens type A non-food-borne human gastrointestinal disease isolates. J Bacteriol **188:**1585-1598.

135. **Miyamoto, K., Q. Wen, and B. A. McClane.** 2004. Multiplex PCR genotyping assay that distinguishes between isolates of *Clostridium perfringens* type A carrying a chromosomal enterotoxin gene (cpe) locus, a plasmid cpe locus with an IS1470-like sequence, or a plasmid cpe locus with an IS1151 sequence. J Clin Microbiol **42:**1552-1558.
136. **Miyata, S., O. Matsushita, J. Minami, S. Katayama, S. Shimamoto, and A. Okabe.** 2001. Cleavage of a C-terminal peptide is essential for heptamerization of *Clostridium perfringens* epsilon-toxin in the synaptosomal membrane. J Biol Chem **276:**13778-13783.
137. **Miyata, S., J. Minami, E. Tamai, O. Matsushita, S. Shimamoto, and A. Okabe.** 2002. *Clostridium perfringens* epsilon-toxin forms a heptameric pore within the detergent-insoluble microdomains of Madin-Darby canine kidney cells and rat synaptosomes. J Biol Chem **277:**39463-39468.
138. **Modi, N., and M. H. Wilcox.** 2001. Evidence for antibiotic induced *Clostridium perfringens* diarrhoea. J Clin Pathol **54:**748-751.
139. **Mpamugo, O., T. Donovan, and M. M. Brett.** 1995. Enterotoxigenic *Clostridium perfringens* as a cause of sporadic cases of diarrhoea. J Med Microbiol **43:**442-445.
140. **Myers, G. S., D. A. Rasko, J. K. Cheung, J. Ravel, R. Seshadri, R. T. DeBoy, Q. Ren, J. Varga, M. M. Awad, L. M. Brinkac, S. C. Daugherty, D. H. Haft, R. J. Dodson, R. Madupu, W. C. Nelson, M. J. Rosovitz, S. A. Sullivan, H. Khouri, G. I. Dimitrov, K. L. Watkins, S. Mulligan, J. Benton, D. Radune, D. J. Fisher, H. S. Atkins, T. Hiscox, B. H. Jost, S. J. Billington, J. G. Songer, B. A. McClane, R. W. Titball, J. I. Rood, S. B. Melville, and I. T. Paulsen.** 2006. Skewed genomic variability in strains of the toxigenic bacterial pathogen, *Clostridium perfringens*. Genome Res **16:**1031-1040.
141. **Nagahama, M., S. Hayashi, S. Morimitsu, and J. Sakurai.** 2003. Biological activities and pore formation of *Clostridium perfringens* beta toxin in HL 60 cells. J Biol Chem **278:**36934-36941.
142. **Nagahama, M., A. Yamaguchi, T. Hagiyama, N. Ohkubo, K. Kobayashi, and J. Sakurai.** 2004. Binding and internalization of *Clostridium perfringens* iota-toxin in lipid rafts. Infect Immun **72:**3267-3275.
143. **Nichols, L. S., R. Ashfaq, and C. A. Iacobuzio-Donahue.** 2004. Claudin 4 protein expression in primary and metastatic pancreatic cancer: support for use as a therapeutic target. Am J Clin Pathol **121:**226-230.
144. **Niilo, L.** 1971. Mechanism of Action of the Enteropathogenic Factor of *Clostridium perfringens* Type A. Infect Immun **3:**100-106.
145. **Nusrat, A., C. A. Parkos, P. Verkade, C. S. Foley, T. W. Liang, W. Innis-Whitehouse, K. K. Eastburn, and J. L. Madara.** 2000. Tight junctions are membrane microdomains. J Cell Sci **113 (Pt 10):**1771-1781.
146. **O'Brien, D. K., and S. B. Melville.** 2004. Effects of *Clostridium perfringens* alpha-toxin (PLC) and perfringolysin O (PFO) on cytotoxicity to macrophages, on escape from the phagosomes of macrophages, and on persistence of C. perfringens in host tissues. Infect Immun **72:**5204-5215.

147. **Ogawa-Goto, K., K. Tanaka, T. Ueno, T. Kurata, T. Sata, and S. Irie.** 2007. p180 is involved in the interaction between the endoplasmic reticulum and microtubules through a novel microtubule-binding and bundling domain. Mol Biol Cell **18:**3741-3751.
148. **Ouban, A., and A. A. Ahmed.** 2010. Claudins in human cancer: a review. Histol Histopathol **25:**83-90.
149. **Pei, J., J. E. Turse, Q. Wu, and T. A. Ficht.** 2006. *Brucella abortus* rough mutants induce macrophage oncosis that requires bacterial protein synthesis and direct interaction with the macrophage. Infect Immun **74:**2667-2675.
150. **Philippe, V. A., M. B. Mendez, I. H. Huang, L. M. Orsaria, M. R. Sarker, and R. R. Grau.** 2006. Inorganic phosphate induces spore morphogenesis and enterotoxin production in the intestinal pathogen *Clostridium perfringens*. Infect Immun **74:**3651-3656.
151. **Pigott, C. R., and D. J. Ellar.** 2007. Role of receptors in *Bacillus thuringiensis* crystal toxin activity. Microbiol Mol Biol Rev **71:**255-281.
152. **Pike, L. J.** 2006. Rafts defined: a report on the Keystone Symposium on Lipid Rafts and Cell Function. J Lipid Res **47:**1597-1598.
153. **Pituch, H., N. van den Braak, A. van Belkum, W. Van Leeuwen, P. Obuch-Woszczatynski, M. Luczak, H. Verbrugh, F. Meisel-Mikolajczyk, and G. Martirosian.** 2002. Characterization of *Clostridium perfringens* strains isolated from Polish patients with suspected antibiotic-associated diarrhea. Med Sci Monit **8:**BR85-88.
154. **Prevention, C. f. D. C. a.** 2009. *Clostridium perfringens* infection among inmates at a county jail--Wisconsin, August 2008. MMWR Morb Mortal Wkly Rep **58:**138-141.
155. **ProMED-mail.** 2010. *C. perfringens* food intoxication, fatal - USA: (LA) nosocomial. ProMED-mail 2010, vol. 30 May.
156. **Qin, S., H. Wang, R. Yuan, H. Li, M. Ochani, K. Ochani, M. Rosas-Ballina, C. J. Czura, J. M. Huston, E. Miller, X. Lin, B. Sherry, A. Kumar, G. Larosa, W. Newman, K. J. Tracey, and H. Yang.** 2006. Role of HMGB1 in apoptosis-mediated sepsis lethality. J Exp Med **203:**1637-1642.
157. **Robertson, S. L., J. G. Smedley, 3rd, and B. A. McClane.** 2010. Identification of a claudin-4 residue important for mediating the host cell binding and action of *Clostridium perfringens* enterotoxin. Infect Immun **78:**505-517.
158. **Robertson, S. L., J. G. Smedley, 3rd, U. Singh, G. Chakrabarti, C. M. Van Itallie, J. M. Anderson, and B. A. McClane.** 2007. Compositional and stoichiometric analysis of *Clostridium perfringens* enterotoxin complexes in Caco-2 cells and claudin 4 fibroblast transfectants. Cell Microbiol.
159. **Rodewald, M., D. Herr, W. C. Duncan, H. M. Fraser, G. Hack, R. Konrad, F. Gagsteiger, R. Kreienberg, and C. Wulff.** 2009. Molecular mechanisms of ovarian hyperstimulation syndrome: paracrine reduction of endothelial claudin 5 by hCG in vitro is associated with increased endothelial permeability. Hum Reprod **24:**1191-1199.
160. **Rupnik, M., M. H. Wilcox, and D. N. Gerding.** 2009. *Clostridium difficile* infection: new developments in epidemiology and pathogenesis. Nat Rev Microbiol **7:**526-536.
161. **Saeki, R., M. Kondoh, H. Kakutani, S. Tsunoda, Y. Mochizuki, T. Hamakubo, Y. Tsutsumi, Y. Horiguchi, and K. Yagi.** 2009. A novel tumor-targeted therapy using a claudin-4-targeting molecule. Mol Pharmacol **76:**918-926.
162. **Samuel, S. C., P. Hancock, and D. A. Leigh.** 1991. An investigation into *Clostridium perfringens* enterotoxin-associated diarrhoea. J Hosp Infect **18:**219-230.

163. **Santin, A. D., S. Bellone, E. R. Siegel, J. K. McKenney, M. Thomas, J. J. Roman, A. Burnett, G. Tognon, E. Bandiera, and S. Pecorelli.** 2007. Overexpression of *Clostridium perfringens* Enterotoxin Receptors Claudin-3 and Claudin-4 in Uterine Carcinosarcomas. Clin Cancer Res **13:**3339-3346.
164. **Santin, A. D., S. Cane, S. Bellone, M. Palmieri, E. R. Siegel, M. Thomas, J. J. Roman, A. Burnett, M. J. Cannon, and S. Pecorelli.** 2005. Treatment of chemotherapy-resistant human ovarian cancer xenografts in C.B-17/SCID mice by intraperitoneal administration of *Clostridium perfringens* enterotoxin. Cancer Res **65:**4334-4342.
165. **Sarker, M. R., R. J. Carman, and B. A. McClane.** 1999. Inactivation of the gene (cpe) encoding *Clostridium perfringens* enterotoxin eliminates the ability of two cpe-positive *C. perfringens* type A human gastrointestinal disease isolates to affect rabbit ileal loops. Mol Microbiol **33:**946-958.
166. **Sarker, M. R., R. P. Shivers, S. G. Sparks, V. K. Juneja, and B. A. McClane.** 2000. Comparative experiments to examine the effects of heating on vegetative cells and spores of *Clostridium perfringens* isolates carrying plasmid genes versus chromosomal enterotoxin genes. Appl Environ Microbiol **66:**3234-3240.
167. **Sayeed, S., J. Li, and B. A. McClane.** 2010. Characterization of virulence plasmid diversity among *Clostridium perfringens* type B isolates. Infect Immun **78:**495-504.
168. **Sayeed, S., J. Li, and B. A. McClane.** 2007. Virulence plasmid diversity in *Clostridium perfringens* type D isolates. Infect Immun **75:**2391-2398.
169. **Sayeed, S., F. A. Uzal, D. J. Fisher, J. Saputo, J. E. Vidal, Y. Chen, P. Gupta, J. I. Rood, and B. A. McClane.** 2008. Beta toxin is essential for the intestinal virulence of *Clostridium perfringens* type C disease isolate CN3685 in a rabbit ileal loop model. Mol Microbiol **67:**15-30.
170. **Scaffidi, P., T. Misteli, and M. E. Bianchi.** 2002. Release of chromatin protein HMGB1 by necrotic cells triggers inflammation. Nature **418:**191-195.
171. **Severson, E. A., and C. A. Parkos.** 2009. Structural determinants of Junctional Adhesion Molecule A (JAM-A) function and mechanisms of intracellular signaling. Curr Opin Cell Biol **21:**701-707.
172. **Shandera, W. X., C. O. Tacket, and P. A. Blake.** 1983. Food poisoning due to *Clostridium perfringens* in the United States. J Infect Dis **147:**167-170.
173. **Sherman, S., E. Klein, and B. A. McClane.** 1994. *Clostridium perfringens* type A enterotoxin induces tissue damage and fluid accumulation in rabbit ileum. J Diarrhoeal Dis Res **12:**200-207.
174. **Shimizu, T., K. Ohtani, H. Hirakawa, K. Ohshima, A. Yamashita, T. Shiba, N. Ogasawara, M. Hattori, S. Kuhara, and H. Hayashi.** 2002. Complete genome sequence of *Clostridium perfringens*, an anaerobic flesh-eater. Proc Natl Acad Sci U S A **99:**996-1001.
175. **Simons, K., and E. Ikonen.** 1997. Functional rafts in cell membranes. Nature **387:**569-572.
176. **Sims, J. E., and D. E. Smith.** 2010. The IL-1 family: regulators of immunity. Nat Rev Immunol **10:**89-102.
177. **Singh, A. B., and R. C. Harris.** 2004. Epidermal growth factor receptor activation differentially regulates claudin expression and enhances transepithelial resistance in Madin-Darby canine kidney cells. J Biol Chem **279:**3543-3552.

178. **Singh, U., L. L. Mitic, E. U. Wieckowski, J. M. Anderson, and B. A. McClane.** 2001. Comparative biochemical and immunocytochemical studies reveal differences in the effects of *Clostridium perfringens* enterotoxin on polarized CaCo-2 cells versus Vero cells. J Biol Chem **276:**33402-33412.
179. **Singh, U., C. M. Van Itallie, L. L. Mitic, J. M. Anderson, and B. A. McClane.** 2000. CaCo-2 cells treated with *Clostridium perfringens* enterotoxin form multiple large complex species, one of which contains the tight junction protein occludin. J Biol Chem **275:**18407-18417.
180. **Skjelkvale, R., H. Tolleshaug, and T. Jarmund.** 1980. Binding of enterotoxin from *Clostridium perfringens* type A to liver cells in vivo and in vitro. The enterotoxin causes membrane leakage. Acta Pathol Microbiol Scand B **88:**95-102.
181. **Skjelkvale, R., and T. Uemura.** 1977. Experimental Diarrhoea in human volunteers following oral administration of *Clostridium perfringens* enterotoxin. J Appl Bacteriol **43:**281-286.
182. **Smedley, J. G., 3rd, and B. A. McClane.** 2004. Fine mapping of the N-terminal cytotoxicity region of *Clostridium perfringens* enterotoxin by site-directed mutagenesis. Infect Immun **72:**6914-6923.
183. **Smedley, J. G., 3rd, J. Saputo, J. C. Parker, M. E. Fernandez-Miyakawa, S. L. Robertson, B. A. McClane, and F. A. Uzal.** 2008. Noncytotoxic *Clostridium perfringens* enterotoxin (CPE) variants localize CPE intestinal binding and demonstrate a relationship between CPE-induced cytotoxicity and enterotoxicity. Infect Immun **76:**3793-3800.
184. **Smedley, J. G., III, F. A. Uzal, and B. A. McClane.** 2007. Identification of a Prepore Large-Complex Stage in the Mechanism of Action of *Clostridium perfringens* Enterotoxin. Infect. Immun. **75:**2381-2390.
185. **Song, L., M. R. Hobaugh, C. Shustak, S. Cheley, H. Bayley, and J. E. Gouaux.** 1996. Structure of staphylococcal alpha-hemolysin, a heptameric transmembrane pore. Science **274:**1859-1866.
186. **Songer, J. G.** 1996. Clostridial enteric diseases of domestic animals. Clin Microbiol Rev **9:**216-234.
187. **Sonoda, N., M. Furuse, H. Sasaki, S. Yonemura, J. Katahira, Y. Horiguchi, and S. Tsukita.** 1999. *Clostridium perfringens* enterotoxin fragment removes specific claudins from tight junction strands: Evidence for direct involvement of claudins in tight junction barrier. J Cell Biol **147:**195-204.
188. **Stark, R. L., and C. L. Duncan.** 1971. Biological characteristics of *Clostridium perfringens* type A enterotoxin. Infect Immun **4:**89-96.
189. **Sugimoto, N., Y. M. Chen, S. Y. Lee, M. Matsuda, and C. Y. Lee.** 1991. Pathodynamics of intoxication in rats and mice by enterotoxin of *Clostridium perfringens* type A. Toxicon **29:**751-759.
190. **Sugimoto, N., K. Ozutsumi, and M. Matsuda.** 1985. Morphological alterations and changes in cellular cations induced by *Clostridium perfringens* type A enterotoxin in tissue culture cells. Eur J Epidemiol **1:**264-273.
191. **Sugimoto, N., M. Takagi, K. Ozutsumi, S. Harada, and M. Matsuda.** 1988. Enterotoxin of *Clostridium perfringens* type A forms ion-permeable channels in a lipid bilayer membrane. Biochem Biophys Res Commun **156:**551-556.

192. **Takahashi, A., E. Komiya, H. Kakutani, T. Yoshida, M. Fujii, Y. Horiguchi, H. Mizuguchi, Y. Tsutsumi, S. Tsunoda, N. Koizumi, K. Isoda, K. Yagi, Y. Watanabe, and M. Kondoh.** 2008. Domain mapping of a claudin-4 modulator, the C-terminal region of C-terminal fragment of *Clostridium perfringens* enterotoxin, by site-directed mutagenesis. Biochem Pharmacol **75:**1639-1648.
193. **Takahashi, A., M. Kondoh, A. Masuyama, M. Fujii, H. Mizuguchi, Y. Horiguchi, and Y. Watanabe.** 2005. Role of C-terminal regions of the C-terminal fragment of *Clostridium perfringens* enterotoxin in its interaction with claudin-4. Journal of Controlled Release **108:**56-62.
194. **Tanaka, D., K. Kimata, M. Shimizu, J. Isobe, M. Watahiki, T. Karasawa, T. Yamagishi, S. Kuramoto, T. Serikawa, F. Ishiguro, M. Yamada, K. Yamaoka, M. Tokoro, T. Fukao, M. Matsumoto, R. Hiramatsu, C. Monma, and Y. Nagai.** 2007. Genotyping of *Clostridium perfringens* isolates collected from food poisoning outbreaks and healthy individuals in Japan based on the cpe locus. Jpn J Infect Dis **60:**68-69.
195. **Thumbikat, P., T. Dileepan, M. S. Kannan, and S. K. Maheswaran.** 2005. Mechanisms underlying Mannheimia haemolytica leukotoxin-induced oncosis and apoptosis of bovine alveolar macrophages. Microb Pathog **38:**161-172.
196. **Tilley, S. J., and H. R. Saibil.** 2006. The mechanism of pore formation by bacterial toxins. Current Opinion in Structural Biology **16:**230-236.
197. **Titball, R. W.** 1993. Bacterial phospholipases C. Microbiol Rev **57:**347-366.
198. **Todd, E. C.** 1989. Costs of acute bacterial foodborne disease in Canada and the United States. Int J Food Microbiol **9:**313-326.
199. **Tsukita, S., M. Furuse, and M. Itoh.** 2001. Multifunctional strands in tight junctions. Nat Rev Mol Cell Biol **2:**285-293.
200. **Tweten, R. K.** 2005. Cholesterol-dependent cytolysins, a family of versatile pore-forming toxins. Infect Immun **73:**6199-6209.
201. **Uchida, H., M. Kondoh, T. Hanada, A. Takahashi, T. Hamakubo, and K. Yagi.** 2010. A claudin-4 modulator enhances the mucosal absorption of a biologically active peptide. Biochem Pharmacol **79:**1437-1444.
202. **Uzal, F. A., J. Saputo, S. Sayeed, J. E. Vidal, D. J. Fisher, R. Poon, V. Adams, M. E. Fernandez-Miyakawa, J. I. Rood, and B. A. McClane.** 2009. Development and application of new mouse models to study the pathogenesis of *Clostridium perfringens* type C Enterotoxemias. Infect Immun **77:**5291-5299.
203. **Vaishnavi, C., and S. Kaur.** 2008. *Clostridium perfringens* enterotoxin in antibiotic-associated diarrhea. Indian J Pathol Microbiol **51:**198-199.
204. **Van Itallie, C. M., and J. M. Anderson.** 2004. The molecular physiology of tight junction pores. Physiology (Bethesda) **19:**331-338.
205. **Van Itallie, C. M., L. Betts, J. G. Smedley, 3rd, B. A. McClane, and J. M. Anderson.** 2008. Structure of the claudin-binding domain of *Clostridium perfringens* enterotoxin. J Biol Chem **283:**268-274.
206. **Varga, J., V. L. Stirewalt, and S. B. Melville.** 2004. The CcpA protein is necessary for efficient sporulation and enterotoxin gene (cpe) regulation in *Clostridium perfringens*. J Bacteriol **186:**5221-5229.
207. **Vidal, J. E., B. A. McClane, J. Saputo, J. Parker, and F. A. Uzal.** 2008. Effects of *Clostridium perfringens* beta-toxin on the rabbit small intestine and colon. Infect Immun **76:**4396-4404.

208. **Vieira, F. S., G. Correa, M. Einicker-Lamas, and R. Coutinho-Silva.** 2010. Host-cell lipid rafts: a safe door for micro-organisms? Biol Cell **102:**391-407.
209. **Waheed, A. A., Y. Shimada, H. F. Heijnen, M. Nakamura, M. Inomata, M. Hayashi, S. Iwashita, J. W. Slot, and Y. Ohno-Iwashita.** 2001. Selective binding of perfringolysin O derivative to cholesterol-rich membrane microdomains (rafts). Proc Natl Acad Sci U S A **98:**4926-4931.
210. **Wallace, F. M., A. S. Mach, A. M. Keller, and J. A. Lindsay.** 1999. Evidence for *Clostridium perfringens* enterotoxin (CPE) inducing a mitogenic and cytokine response in vitro and a cytokine response in vivo. Curr Microbiol **38:**96-100.
211. **Weinrauch, Y., and A. Zychlinsky.** 1999. The induction of apoptosis by bacterial pathogens. Annu Rev Microbiol **53:**155-187.
212. **Wen, Q., and B. A. McClane.** 2004. Detection of enterotoxigenic *Clostridium perfringens* type A isolates in American retail foods. Appl Environ Microbiol **70:**2685-2691.
213. **Wieckowski, E. U., J. F. Kokai-Kun, and B. A. McClane.** 1998. Characterization of membrane-associated *Clostridium perfringens* enterotoxin following pronase treatment. Infect Immun **66:**5897-5905.
214. **Wieckowski, E. U., A. P. Wnek, and B. A. McClane.** 1994. Evidence that an approximately 50-kDa mammalian plasma membrane protein with receptor-like properties mediates the amphiphilicity of specifically bound *Clostridium perfringens* enterotoxin. J Biol Chem **269:**10838-10848.
215. **Winkler, L., C. Gehring, A. Wenzel, S. L. Muller, C. Piehl, G. Krause, I. E. Blasig, and J. Piontek.** 2009. Molecular determinants of the interaction between *Clostridium perfringens* enterotoxin fragments and claudin-3. J Biol Chem **284:**18863-18872.
216. **Wnek, A. P., and B. A. McClane.** 1983. Identification of a 50,000 Mr protein from rabbit brush border membranes that binds *Clostridium perfringens* enterotoxin. Biochem Biophys Res Commun **112:**1099-1105.
217. **Wnek, A. P., and B. A. McClane.** 1989. Preliminary evidence that *Clostridium perfringens* type A enterotoxin is present in a 160,000-Mr complex in mammalian membranes. Infect Immun **57:**574-581.
218. **Wnek, A. P., R. J. Strouse, and B. A. McClane.** 1985. Production and characterization of monoclonal antibodies against *Clostridium perfringens* type A enterotoxin. Infect Immun **50:**442-448.
219. **Wong, V.** 1997. Phosphorylation of occludin correlates with occludin localization and function at the tight junction. Am J Physiol **273:**C1859-1867.
220. **Yamamoto, K., I. Ohishi, and G. Sakaguchi.** 1979. Fluid accumulation in mouse ligated intestine inoculated with *Clostridium perfringens* enterotoxin. Appl Environ Microbiol **37:**181-186.
221. **Yamazaki, Y., K. Okawa, T. Yano, and S. Tsukita.** 2008. Optimized proteomic analysis on gels of cell-cell adhering junctional membrane proteins. Biochemistry **47:**5378-5386.
222. **Young, J. A., and R. J. Collier.** 2007. Anthrax toxin: receptor binding, internalization, pore formation, and translocation. Annu Rev Biochem **76:**243-265.
223. **Yu, A. S., K. M. McCarthy, S. A. Francis, J. M. McCormack, J. Lai, R. A. Rogers, R. D. Lynch, and E. E. Schneeberger.** 2005. Knockdown of occludin expression leads

to diverse phenotypic alterations in epithelial cells. Am J Physiol Cell Physiol **288:**C1231-1241.

224. **Yuan, X., X. Lin, G. Manorek, I. Kanatani, L. H. Cheung, M. G. Rosenblum, and S. B. Howell.** 2009. Recombinant CPE fused to tumor necrosis factor targets human ovarian cancer cells expressing the claudin-3 and claudin-4 receptors. Mol Cancer Ther **8:**1906-1915.
225. **Zhao, Y., and S. B. Melville.** 1998. Identification and characterization of sporulation-dependent promoters upstream of the enterotoxin gene (cpe) of *Clostridium perfringens*. J Bacteriol **180:**136-142.
226. **Zheng, A., F. Yuan, Y. Li, F. Zhu, P. Hou, J. Li, X. Song, M. Ding, and H. Deng.** 2007. Claudin-6 and claudin-9 function as additional coreceptors for hepatitis C virus. J Virol **81:**12465-12471.
227. **Zhou, X., M. E. Konkel, and D. R. Call.** 2009. Type III secretion system 1 of *Vibrio parahaemolyticus* induces oncosis in both epithelial and monocytic cell lines. Microbiology **155:**837-851.
228. **Zitzer, A., O. Zitzer, S. Bhakdi, and M. Palmer.** 1999. Oligomerization of *Vibrio cholerae* cytolysin yields a pentameric pore and has a dual specificity for cholesterol and sphingolipids in the target membrane. J Biol Chem **274:**1375-1380.